Cortical and Subcortical Correlates of Emotional Control

Across Adolescent Development

A DISSERTATION
SUBMITTED TO THE FACULTY OF THE GRADUATE SCHOOL
OF THE UNIVERSITY OF MINNESOTA
BY

James Norby Porter

IN PARTIAL FULFILLMENT OF THE REQUIREMENTS
FOR THE DEGREE OF
DOCTOR OF PHILOSOPHY

Adviser: Monica Luciana, Ph.D.

August 2013

Acknowledgements

Many thanks to my adviser, Monica Luciana, for her continual support and improvement of my work. Thank you to Paul Collins, Ryan Muetzel, and Dan Johnson for their years of comradeship, assistance in data collection, and their insights into the delicate processes of neuroimaging analysis. Thank you to all Luciana lab members for your friendship, support, and encouragement. Thank you to my dissertation committee members, Angus MacDonald III, Katie Thomas, and Bonnie Kilmes-Dougan, for their insightful comments and invaluable guidance. Last, but not least, thank you to the study participants, without whom none of this work would be possible.

The funding for MRI scanning in this study was provided by the University of Minnesota's College of Liberal Arts Brain Imaging Initiative. Scanning took place at the University of Minnesota Center for Magnetic Resonance Research, which was funded in part by National Center for Research Resources grant P41 RR008079 and National Institute of Neurological Disorders and Stroke grant P30 NS057091.

Additional support was provided by training grants from the National Institute of Mental Health (NIMH T32-MH017069, Neurobehavioral Aspects of Personality and Psychopathology) and the Eunice Kennedy Shriver National Institute of Child Health and Human Development (NICHD T32-HD007151, Interdisciplinary Training Program in Cognitive Science).

Dedication

This dissertation is dedicated to my family: my beautiful daughter, Audrey, and my wonderful wife, Esther. Without you, I can barely remember how to tie my shoes, and here I am earning a Ph.D.

Abstract

The neural mechanisms of motivational and emotional processing are of particular interest to the study of adolescent development. Magnetic resonance imaging (MRI) studies show the ventral striatum (especially nucleus accumbens [NAcc]), the amygdala, and the prefrontal cortex (PFC) to be reliable neural correlates of processing stimuli with hedonically valenced content. Current models theorize that the relative levels of maturity of these three regions, from both structural and functional standpoints, strongly influence an individual's tendencies towards impulsive, risky decision-making in the presence of motivationally salient stimuli. This study recruited pre- to early-adolescents, adolescents, and young adults to assess neural correlates of control over emotional reactivity while performing a novel functional MRI (fMRI) task, referred to here as the interval timing task. The task tested individual's abilities to perceive and recreate discrete time intervals, and required deliberate perceptual, cognitive, and motor control in the presence of strongly and weakly valenced visual stimuli. This paper describes the development of the interval timing task and presents comprehensive analyses of alterations due to task parameters as well as inter-individual characteristics of age and sex upon both participants' behavioral performances and their blood-oxygen-level-dependent (BOLD) responses. Additionally, this paper presents an alternative analysis of the fMRI data that can inform the current debate on the extent to which the NAcc displays a specificity for processing positively valenced information or if it is also integral to the processing of negatively valenced information.

Table of Contents

List of Tables

List of Figures

General Introduction

Motivational control, or the ability to modulate one's behavior by inhibiting a prepotent response to a concrete and proximal stimulus (of either positive or negative hedonic value) in the service of a more abstract or distal goal, is a key topic in affective neuroscience. The neural mechanisms of processing both appetitive and aversive information are of particular interest to the study of adolescent development of motivational control, as adolescence is a period of life characterized by increased health and vigor but also increased mortality and psychiatric morbidity, often due to impulsiveness or emotional undercontrol (Dahl, 2004). Two[1] broadly defined neural systems involved in motivational control are evident in the literature: one system that is primarily subcortical and related to the identification of motivationally salient environmental stimuli, and another system that is primarily prefrontal in localization and is related to the representation of long-term goal states and exertion of control over automatic behaviors. Within the motivational system, the striatum (particularly nucleus accumbens [NAcc]), amygdala, and ventromedial prefrontal cortex (VMPFC) are key structures. For the control system, dorsolateral PFC (DLPFC), ventrolateral PFC (VLPFC), and anterior cingulate cortex (ACC) are critical regions.

Traditional explanations of adolescent behavioral problems stemming from low motivational control have relied on evidence indicating that prefrontal development is not

[1] The broader motivational system may be conceptualized as containing two subsystems: one that responds to positive/rewarding stimuli, and one that responds to negative/threatening stimuli. It is therefore also possible to present this discussion in terms of three (or more) systems, and there is continued debate over the brain regions contained within such categories.

yet complete over the teen years, and that proper behavioral control will reach adult levels once cortical maturation is complete. However, such theories do not explain the nonlinear developmental trajectories of sensation-seeking and risk-taking, with adolescents displaying greater tendencies toward those traits than do either children or adults. That is to say, a prefrontal immaturity theory would predict that children would be even more prone to risky behavior than adolescents, as they have even more immature prefrontal cortices. Building upon animal models of brain development and reward responsivity (Bourgeois et al., 1994; Panksepp, 1998; Spear, 2000) and structural neuroimaging studies of brain development that showed disparate maturational trajectories across the brain (Giedd et al., 1999; Sowell et al., 1999, 2004), several research groups have recently proposed multisystem models of brain development that purport to explain the biological basis of increased adolescent sensation-seeking and risk-taking in the face of low motivational control (e.g., Casey, Jones, & Hare, 2008; Ernst, Romeo, & Andersen, 2009; Luciana, Wahlstrom, Porter, & Collins, 2012; Luna, 2009; Steinberg, 2010).

The brain's "reward system" has largely been ascribed to the striatum, and particularly the ventral striatum (VS; Ikemoto & Wise, 2004; Knutson & Greer, 2008; Robinson & Berridge, 2003) operating in concert with other subcortical and frontal regions (Haber & Knutson, 2010; Sesack & Grace, 2010). A number of studies have compared striatal responses to incentives in adults and adolescents (for reviews see Casey, Duhoux, & Malter-Cohen, 2010; Ernst et al., 2009) and many have reported enhanced activation in this region, particularly within the nucleus accumbens (NAcc), a

key component of the VS. However, the findings of enhanced or exaggerated striatal activity or insufficient activity within cognitive control regions (i.e., PFC) within adolescents are not universal, with some studies reporting either less involvement of these regions during reward tasks or no activation differences at all between adolescents and other age groups (Bjork et al., 2004, 2010; Geier et al., 2010; May et al., 2004). Many reasons can explain these inconsistencies, including the type of reward paradigm employed, sample characteristics, and analytic techniques (see Richards, Plate, & Ernst, 2013 for a comprehensive review).

Additionally, the degree to which the cortical and subcortical components of the putative reward system are truly specific to processing rewarding information has shifted in recent years. In one leading account of how the brain differentially processes reward-related and threat-related information over adolescence, Ernst and colleagues (2006, 2009) proposed the triadic model of adolescent behavior, which contains three main neural hubs (i.e., VS, amygdala, and PFC) that are all hypothesized to contribute to approach, avoidance, and executive control. Activation in each node can be viewed from a dimensional perspective, and the triadic model conceptualizes behavior as a function of changes in the patterning of activity, or relative extents of activations, across the different dimensions. The anterior NAcc, basolateral amygdala, and ventromedial PFC (VMPFC) are associated with approach signals; the central amygdala, posterior NAcc, and ventrolateral PFC (VLPFC) are associated with avoidance signals; the dorsolateral PFC

(DLPFC) and the afferent projections from NAcc and amygdala to the PFC are associated with modulation of behaviors[2] (Ernst & Fudge, 2009).

This heuristic model of VS-amygdala-PFC coordination does not purport to fully describe the array of brain regions that contribute to approach, avoidance, and control (i.e., motivated) behaviors, and major roles have been outlined for regions of the temporal lobes (Nelson, Liebenluft, McClure, & Pine, 2005), the insula (Bernston et al., 2011; Menon & Uddin, 2010), and ACC (Groenewold et al., 2013). The temporal lobes are thought to interface with the triadic model nodes particularly when motivational behaviors are related to accurate detection and decoding of socially important sensory information, such as the presence of peers and their projected expectations or intentions within the current situation (Nelson et al., 2005). The role of the insula is more broadly conceived as an alliesthetic integrator, combining homeostatic interoceptive information into subcortical approach/avoidance signals and medial-prefrontally-generated goal states (Craig, 2009a; Stein & Paulus, 2008). In this view, the insula provide "weighting" for evaluation of external stimuli according to drives towards achieving homeostasis, and dysfunction among, or imbalance between, insula, VS, and amygdala signaling may be a biomarker for disorders characterized by emotional and motivational dysregulation (Aupperle & Paulus, 2010; Paulus, Tapert, & Sculteis, 2009). A recent meta-analysis of over 200 fMRI studies on the perception of subjective valence provided additional support for the general anterior-positivity/posterior-negativity functional gradient within

[2] While such a model proposes a general functional gradient of anterior-positivity/posterior-negativity within NAcc as well as basolateral-positivity/central-negativity biases in the amygdala, technical limitations on fMRI resolution limit the ability to derive reliably distinct signals from the subdivisions of NAcc and amygdala, and they are most commonly investigated as unitary structures in human studies.

the basal ganglia and confirmed that both dorsal medial PFC (including ACC) and anterior insula were reliably associated with experiencing both positive and negative valence (Bartra et al., 2013). Indeed, since its initial presentation (Ernst, Pine, & Hardin, 2006), the triadic model has been significantly modulated and has recently begun to incorporate roles for the ACC and insula, as well as the hippocampus (Richards et al., 2013), though the extent to which these structures would be expected to show adolescent-specific alterations in activity have not been fully defined.

Methodologically, most of the task-based fMRI studies contributing to the development of the models discussed above employed the approach of using subtractive contrasts to isolate sets of brain regions important for particular task conditions, and through agglomerations of results over time, "network" statuses were ascribed to brain regions consistently co-activated across similar task conditions. Using subtractive contrasts in fMRI is a time-tested analytic strategy, and is also the approach that was taken in the current study. However, there are many ways to define a network of brain regions, and results from one analytic view can be used to constrain or enhance the interpretations of another.

Clearly, the individual anatomical components of proposed appetitive approach, aversive withdrawal, and cognitive control networks in the brain are not exclusively dedicated to the processing of just one type of stimulus or facet of information. All brain regions discussed above have afferent and efferent connections to multiple other sites, often distributed widely across the brain, and they participate in myriad aspects of conscious and non-conscious experiences. In addition to "hard-wired" networks for

which direct axonal and synaptic connections exist, catalogs of persistently (and thus presumably, importantly) physiologically correlated networks, known as intrinsic connectivity networks (ICNs) are being built through resting state fMRI studies (Damoiseaux et al. 2006; Fox et al., 2005; Laird et al., 2011; Smith et al., 2009; Sporns, 2011).

Many ICNs share aspects with, and interact with, the motivational systems described above. The concept of the ICN became influential with the recognition of a coherent set of brain regions that reliably deactivates (i.e., shows negative BOLD signal change) when subjects engage in a wide array of cognitive tasks and was, conversely, coherently active during rest. This so-called "default mode network" includes the VMPFC, portions of the medial temporal lobes, posterior cingulate cortex (PCC), and angular gyrus (Raichle et al., 2001), and is thought to function as an internal monitoring and self-integration network. More recently, Seeley and colleagues (2007) described two ICNs involved in directing one's attention outward and putting forth concerted effort. Their "salience network" included dorsal ACC and anterior insula, whereas the "central executive network" included portions of DLPFC and lateral parietal cortex (e.g., angular gyrus, superior parietal lobule). One way that the insula may be related to emotional processing irrespective of valence is through its role in a salience network, where its role as a crossover point for simultaneous processing of interoceptive and cognitive information (Laird et al., 2011) allows it to integrate alerting signals with internal state signals and facilitate switching out of the resting/readiness default mode network and into

other active processing systems like the central executive network (Menon & Uddin, 2010).

Regardless of methodology used to define functionally coupled or interactive brain networks, the current consensus view is that the basal ganglia (particularly the VS), amygdala, and insula are important for instantiation of reward/punishment and prediction/learning signals underlying goal-directed behaviors, whereas subdivisions of the PFC are variously responsible for evaluation of changes in contextual information (e.g., ACC), evaluation of hedonic value (e.g., VMPFC/VLPFC), and selection of actions (e.g., DLPFC/inferior frontal gyrus (IFG)). The emerging consensus on developmental aspects of these regions is that the unsynchronized timing of functional maturity (i.e., these are developmental lag, developmental mismatch, or unbalanced development models) within subcortical and prefrontal cortical structures is key to understanding the development of emotional/motivational regulation and cognitive control across childhood, adolescence, and young adulthood (Ernst et al., 2009; Luna, 2009; Somerville, Jones, & Casey, 2010; Steinberg, 2010).

With humans' exceptionally outsized cognitive capacities, motivational control can be assessed with a wide array of tasks and paradigms. Most of the studies contributing to the consensus view above have been concerned with studying decision-making processes, approach behaviors, and receipt of rewards (Ernst & Paulus, 2005; Richards et al., 2013). However, studies of adolescent reward responsiveness and emotional control do not often use paradigms that secondarily elicit appetitive and aversive processing within a context of primary demands for executive control. Outside

of explicit motivational contexts, skills of cognitive control increase from childhood to adulthood on a variety of executive function and working memory tasks, such as the Tower of London (Luciana, Collins, Olson, & Schissel, 2009), the antisaccade task (Luna et al., 2001), the go/no-go task (Casey et al., 1997), the stop signal task (Carver, Livesey, & Charles, 2001), the Stroop task (Adelman et al., 2002), set shifting tasks (Kalkut et al., 2009), and the flanker task (Bunge et al., 2002). The developmental trajectories of performances on such control tasks generally show a linear increase across childhood until reaching asymptotic (i.e., adult-like) performance levels in mid- to late-adolescence (Best, Miller, & Jones, 2009; Davidson, Amso, Anderson, & Diamond, 2006; Luciana & Nelson, 2002; Luciana et al., 2005; Yurgelun-Todd, 2007).

In order to move from neutral states or "cold" cognitive states into "hot" motivational conditions, it is common to alter tasks with the inclusion of explicitly valenced stimuli, such as emotionally expressive photographs (e.g., Hardin et al., 2009) or pleasant and aversive sounds (e.g., Levita et al., 2009), or to induce motivated states through the addition of performance-based monetary incentives (e.g., Bjork et al., 2004; Galvan et al., 2006). Thus, the broad goal of this study was to design a novel fMRI task that would facilitate investigations of the development of control over emotional reactivity across adolescence, through the employment of an underlying "cool" control task altered with "hot" appetite and aversive stimuli, with the intent of determining the extent to which control processes can be exerted in the presence of valenced stimuli intended to be distracting or disruptive to accurate task performance.

The task is referred to herein as the interval timing task. Three projects will be described in relation to the task's design and development (Chapter 1), behavioral findings in an adolescent sample (Chapter 1), functional imaging correlates for the task parameters and inter-individual differences (Chapter 2), and a post-hoc use of the dataset to attempt a conceptual replication and extension of a recent fMRI study that explored NAcc responses to both appetitive and aversive stimuli.

Chapter 1. Creation of the Interval Timing Task and Comprehensive Behavioral Analyses

Introduction

The task that was developed attempts to assess cognitive and emotional influences over internal interval timing skills. Interval timing refers to one's "sense of time," that is, being able to judge how much time has elapsed and/or being able to reproduce a specific time interval when asked (cf., Buhusi & Meck, 2005; Matell & Meck, 2000). Accurate timing judgments of this sort require executive attention as well as self-monitoring, both important aspects of cognitive control. This study sought to determine whether timing skills are affected by age over an adolescent developmental range, as well as to determine if experimental manipulations of emotional valence and arousal would differentially impact interval timing skills.

The perception and tracking of the passage of time is an integral component of many human behaviors, from pacing one's workday to performing complicated dance routines. Before the invention of clocks, timers, and metronomes (a time span including all but the last fraction of human evolution), tasks requiring the correct timing of events relied solely upon an individual's ability to track time internally. Thus, the internal (i.e., neural) mechanisms of interval timing are expected to be highly conserved through evolutionary processes and relatively invariant across humans (Matell & Meck, 2000).

The subcortical regions implicated in interval timing include the caudate, putamen, pallidum, hippocampus, anterior insula, thalamus, and cerebellum, and the

cortical regions most often cited are posterior parietal cortex, supramarginal gyrus, central and frontal opercula, supplementary motor area (SMA), DLPFC, and IFG (Buhusi & Meck, 2005; Matell & Meck, 2000; Meck, 2005). The extent to which these areas appear in timing research reports appears to be dependent upon interval duration, reflecting the shifting biological substrates for timing intervals shorter or longer than just a few seconds (Meck, 2005), and upon task difficulty, indicating that interval timing networks interact with executive control regions, particularly when the timing is overt and not incidental (Livesey, Wall, & Smith, 2007).

The current study used overt interval timing as a method to engage executive processes, including attention and cognitive control, and then attempted to tax control systems through manipulations of emotional valence and arousal. The design of an interval timing task to be used in an fMRI context was predicated on the assumption that valence- and arousal-based alterations to stimuli used in the task would differentially affect activation levels within cortical and subcortical regions that underlie emotional reactivity and that these activations might impact the levels of effortful executive and motivational control to be exerted during task performance. For instance, under conditions of high arousal, one's perception of the pace of time accelerates; under conditions of low arousal, time seems to slow down (Droit-Volet & Meck, 2007; Wittman, 2009). Notably, various PFC regions and the insula have been shown to be involved in prior timing studies, while the NAcc and amygdala are two regions that have not been directly implicated in timing processes but are involved in the generation of positive incentive and threat-based states.

Interval Timing Task Creation

The fundamental research questions behind this task design were aimed at understanding how much control (reflected by accurate performance) could be exerted under conditions of appetitive versus aversive arousal, as well as the extent to which there may be developmental influences over that process. For instance, if adolescents are particularly sensitive to positive incentives, then the induction of positive motivation might be expected to more strongly interfere with performance accuracy as compared to the induction of negative motivation. The basic premise of the interval timing task was for participants to view an image, which was presented for a discrete length of time, and then, after a brief delay, attempt to recreate the time interval they had just experienced. In its basic form, such a task requires attention, monitoring, memory, and cognitive control. However, there were additional affective manipulations included in the interval timing task. First, the images used varied in their emotional properties. Some were neutral (e.g., pictures of common objects or landscapes), some were positive (e.g., pictures of attractive people, appetizing foods), and some were negative (e.g., menacing animals, unsightly physical features, disgusting things such as vomit or excrement). Within the positive and negative categories, stimuli also varied in the extent to which they elicited arousal. All images were sourced from publicly available web sites, and were found through targeted queries to image search engines for terms such as “cute kittens” or “snarling dogs.”

The images used in this study were designed to replicate the effects of the International Affective Picture Set (IAPS; Lang, Bradley, & Cuthbert, 1999), a collection of images with known features on the dimensions of valence (emotional appeal or dislike) and arousal (excitement/engagement or neutrality). Rather than use IAPS images, the current study sourced new images of improved photographic quality and subject matter relevant to a contemporary adolescent audience. Before the current fMRI study, a separate study was run to acquire mean valence and arousal image ratings for images that might be used in the current study. Thirty undergraduate students (15 males, 15 females) rated a collection of 166 candidate images on 5-point scales of positivity, negativity, and arousal. The 72 images most reliably mapping onto the positive, negative, and neutral domains of the IAPS-style valence/arousal ratings space were chosen for use in the current study. The images were also selected for appropriateness of content for a developmental sample, which is to say that none of the images were outside of the realm of exposure that the participants could access through public media such as news outlets, television, print or billboard advertising, or age-appropriate cinematic entertainment. Extremely graphic images (e.g., sexually explicit erotica, mutilations) were not chosen for this study. For examples of images used in this study, see Figure 1.1.

The other main task manipulation involved the duration of image presentation. This manipulation was chosen because current models of the experiential integration of temporal units suggest that around two to three seconds may be a universal cutoff for the experience and cognitive processing of discrete moments[3] (Pöppel, 2009; Ulbrich,

[3] That is to say, at any given moment, one's experience of "right now" is actually an accumulation of internal experiences over a sliding window of two to three seconds.

Churan, Fink, & Wittmann, 2007). Furthermore, current models of the neural basis for interval timing suggest that as intervals bordering on, or less than, one second in length should more strongly engage subcortical and cerebellar timing systems, whereas the tracking of multi-second or greater intervals should be more dependent upon higher cortical systems (Buhusi & Meck, 2005; Lewis & Miall, 2003; Matell & Meck, 2000; Meck, 2005; Wittmann, 2009). Though including intervals shorter than one second would be most appropriate for attempts to parse out cerebellar versus cortico-striatal timing networks, this task was designed for an fMRI study, which, due to fMRI's limited temporal resolution, meant that the use of trials with subsecond timing intervals would be ill-advised. Additionally, complete separation of such timing networks was not a focus of the study. Thus, the task contained trials that were short, with intervals of 1, 1.5, and 2 seconds, and trials that were long, with intervals of 5, 5.5, and 6 seconds.

The basic trial structure was to have participants experience a discrete time interval through the presentation of an image (e.g., from Figure 1.1), and then, after a brief delay, to reproduce the just-experienced interval by viewing another image and making it go away with a button press. The initial viewing images were different on every trial and varied on levels of valence and arousal, whereas the image used in the reproduction period was the same on every trial (see Methods section and Figure 1.2 below for more details on trial layout).

Figure 1.1: A selection from the 72 images used in the interval timing task. The top row contains negative images, the middle row contains neutral images, and the bottom row contains positive images.

Hypotheses

Valence and Arousal. The main expectation during task design was that the manipulations of image content would yield differential performance levels across image valence and arousal categories. It was expected that neutral images would serve as a baseline for task performance, and that positive and negative images would influence the accuracy of interval timing. However, the directions of such performance alterations were not set *a priori*, as valenced stimuli could be either performance-detracting distractions or they could aid with sustained interest and task engagement, potentially improving performance compared to neutral trials (Droit-Volet & Meck, 2007; Wittman, 2009). However, for the manipulation of arousal levels, increasing arousal was expected to tip

the balance towards distraction and consequent performance declines (Droit-Volet & Meck, 2007; Gil & Droit-Volet, 2012).

Duration. There was not a clear expectation during task development of whether or not participants would be better or worse at longer or shorter trials, or whether image content manipulations would differentially impact short and long trials.

Age. In general, the expectation in cognitive testing is that children will show lower performance levels compared to adults. Younger participants were expected to demonstrate less cognitive control over emotional reactions to the task stimuli, lowering their performance levels. Moreover, the study recruited a developmental sample (pre-teens to young adults) to allow for the testing of hypotheses that adolescents would show greater emotional reactivity and thus less cognitive control than younger or older participants.

Sex. No specific directional hypotheses for sex differences were made during task design.

Methods

Participants

The recruitment strategy for the fMRI study targeted three age groups: ages 11–13, 15–18, and 19–24. Parents of children and adolescents were contacted through a subject database maintained by the University of Minnesota's Institute for Child Development (ICD). The Institute contacts parents listed in public birth records, and those who indicate a willingness to be contacted in the future for study participation are added to the database. Families with children within the targeted age ranges were chosen

via random selection from the database and contacted about possible participation. Participants age 18 and above were solicited through the University of Minnesota Psychology Department's Research Experience Program, which provides undergraduate students with extra class credit for participation in university research studies. Potential participants were screened via telephone interviews for exclusion criteria, including a) major physical or genetic abnormalities, b) mental retardation, c) head injuries that resulted in loss of consciousness, d) current or past neurological, psychological, or psychiatric illnesses, e) learning disabilities, f) tobacco, alcohol, or drug abuse, g) current or past use of psychoactive medications, h) being a non-native English speaker, i) abnormal or uncorrected vision and hearing, and j) MRI contraindications (e.g., severe claustrophobia, braces, pregnancy, medical implants). The University of Minnesota's Institutional Review Board approved the protocol. Adults and parents of minors all provided informed consent, and all minor children assented to participate in the study. Parents were shown the images used in the task prior to giving consent for their children's participation.

A total of 33 participants aged 11 through 24 years were enrolled in the study. Data from two participants were not analyzed, as they were unable to provide both behavioral and fMRI data that met quality assurance standards. The final sample thus contained 31 participants (16 females, 15 males, age M=17.22, SD=3.69). Across the target age groups, the final sample contained 9 11–13-year-olds (F=4, M=5), 9 15–18-year-olds (F=5, M=4), and 13 19–24-year-olds (F=7, M=6). All participants spent approximately 2 hours completing the study, which included an MRI protocol as well as

the completion of various self-report measures. All minors were paid $20 for their time and effort, as well as up to a $5 "bonus" based on timing task performance. Undergraduate participants received either $20 or extra credit points in a psychology course for participating, along with up to $5 in task-based bonus payments.

Interval Timing Trial Layout and Task Parameters

As noted above, the interval timing task required participants to experience a discrete time interval through viewing an image, and then to attempt to reproduce that same interval. During short presentation trials, images were displayed to the participants for 1000–2000 ms, whereas long presentation trials held images on-screen for 5000–6000 ms. Participants' interval timing reproductions were indicated on each trial by a single right-handed button press. During the self-paced timing reproduction phase of every trial, the same image of a blank stopwatch was shown to the participants (see Figure 1.2). Participants were instructed to press a button to make the stopwatch go away when they felt that the stopwatch image had been shown to them for as much time as the prior image (in Figure 1.2, the kitten) had been shown to them.

Participants received performance feedback on each trial, which was designed to assist with improving subsequent performances. The feedback images conveyed two pieces of information: 1) whether or not the timing reproduction was accurate enough (±20% of true duration) to have won money on the trial, and 2) whether the timing reproduction was faster or slower than the target duration (see Figure 1.2 inset). Precise feedback of timing error in raw milliseconds was not given for two related reasons: 1) to reduce the amount and complexity of information shown on-screen, and 2) simplifying

performance outcomes to close enough/not close enough was intended to increase ambiguity, such that performances would be more likely to be based on participants "gut feelings" rather than engagement of excessively cognitive, calculation-based strategies. Each participant was able to win up to $5.00 based on his or her cumulative task performance. Participants were not punished by subtracting money from their running totals when their reproductions were outside of the accuracy cutoffs. Thus, trial outcomes were either wins or non-wins. However, to aid with textual clarity throughout this paper, reproductions that were ±20% of the true target duration are referred to as wins, and those that were either less than 80% or more the 120% of the true target duration are referred to as losses.

The task was performed during fMRI scanning, and was broken into four separate 5-minute blocks (for full fMRI timing parameters, see the Methods section in Chapter 2). Each block contained 18 trials, for a total of 72 trials in the entire task. Based on the prior responses of undergraduate image raters, an evenly balanced set of 24 positive images, 24 negative images, and 24 neutral images were chosen for the fMRI study. There were 12 high arousal images and 12 low arousal images within each of the positive and negative image sets (all 24 neutral images were necessarily of low arousal). The trials were divided evenly between short and long durations, and the valence and arousal categories were evenly distributed within short and long trials. No images were repeated during the task. The task was administered using E-Prime software (Psychology Software Tools, Inc, Pittsburgh, PA).

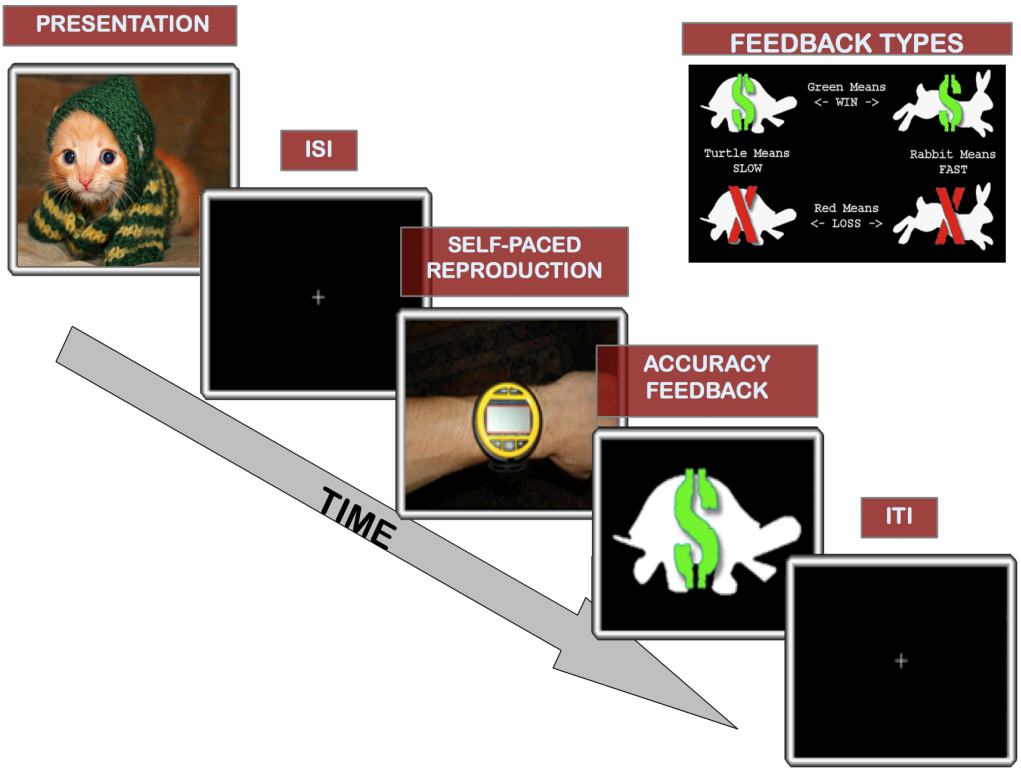

Figure 1.2: Sample trial layout. Target interval presentations varied in duration (either short or long) and contained a unique image on every trial. The interstimulus interval (ISI) varied between 1000 and 1500 ms. Reproduction periods began when the stopwatch image appeared, and ended when participants pressed a button to make the stopwatch go away. Feedback was provided on the relative length of reproductions (slower or faster than the target) and on whether or not reproductions were accurate enough to have won money on the trial. The intertrial interval (ITI) varied in length, depending on reproduction times. (See Chapter 2 for details on the pacing of the task during fMRI scanning.)

Confirmations of Image Ratings. After the scanning session, all participants rated the 72 task images on 5-point scales of positivity, negativity, and arousal. Overall image valence ratings were taken as the participant's positivity rating minus the negativity rating and ran on a scale from -4 to 4.

Statistical Approach

The goals of these analyses were to validate the valence and arousal ratings of the images selected for this study, and to confirm that the elements of task and study design (e.g., duration, valence, arousal, age-based development) were truly impactful upon task performance, through direct comparisons of multiple explanatory models.

Two approaches were taken to understanding the image rating data. First, group mean valence and arousal ratings were calculated for each image across the 31 subjects. Statistical tests of mean image ratings across the image categories were carried out to ensure that the three valence and two arousal groups did actually differ on their mean ratings, but also to ensure that the image ratings were not confounded across valence and arousal groups (to ensure that, e.g., all positive images were not rated as low arousal, all negative images were not highly arousing). High versus low arousal image comparisons were made with *t*-tests, and ANOVAs with Bonferroni-corrected follow-up *t*-tests were carried out for the positive/negative/neutral valence comparisons.

In the second approach to analyzing the image ratings, repeated-measures ANCOVAs were run to test the effects of sex and age upon participants' mean image ratings within each category. Two ANCOVAs were run. The first looked at effects upon valence ratings across the valence categories, with mean positive, negative, and neutral valence ratings as within-subjects factors, sex as a categorical between-subjects factor, and age as a continuous covariate. The second looked at effects upon arousal ratings across arousal categories, with mean high and low arousal ratings as within-subjects

factors, sex as a between-subjects factor, and age as a covariate. All *p*-values were Bonferroni-corrected within each ANCOVA.

Exploratory, Descriptive Plotting of Task Performance Data. The study design was predicated on the hypotheses that task performances would be influenced by interval duration, image valence, image arousal, and participant age, but as this was a novel task it was imperative that a variety of potential explanatory factors be explored. A two-stage approach of visual inspection of the data followed by a series of model comparisons was used in this study.

The exploratory plotting of the data was carried out to assess basic distributional characteristics of reproduction performances as well as to provide guidance for the selection of interaction effects to include in later model-fitting comparisons (described in detail below), as well as to provide the reader with a fuller understanding of the data. Only descriptive statistics were calculated in association with the plots; no inferential statistics were generated in this stage. Barplots were drawn with standard error bars to provide a general depiction of variance in task performances, but these error bars were not used to provide formal inferences of statistically significant differences between groups.

All but one of the plots presented used the number of wins divided by the total number of trials, referred to as the "win ratio," as the dependent variable. Perfect performance on all trials would produce a win ratio of 1.0, whereas for complete failure it would equal 0.0. Thus, the win ratio represents a summary score of performances across all of a participant's individual win/loss trial outcomes, which were the dependent

variables for the later inferential statistical analyses (see below). Looking at the dependent variable from a continuous perspective (e.g., proportion reproduced, raw milliseconds reproduced) would be meaningful in an investigation of absolute accuracy. However, as noted above, the task was designed to provide feedback based on a dichotomous outcome: being "accurate enough" to win money on a trial or being "too inaccurate" and losing the opportunity to win money on a trial. As such, analyzing performances with a binary response variable allows for an examination of behavioral data that mirrors the performance-guiding information that was available to each participant.

All plots were generated for the short and long duration trials separately. Histograms of participants' proportional interval reproduction values (reproduction times divided by the true interval duration) allowed for visualization of the accuracy of individual trial reproductions as well as the relative frequency of wins to losses across the whole sample. All other plots used the win ratio as the summary variable. Histograms of win ratios were generated to visualize performance distributions across short and long interval durations. Barplots were used to inspect the mean performances across images valences (positive, negative, and neutral), across image arousal levels (high and low), and across the five image categories representing the interaction of valence and arousal (positive/high, positive/low, negative/high, negative/low, and neutral). Potential sex effects were also explored with barplots. Potential linear effects of age upon performance, was well as potential age × sex interactions, were explored with scatterplots. After the exploratory, descriptive inspection of data, inferential statistics for task performances

were then employed during a multi-step, forward-selection model fitting and comparison procedure.

Model Selection Procedures. The model selection analyses were aimed at understanding the factors that would best predict wins and losses in the timing task. Conventionally, this type of analysis would likely be carried out with repeated-measures ANOVA, but here a linear mixed effects regression (LMER) approach has been taken. The use of LMER allows for the direct assessment of the impact of individual variability in intercepts and slopes in the expression of task proficiency. Perhaps more importantly, the reason to favor an LMER approach over ANOVA in this case is that the use of Maximum Likelihood estimation procedures within an LMER framework allows for the direct comparison, via fit indices, of non-nested models to determine the combinations of fixed and random effects that best account for task performance. Additionally, as there are no *p*-values associated with the fit statistics, fit index comparison approaches are not subject to the family-wise error rate inflation restrictions of typical null-hypothesis statistical testing (Long, 2012). Since family-wise error inflation is not an issue with fit indices (again, no *p*-values are calculated), concerns over testing too many models at one time are minimized, and alternative models and factors that may have been otherwise uninvestigated or overlooked can be included in the model comparison sets. This "no stone unturned" approach is important to this study, as the interval timing task was a novel development. Although the task was designed with specific expectations that participant age and categories of valence, arousal, and duration would influence task performance, there may have been unexpected factors, or combinations of factors, that

influenced task performance in addition to or in place of design expectations. Were such factors present and left unexamined, the study's interpretations and conclusions would be in doubt. In situations where tasks are well established and their performance determinants are well known, the number of models fit and compared would be far more constrained than in an exploratory analysis such as this.

Although the use of Maximum Likelihood, LMER, and fit indices in this context preempts concerns over error rate inflation due to multiple comparisons, it certainly does not guarantee that the "correct" model will be identified, nor does it fully protect against identifying a model that could be specific to only this sample and ungeneralizable. That is to say, these procedures do not, and cannot, prevent the problem of "over-fitting." (Notably, conventional null hypothesis statistical testing cannot make such guarantees, either.) The choice of a penalized fit index—one that reduces the fit score given to a model as it becomes more complex—provides partial protection from over-fitting, favoring parsimony over a perfect description of the data at hand. In this set of analyses, the use of the corrected Akaike information criterion (AICc; Hurvich & Tsai, 1989) ensures that any parameters added across models will be rejected unless they contribute substantial improvement in model fit. This is done by reducing maximized log likelihood values (and thus worsening AICc values) by two times the number of parameters included in the model. In these analyses, reducing the number of tested interaction terms was also taken as a safeguard against over-fitting. Unless exploratory plotting clearly indicated the presence of markedly different slopes across levels of a variable, only intercept effects were tested. Additionally, the inclusion of a nil model (intercept effects

only) within the comparison set provided a basic check that the independent variables built into the task actually altered performances beyond each individuals' inherent abilities to experience and reproduce discrete time intervals.

In sum, these analyses should be viewed as exploratory model analyses testing the relative strengths of effects of trial duration, image content manipulations, age, and sex upon task performance. A multi-step, forward-selection approach was taken to determine which task parameter variables most completely, but succinctly, captured win/loss variance across the whole task, using logistic regression methods to predict wins and losses (coded as binary 1/0 outcomes) from regressors based on task parameters, sex, and age. Simple models of single predictors, complex models of multiple predictor combinations, as well as a "nil" model containing only fixed and random intercept terms were included in comparison sets across three tiers of analyses. All models within a step were estimated separately (through logistic LMER procedures) and then compared simultaneously by examinations of AICc model fit values before moving on to the next step. All model and fit index calculations were performed in R (R Development Core Team, 2012), using the *lme4* and *bblme* packages.

Model Building and Estimation Procedures. In the first step, combinations of only the task parameters were examined. Parameters tested included trial duration and categorical distinctions of valence and arousal, as well as subject-specific image ratings for valence and arousal. Since there were no neutral valence/high arousal images, a recoding of categorical valence was required in order to make models with a valence × arousal factor mathematically tractable. Negative images were recoded as -1, positive

images as 1, and neutral images as 0. An additional benefit to this recoding is that the vectors for valence and valence × arousal both coded neutral images as 0, making neutral images the comparative basis for interpreting the model weights. Thus, the first model selection step identified which task parameters were most robustly predictive of trial success (a binary dependent variable, win=1, loss=0), with an added comparison of whether or not individual's image ratings provided greater predictive power over mean image categorizations. Only fixed effects terms for task parameters were examined in this step, but each model included a random effects intercept term (by necessity, in LMER). A total of 34 models were examined in the first step (see Table 1.2).

The second step sought to determine if the inclusion of random effects terms for best-performing parameters from the first step would provide additional predictive power beyond a model with only fixed effects for task parameters and a random intercepts term. For example, if the first step indicated that image valence and arousal were to be retained as fixed effect terms, then comparisons of models with additional random effects for valence and arousal were entered in the comparison set. In order to reduce the likelihood of over-fitting and to constrain interpretive complexity, slope effects (e.g., for valence × arousal) were entered as fixed effects terms but their random effects were not examined. In order for a random effects variable to continue on to the next step, the model containing that variable had to provide a greater weight of evidence (see below) than the fixed effects model carried forward from step one.

In the third and final step, combinations of fixed effects terms for age and sex were added to the best-fitting model from step two, to see if they provided additional meaningful predictions of task performance.

Model Comparison Procedures. For all steps, comparisons of model fits were performed by transforming model AICc values into "weight of evidence" ratios. Among the set of compared models, the model with the minimum AICc value was identified and then used to calculate an AICc difference score (dAICc) for each model. The weight of evidence score was then calculated as the ratio of a model's exponential distance from the minimum AICc in the set to the sum of all such distances in the set (see formula below). The weights within any comparison set sum to 1, and when multiplied by 100 they can be interpreted as the percent chance that, among all the models in the comparison set, the model at hand is the true model underlying the data (Long, 2012).

$$\frac{\exp\left(-dAICc/2\right)}{\sum\exp\left(-dAICc/2\right)}$$

Dividing the weight of evidence values by the largest weight value in the set yields a relative weight value. The model with the smallest AICc value always has a relative weight of 1, and all other models' relative weight values are interpreted like an odds ratio, as how many times more likely it is that the smallest AICc reference model is the true model compared to that particular model (Long, 2012).

Results

Thirty-one participants successfully completed the interval timing task while undergoing fMRI scanning. Due to computer errors, timing task administration was interrupted by the computer's operating system at the close of the task for two

participants. These two participants missed a total of three trials and one other subject did not respond to one trial, but all other participants completed the task in full. Overall, this represents over 99% complete data. Computation errors within E-Prime led to participants receiving erroneous loss feedback on a subset of 1000 ms trials. All participants were affected. Across all participants, the total percentage of false feedbacks on 1000 ms trials was 51.35%. The number of false feedbacks per participant varied by individual performance levels on the 1000 ms trials, ranging from 3 to 10 erroneous feedbacks (M=6.13, SD=1.86). Those trials were recoded as wins for the purposes of the behavioral analyses, but were excluded from the later fMRI analyses when looking at feedback-related neural activations.

Confirmation of Image Ratings

The mean valence and arousal ratings of the images showed that the participants perceived the image content largely as intended (see Figure 1.3 and Table 1.2). The categorization of images was fairly stable from the previously mentioned undergraduate image raters to the fMRI study participants. Some of the images previously classified as positive had different mean ratings for the fMRI participants, leading to slightly non-balanced cells in the task design. Three positive/low images were rated as neutral, and one positive/low image shifted to the positive/high category. The image category classifications shown in Table 1.1 were used in all behavioral and fMRI analyses.

Figure 1.3 shows a scatterplot of the two-dimensional valence × arousal content ratings for all images, which replicates the IAPS' characteristic "boomerang" shape

(Lang et al., 1999), indicating that the images were properly dissociated between valence and arousal dimensions.

Table 1.1
Cross-tabulation of image categorizations based on participant ratings of valence and arousal.

	High Arousal	Low Arousal
Negative	12	12
Neutral	0	27
Positive	13	8

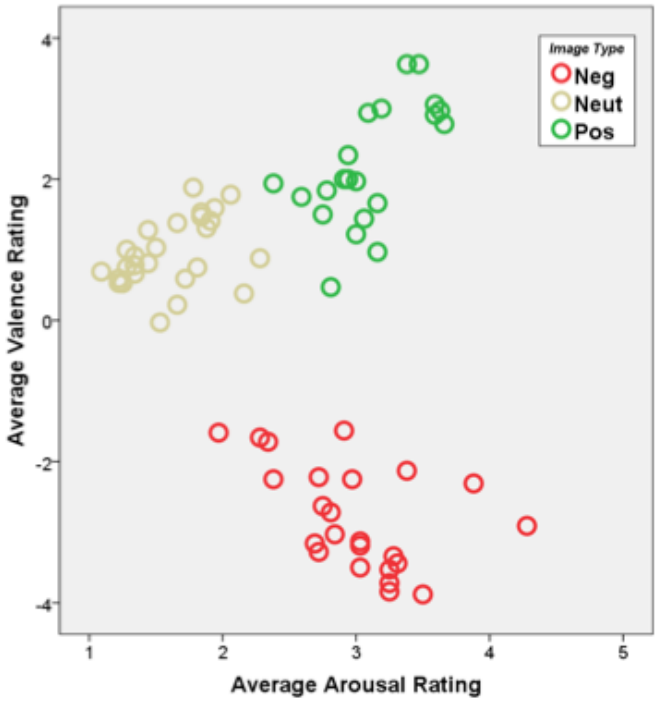

Figure 1.3: Scatterplot of mean arousal ratings by mean valence ratings. Points are color-coded by valence group membership.

Table 1.2

Mean valence and arousal ratings for each image category.

Image Type	Mean (SD) Valence	Mean (SD) Arousal
Positive	2.19 (0.86)	3.09 (0.35)
Negative	-2.79 (0.74)	2.99 (0.51)
Neutral	0.93 (0.48)	1.59 (0.33)
High Arousal	-0.27 (3.00)	3.34 (0.31)
Low Arousal	0.23 (1.64)	2.05 (0.62)

Note: Valence ratings were calculated by combining individual positivity ratings (1 to 5) and negativity (1 to 5) ratings, producing a scale of -4 to 4. Arousal ratings were made on a single scale of 1 to 5.

Comparisons of Mean Valence and Arousal Ratings Across Image Types. A *t*-test on mean ratings showed that images categorized as high and low arousal did differ significantly on arousal ratings ($t(70)=9.75$, $p<0.05$). An *F*-test and follow-up pairwise comparisons on valence ratings across valence categories showed that all three categories were significantly different from each other ($F(2,69)=319.84$, $p<0.05$). Positive image valence ratings were higher than those for both neutral ($t(46)=6.40$, $p<0.05$) and negative ($t(43)=20.86$, $p<0.05$) images, and negative images were rated with lower valences than neutral images ($t(49)=-21.47$, $p<0.05$). For arousal ratings, there was a main effect across valence types ($F(2,69)=109.29$, $p<0.05$), driven by the fact that neutral images were less arousing than both positive images ($t(46)=-15.30$, $p<0.05$) and negative images ($t(49)=-11.83$, $p<0.05$). Importantly, positive and negative images did not differ in mean arousal ratings ($t(43)=0.79$, *n.s.*). All tests remained statistically significant after Bonferroni correction for multiple comparisons. Mean ratings for valence ($t(70)=0.14$, *n.s.*) and arousal ($t(70)=0.05$, *n.s.*) did not differ across images used for the short and long duration

trials. Figure 1.4 contains barplots depicting mean ratings values for the various image types.

Repeated-Measures ANCOVA Tests for Effects of Sex and Age. The repeated-measures ANCOVA investigating age and sex effects upon valence ratings across valence categories reaffirmed the findings above, showing a significant main effect for valence category upon valence ratings ($F(2,27)=25.54$, $p<0.05$). There were no between-subjects main effects for age ($F(1,28)=0.29$, *n.s.*) or for sex ($F(1,28)=0.21$, *n.s.*). There was no interaction effect for valence and age ($F(2,27)=1.57$, *n.s.*), but there was a significant interaction effect for valence and sex ($F(2,27)=3.84$, $p<0.05$, partial eta-squared=0.22). Follow-up *t*-tests showed that females tended to rate negative images more negatively (M(SD)=-2.96(0.54)) than males did (M(SD)=-2.57(0.39), $t(29)=2.27$, $p<0.05$). Likewise, females tended to rate positive images more positively (M(SD)=3.35(0.70)) than males did (M(SD)=2.82(0.57)), $t(29)=-2.32$, $p<0.05$).

The ANCOVA investigating age and sex effects upon arousal ratings across arousal categories again reaffirmed that high and low arousal categories did significantly differ in mean arousal ratings ($F(1,28)=7.23$, $p<0.05$). There were no between-subjects main effects for age ($F(1,28)=2.23$, *n.s.*), nor was there a significant interaction of age and arousal category ($F(1,28)=0.91$, *n.s.*). There was a significant main effect for sex upon arousal ratings ($F(1,28)=4.40$, $p<0.05$, partial eta-squared=0.14), but there was no interaction effect for arousal and sex ($F(1,28)=0.34$, *n.s.*). The follow-up *t*-test for sex effects showed that females tended to rate images as more arousing (M(SD)=2.71(0.63)) than males did (M(SD)=2.26(0.43), $t(29)=2.28$, $p<0.05$).

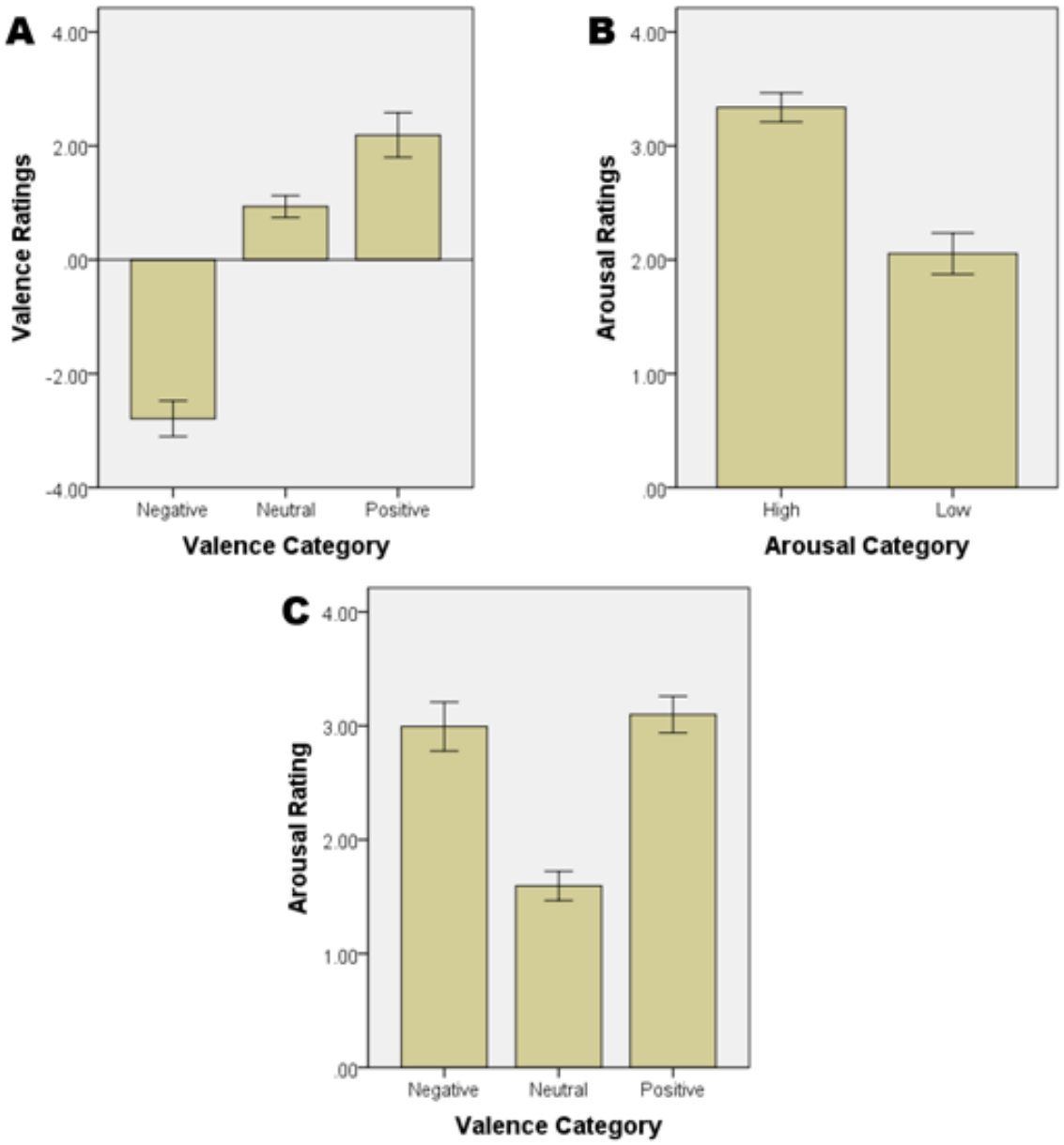

Figure 1.4: Barplots depicting mean valence and arousal ratings for the image categories. (A) Valence ratings across the valence categories. (B) Arousal ratings across the arousal categories. (C) Arousal ratings across the valence categories. Statistical comparisons between all groups were significant, except for the comparison of arousal ratings between positive and negative valence groups (means shown in panel C). Error bars represent 95% confidence intervals.

Descriptive and Exploratory Plotting of Timing Task Performance Data

Histograms of Win Ratios. No gross differences from normally distributed performances were visible in the histograms of reproduction proportions (Figure 1.5), though long trial reproductions were somewhat leptokurtic compared to the distribution of short trial reproductions, indicative of greater accuracy rates (less variance) for long compared to short trials.

Barplots of Performances Across Valence and Arousal Categories. Plotting of mean win ratios split by valence (Figure 1.6) also indicated effects of valence within short trials, such that positive images yielded fewer wins. For long trials, negative images yielded fewer wins than positive and neutral trials, but the difference was not clearly meaningful. Likewise, when collapsed across valence levels, arousal effects did not appear to be present for either long or short trials (Figure 1.7).

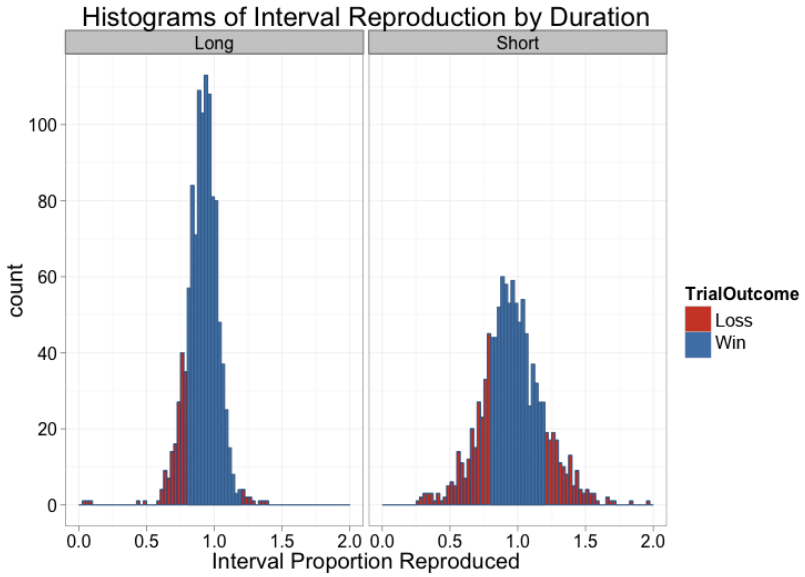

Figure 1.5: Histograms of proportional reproduction times. Distributions of performances are presented for long (left) and short (right) trials. Bars are color-coded by wins (blue) and losses (red).

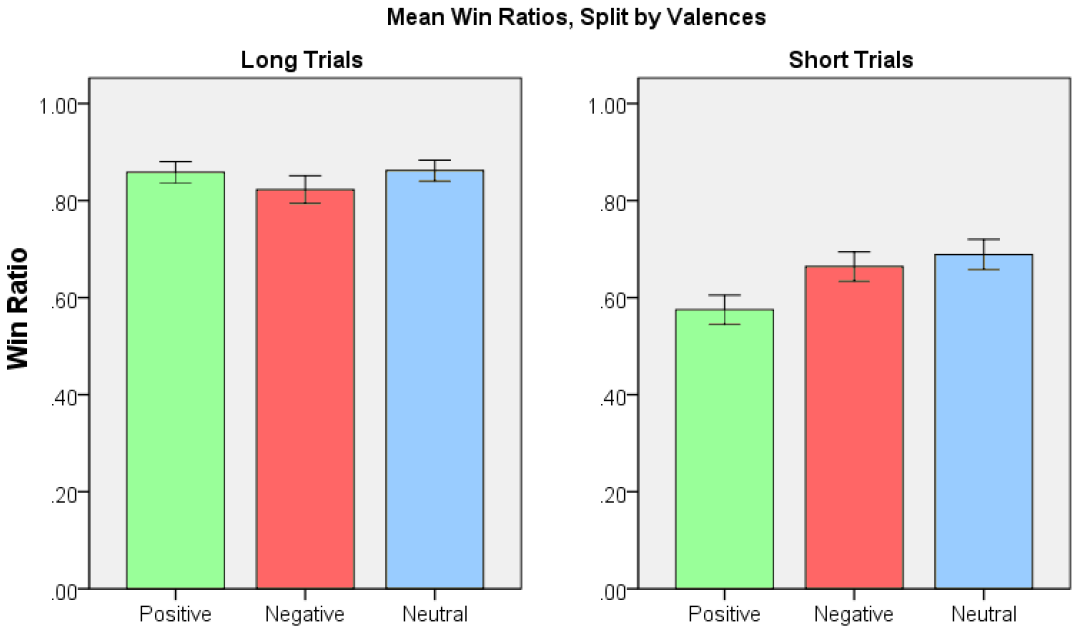

Figure 1.6: Barplots of mean win ratios split by valence groups and duration type. Long trial values are on the left; short trial values are on the right. Green=positive, red=negative, blue=neutral. (Note that error bars (±1standard error) are represented to indicate relative variances, but no inferential tests were carried out during the exploratory plotting phase.)

Barplots of Performances Across Valence × Arousal Categories. For short trials, there appeared to be a valence × arousal interaction (Figure 1.8), with equivalent performances for low arousal images, but, within the high arousal category there were poorer positive image performances and better negative image performances. A somewhat reversed pattern was seen in the long trials, which showed a higher proportion of wins for positive/low images compared to negative/low images, along with apparently equivalent performances across valences in high arousal images.

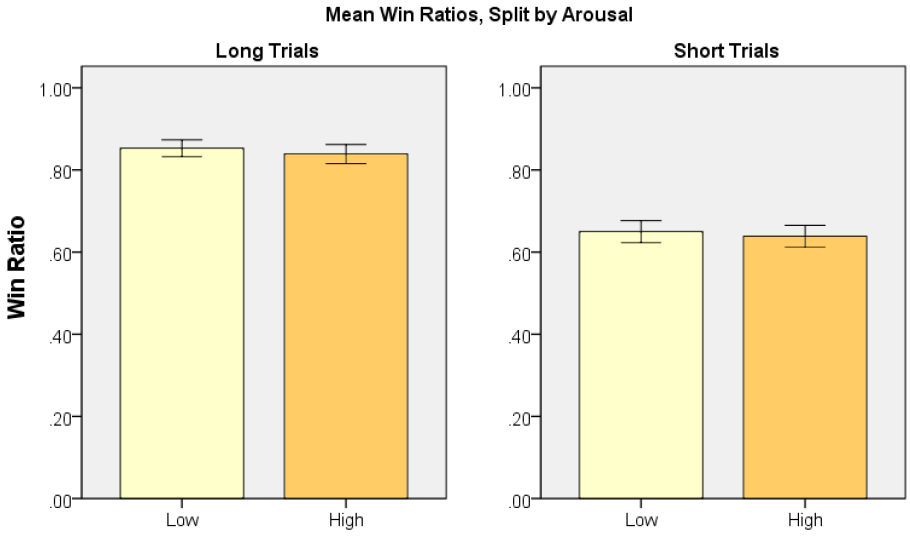

Figure 1.7: Barplots of mean win ratios split by arousal groups and duration type. Long trial values are on the left; short trial values are on the right. Light yellow=low arousal, dark yellow=high arousal. (Note that error bars (±1standard error) are represented to indicate relative variances, but no inferential tests were carried out during the exploratory plotting phase.)

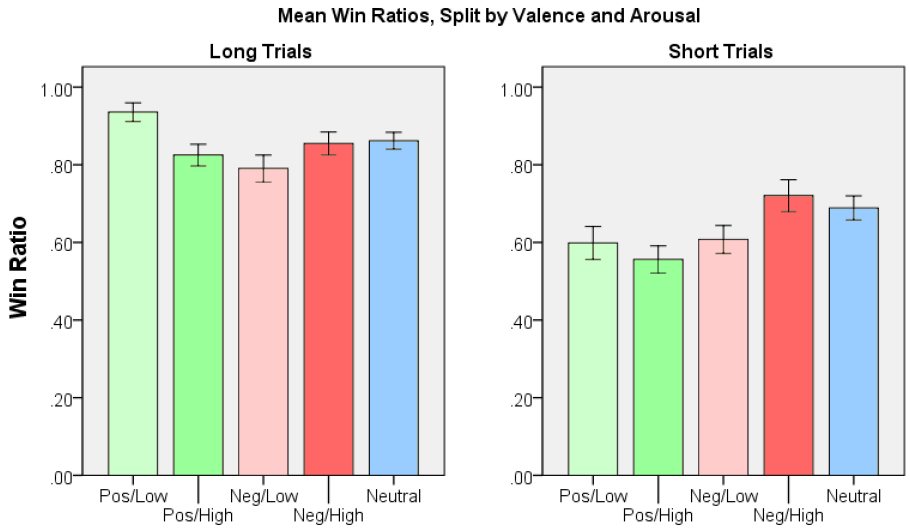

Figure 1.8: Barplots of mean win ratios split by valence groups, arousal groups, and duration type. Long trial values are on the left; short trial values are on the right. Blue=neutral, light green=positive/low arousal, dark green=positive/high arousal, light red=negative/low arousal, dark red=negative/high arousal. (Note that error bars (±1standard error) are represented to indicate relative variances, but no inferential tests were carried out during the exploratory plotting phase.)

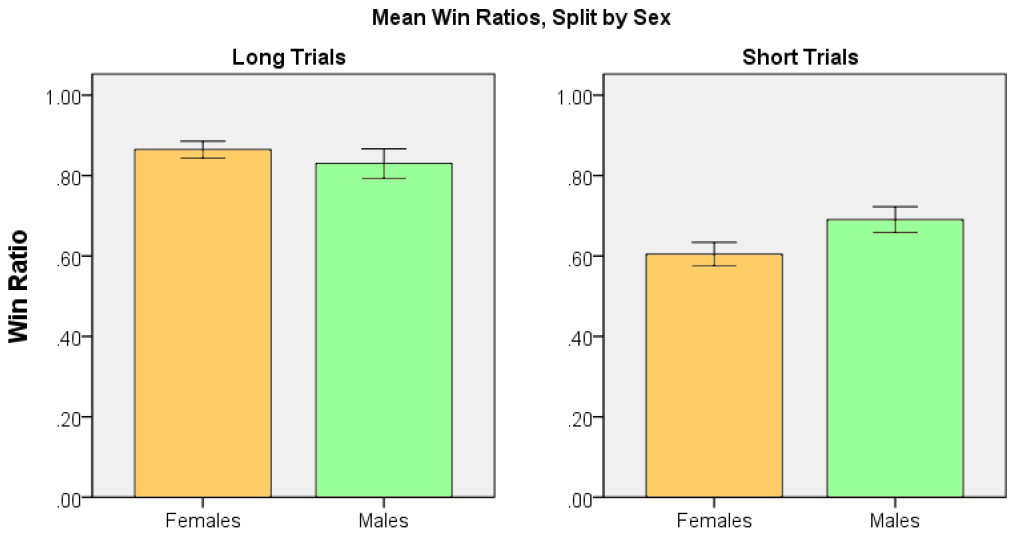

Figure 1.9: Barplots of mean win ratios split by sex and duration type. Long trial values are on the left; short trial values are on the right. Yellow=females, green=males. (Note that error bars (±1standard error) are represented to indicate relative variances, but no inferential tests were carried out during the exploratory plotting phase.)

Plotting of Sex and Age Effects. There appeared to be a difference between males and females for short trial performances (Figure 1.9), with females being less likely to win on short trials. On long trials, females were nominally more likely to have winning performances, but the degree of difference was smaller.

When looking at scatterplots of win ratios over the whole task against participants' ages (Figure 1.10), it appeared that age was positively correlated with performance, with the slope of the line appearing somewhat steeper for long trials. The presence of nonlinear age effect upon performance was not indicated by the arrangement of points in the scatterplot. Splitting the plots by sex indicated that age and win ratio relationships were present for males but not for females.

Overall, exploratory plotting of the data suggested effects upon task performance for trial duration, valence, valence × arousal, valence × arousal × duration, sex, age, and sex × age. Main effects for image arousal levels appeared to be absent.

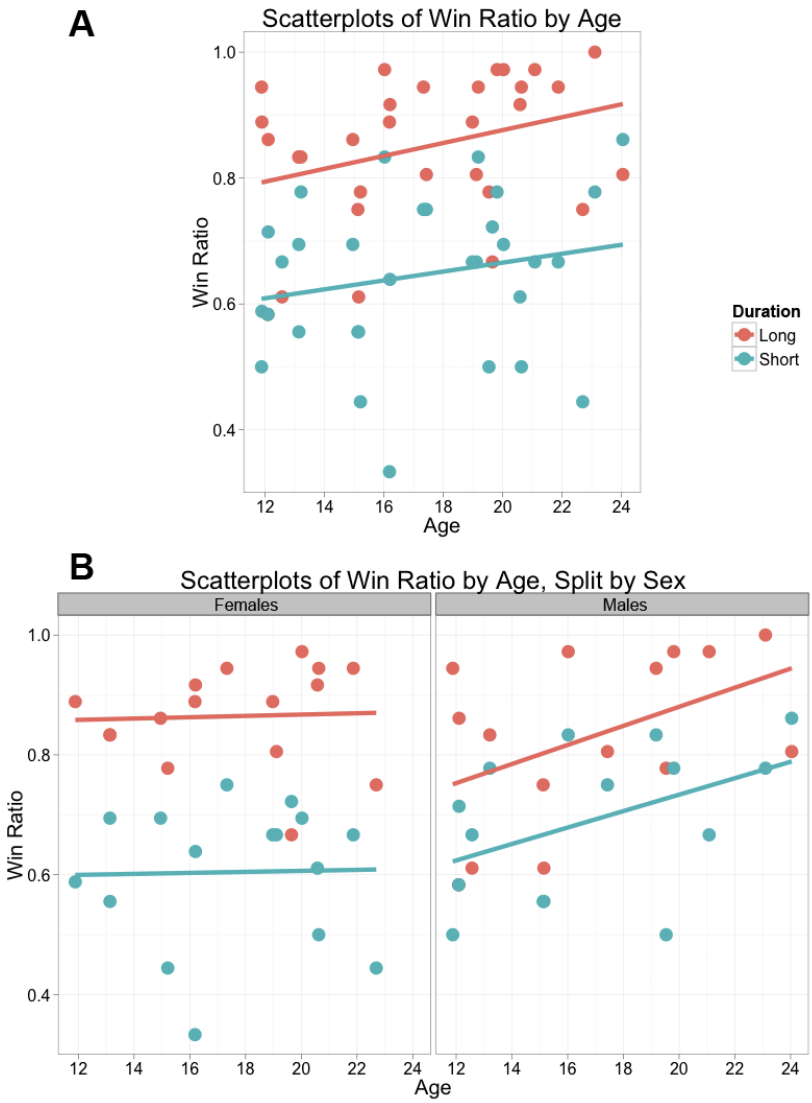

Figure 1.10: Scatterplots of Win Ratios Against Age. (A) Scatterplots for long (right) and short (left) trials for the sample as a whole indicate linear correlations, stronger for long trials. (B) When split by sex, the age correlation appears to be driven soley by male participants, with apparently equal strength for short (blue) and long (red) trials.

Model Fitting and Comparison Results

Model fitting and comparisons were carried out in three steps. A total of 34 models were compared in the first step (Table 1.3). The model set included a 'nil' model containing nothing but fixed and random intercept terms, models with single task parameters, and models with each task parameter in addition to, and in interaction with, trial duration.

Table 1.3
Models compared in the first step of the forward-selection procedures

Model	Fixed Effects	Random Effects	AICc	Weight of Evidence	Relative Weight
1	Intercept	Intercept	2488.30	<0.001	1.58E+30
2	Duration	Intercept	2363.40	<0.001	1142.10
3	Val	Intercept	2482.90	<0.001	1.05E+29
4	Dx + Val	Intercept	2359.60	0.00	178.10
5	Dx + Val + (Dx × Val)	Intercept	2357.00	0.01	47.80
6	Val Rating	Intercept	2489.40	<0.001	2.68E+30
7	Dx + Val Rating	Intercept	2363.80	<0.001	1399.70
8	Dx + Val Rating + (Dx × Val Rating)	Intercept	2362.30	<0.001	674.90
9	Aro	Intercept	2490.20	<0.001	4.08E+30
10	Dx + Aro	Intercept	2364.90	<0.001	2478.40
11	Dx + Aro + (Dx × Aro)	Intercept	2366.80	<0.001	6515.10
12	Aro Rating	Intercept	2488.60	<0.001	1.80E+30
13	Dx + Aro Rating	Intercept	2363.50	<0.001	1239.90
14	Dx + Aro Rating +(Dx × Aro Rating)	Intercept	2365.40	<0.001	3214.10
15	Val + Aro	Intercept	2490.60	<0.001	4.80E+30
16	Dx + Val + Aro	Intercept	2365.60	<0.001	3594.70
17	Dx + Val + Aro + (Dx × Val)	Intercept	2361.00	0.00	343.10
18	Dx + Val + Aro + (Dx × Aro)	Intercept	2367.60	<0.001	9593.40
19	Val + Aro + (Val × Aro)	Intercept	2485.00	<0.001	2.93E+29
20	Dx + Val + Aro + (Val × Aro)	Intercept	2355.50	0.03	22.40
21	**Dx + Val + Aro + (Dx × Val) + (Val × Aro)**	**Intercept**	**2349.30**	**0.63**	**1.00**
22	Dx + Val + Aro + (Dx × Aro) + (Val × Aro)	Intercept	2357.50	0.01	60.20
23	Dx + Val + Aro + (Dx × Val) + (Dx × Aro)	Intercept	2362.80	<0.001	849.80
24	Dx + Val + Aro + (Dx × Val) + (Dx × Aro) + (Val × Aro)	Intercept	2351.20	0.24	2.60
25	Val Rating + Aro Rating	Intercept	2489.60	<0.001	2.90E+30
26	Dx + Val Rating + Aro Rating	Intercept	2363.80	<0.001	1405.30
27	Dx + Val Rating + Aro Rating + (Dx × Val Rating)	Intercept	2362.20	0.00	629.30
28	Dx + Val Rating + Aro Rating + (Dx × Aro Rating)	Intercept	2365.70	<0.001	3694.80
29	Val Rating + Aro Rating + (Val Rating × Aro Rating)	Intercept	2484.20	<0.001	1.96E+29
30	Dx + Val Rating + Aro Rating + (Val Rating × Aro Rating)	Intercept	2357.20	0.01	52.80
31	Dx + Val Rating + Aro Rating + (Dx × Val Rating) + (Val Rating × Aro Rating)	Intercept	2355.90	0.02	28.10
32	Dx + Val Rating + Aro Rating + (Dx × Val Rating) + (Val Rating × Aro Rating)	Intercept	2359.20	0.00	142.80
33	Dx + Val Rating + Aro Rating + (Dx × Val Rating) + (Dx × Aro Rating)	Intercept	2364.10	<0.001	1675.20
34	Dx + Val Rating + Aro Rating + (Dx × Val Rating) + (Dx × Aro Rating) + (Val Rating × Aro Rating)	Intercept	2355.70	0.03	25.00

Note: Dx=Duration, Val=Valence Category, Aro=Arousal Category, Val and Aro Rating=individual image ratings

Comparisons of model fit showed that the 21st model in the set performed the best, with a 63.31% chance of being the true model, compared to the other models. This model was 2.65 times more likely to be the true model than the next best fitting model (#24, which had an additional duration × arousal term), and 22.41 times more likely than the third best fitting model (#20, which removed the duration × valence term). Compared to the nil model of only intercept effects, model 21 was 1.58×10^{30} times more likely to be the true model. Model 21 included fixed effect predictors for duration, valence, arousal, duration × valence, and valence × arousal. This model was carried forward to step two, exploring the inclusion of additional random effects, where a total of eight models were compared (Table 1.4).

Table 1.4
Models compared in the second step of the forward-selection procedures

Model	Fixed Effects	Random Effects	AICc	Weight of Evidence	Relative Weight
1	Dx + Val + Aro + (Dx × Val) + (Val × Aro)	Intercept	2349.3	<0.001	2.17E+3
2	**Dx + Val + Aro + (Dx × Val) + (Val × Aro)**	**Intercept + Dx**	**2333.9**	**0.93205**	**1.00**
3	Dx + Val + Aro + (Dx × Val) + (Val × Aro)	Intercept + Val	2356	<0.001	6.38E+4
4	Dx + Val + Aro + (Dx × Val) + (Val × Aro)	Intercept + Aro	2353	<0.001	1.38E+4
5	Dx + Val + Aro + (Dx × Val) + (Val × Aro)	Intercept + Val + Aro	2363.5	<0.001	2.61E+6
6	Dx + Val + Aro + (Dx × Val) + (Val × Aro)	Intercept + Dx + Val	2343.9	0.00625	149.13
7	Dx + Val + Aro + (Dx × Val) + (Val × Aro)	Intercept + Dx + Aro	2339.4	0.06112	15.25
8	Dx + Val + Aro + (Dx × Val) + (Val × Aro)	Intercept + Dx + Val + Aro	2352.9	<0.001	1.34E+4

Note: Dx=Duration, Val=Valence Category, Aro=Arousal Category, Val and Aro Rating=individual image ratings

Model 2 was the best performing model in the second step comparison set. It had a 93.21% chance of being the true model, compared to the other models. This model was 15.25 times more likely to be the true model than the next best fitting model (#7), and 149.13 times more likely than the third best fitting model (#6). A random effects term for

trial duration was thus carried over to the next step, in which age, sex, and age × sex interaction terms were examined. A total of five models were compared (Table 1.5).

Table 1.5
Models compared in the third step of the forward-selection procedures

Model	Fixed Effects	Random Effects	AICc	Weight of Evidence	Relative Weight
1	Dx + Val + Aro + (Dx × Val) + (Val × Aro)	Intercept + Dx	2333.9	0.093	3.50
2	Dx + Val + Aro + (Dx × Val) + (Val × Aro) + Age	Intercept + Dx	2332.9	0.152	2.13
3	Dx + Val + Aro + (Dx × Val) + (Val × Aro) + Sex	Intercept + Dx	2333.2	0.133	2.44
4	Dx + Val + Aro + (Dx × Val) + (Val × Aro) + Age + Sex	Intercept + Dx	2331.6	0.296	1.09
5	Dx + Val + Aro + (Dx × Val) + (Val × Aro) + Age + Sex + (Age × Sex)	Intercept + Dx	2331.4	0.325	1.00

Note: Dx=Duration, Val=Valence Category, Aro=Arousal Category, Val and Aro Rating=individual image ratings

All models containing age and sex combinations accounted for at least some meaningful additional variance, compared to the task-parameter-only model from step two. Although model 5 offered the lowest AICc value in the set, the differences in fit indices between models 5 and 4 were miniscule. Their AICc value differences were extremely small, model 5 was only 1.09 times more likely to be the true model than model 4, and the two models were both more than 2 to 3.5 times more likely to be the true model than any other model in the comparison set. Consequently, the inclusion of an interaction between age and sex offered very little additional explanatory value, and the more parsimonious model, number 4, was favored.

Thus, the final model for predicting trial wins versus losses included a complex combination of fixed intercept and slope effects and random intercept effects. The model written out in full mathematical notation is as follows:

$$\log\left[\frac{P\left(WinLoss_{ij}=1\right)}{1-P\left(WinLoss_{ij}=1\right)}\right]=\left(\beta_0+b_{0i}\right)+\left(\beta_1+b_{1i}\right)Duration_{ij}+\beta_2 Valence+\beta_3 Arosual+\beta_4 Age_i+\beta_5 Sex_i$$
$$+\beta_6\left(Duration_{ij}\right)\left(Valence_{ij}\right)+\beta_7\left(Valence_{ij}\right)\left(Arousal_{ij}\right)$$

On the first row are the main (intercept) effects. For the fixed effects of task-specific predictors, β_0 is the intercept, β_1 is the effect of effect of trial duration, β_2 is the effect of image valence, and β_3 is the effect of image arousal. For fixed effects of subject-specific predictors, β_4 is the effect of participant age and β_5 is the effect of participant sex. Random effects included in the model are b_{0i}, an intercept term (i.e., the degree to which each individual differs from the mean effect in "raw" ability to perform the task), and b_{1i}, a similarly interpreted individual effect for trial duration. The second row represents the two-way interactions (slope effects) between trial duration × image valence (β_6) and valence × arousal (β_7).

Table 1.6 provides the estimates for the fixed effects along with their standard errors and associated *z*-scores (which provide a guide for interpreting the relative strength of each predictor in the best-fitting model, but in this fit index framework are not associated with significance testing or *p*-values).

Table 1.6
Logistic LMER fixed effect parameter estimates for the final model

Fixed Effect Term	Estimate	Std. Err.	*z*-score
Intercept	0.99	0.47	2.08
Duration	-1.35	0.18	-7.69
Valence	0.46	0.14	3.35
Arousal	-0.09	0.11	-0.83
Age	0.05	0.02	2.18
Sex	0.35	0.17	2.03
Duration × Valence	-0.4	0.14	-2.89
Valence × Arousal	-0.49	0.13	-3.73

Since trial duration and image valence had such large effects upon performance, the same forward model selection procedures were run independently for long and short trials and again after separating out valenced and neutral image trials. In the interest of space, tables of model comparison sets for each of these spilt data sets are not provided here, but the best performing models across the different data splits are presented in Table 1.7.

Table 1.7
Best-fitting models when splitting the data by short/long and valenced/neutral trials

Trials Analyzed	Fixed Effects	Random Effects
All	Dx + Val + Aro + (Dx×Val) + (Val×Aro) + Age + Sex	Intercept + Dx
	Dx + Val + Aro + (Dx×Val) + (Val×Aro) + Age + Sex + (Age×Sex) **	Intercept + Dx
Long	Val + Aro + (Val×Aro) + Age	Intercept
Short	Val Rating + Aro Rating + (Val Rating×Aro Rating) + Sex	Intercept
Valenced	Dx + Val + Aro + (Dx×Val) + (Val×Aro) + Age + Sex	Intercept + Dx
Long Valenced	Val + Aro + (Val×Aro)	Intercept
	Val + Aro + (Val×Aro) + Age**	Intercept
Short Valenced	Val Rating + Aro Rating + (Val Rating×Aro Rating) + Sex	Intercept
Neutral	Dx + Age	Intercept + Dx
Long Neutral	Age	Intercept
Short Neutral	Intercept	Intercept

****Models that provide nominally better fit, but with minute AICc differences the more parsimonious models are favored.**
Note: Dx=Duration, Val=Valence Category, Aro=Arousal Category, Val and Aro Rating=individual image ratings

Discussion

Image Ratings

The images used in this study replicated the characteristics of separable valence and arousal dimensionality as seen in the IAPS, and the images were broadly stable in their categorizations of high/low arousal and positive/negative/neutral valence across two independent samples. Importantly, the valence and arousal categories were not confounded, which allowed for greater confidence in the estimation of each dimension's effects, both in the behavioral analyses and within the later fMRI analyses. Additionally, there were no effects of age upon participants' mean ratings of valence and arousal, though there were ratings differences between males and females, with males showing relatively truncated ratings ranges compared to females (i.e., females rated positive images as more positively, negative images more negatively, and all images overall as more arousing than males did).

LMER-Based Model Selection

On the whole, the model selection procedures verified that the interval timing task was well constructed and largely performed as designed. Short and long trials showed an overall performance difference. Manipulations of image valence and arousal also affected performance, though arousal effects only appeared when in interaction with valence. Furthermore, inter-individual differences of age and sex had influences upon performance above and beyond the task parameters, but differentially so across levels of duration and valence.

In the best-fitting model for the full data set, all predictors but arousal had strong influences upon task performance, which is aligned with the exploratory plotting that indicated no particular differences in win ratios for high and low arousal images. The signs of the parameter estimates in Table 1.6 indicate that longer trial durations[4], more positive image valences, increasing age, and being male all improved task performances. The duration × valence interaction broke down to show that, compared to negative images, positive images produced more wins on long trials but fewer wins on short trials. The valence × arousal interaction was such that negative image trial performances were improved by higher arousal values, whereas positive image trials had better performances if they were minimally arousing.

For all explorations of the split-up data sets, only those containing both short and long trial durations had best-fitting models that included random effects (for duration) above and beyond individual random intercepts. For all long trials, the best fitting model included intercept effects for valence, arousal, and age along with a slope effect for valence × arousal. The best fitting models for short trials took a decidedly different route. Instead of mean image categories, terms for the individuals' ratings of arousal and valence performed best, and sex was the best-performing demographic factor. Task-related parameters included in the best-fitting models did not change when looking at just the trials with positive and negative (i.e., valenced) images, though age no longer provided significant predictive benefit when looking at just the long valenced trials.

[4] The sign for duration's parameter estimate is negative due to alphabetical recoding of factors within the LMER algorithms. A negative sign indicates that as trials move from long to short, the log-likelihood of having a winning trial decreases. Similarly, the positive sign for the parameter estimate of sex indicates that recoded values shifting from female to male are related to increases in performance.

Neutral trial models necessarily could not include categorical valence and arousal terms, as all images were neutral and low arousal. There were no benefits to adding individual ratings of valence and arousal, but the best fitting model did retain duration and age terms. Breaking the neutral data into long and short trials showed that age was related to long trial performances, whereas the best-fitting model for short neutral trials contained only intercept terms. Participant sex did not meaningfully impact neutral trial performances.

Neutral long trial performances were only affected by age, with being older associated with greater likelihoods of winning. The best determinants of neutral short trial outcomes were only the differences in innate ability to perform the task that each participant brought to the testing session (i.e., intercept effects). An interesting difference between short and long valenced trials was that short trial performances were swayed more strongly by individual responses to image content than long trials were, though still in the same direction of the valence, arousal, and valence × arousal effects noted above. Generally, males performed better than females, and task performances improved as participant age increased. The interaction of sex and age indicated by exploratory plotting nominally, but not meaningfully, improved model fit when predicting trial wins and losses across all trial types. Age was a meaningful factor in determining long trial performances, whereas sex was a meaningful factor only for short trial performances.

Limitations

These analyses used trial-by-trial win/loss outcomes as the dependent variable. It would also be reasonable to investigate the behavioral data from the standpoint of the

proportions of target intervals reproduced, or split into binary outcomes of overproduction and underproduction. However, as discussed above, the win/loss variable was chosen for these analyses because it reflects the main performance goal given to the study participants.

Though the image categorizations remained broadly stable from task design to implementation in the current study, the shifting of images almost all came from one category: positive, low arousal. The valence × arousal interaction effects upon performance were driven by the comparison of negative/high trials, of which there were 12 in the task, to positive/low images, of which there were only 8 in the task. Having 25% fewer measurements may have made estimates of mean positive/low trial performances less reliable, and may make the interaction effect less stable. However, differential behavioral effects of valence × arousal in the absence of main effects have been seen in previous timing studies, indicating that this finding is less likely to be one of statistical spuriousness (Angrilli, Cherubini, Pavese, & Manfredini, 1997).

The lack of main effects upon trial outcome for arousal levels may be due to the truncated range of images that could be appropriately shown to a developmental sample. This was a necessary and unavoidable cost of conducting research with a sensitive population. Presumably, the most gruesome mutilations or sexually explicit images contained in a set such as the IAPS would impact performance more deeply than the strongest negative and positive images used in this set (a shark swimming next to a child and a gymnast leaping through the air, see Figure 1.1), though such a presumption would certainly need to be formally tested before discarding the findings of the current study.

Summary

Through pitting multiple models against each other and assessing their relative value at explaining task performance, these analyses have demonstrated that the task performed largely as intended, with few expected variables failing to impact performance and few "surprise" variables coming to the forefront. Differential effects were seen for valence and duration, with interactions for valence × arousal and valence × duration. Arousal was not a very strong determinant of wins and losses independent of valence, which went against predictions. Neutral trials appeared to be a true baseline measure of ability to perform the task, particularly within shorter duration trials. Sex only played a meaningful role in short trials, while age had an impact only for long trials.

If a direct correspondence of task performance to brain activity could be expected, then the behavioral analyses provided a clear set of expectations for the fMRI analyses. Activation differences between the short and long trials would be anticipated, as would effects of valence. Arousal effects could be less impactful when collapsed across valence levels, but interactions effects of valence by arousal would be anticipated. Sex effects within short trials and age effects within long trials would also be predicted. However, such direct brain–behavior relationships are not an established fact. It is possible that a lack of performance differences, such as that seen between overall arousal categories, could be the product of markedly different neural activation patterns. Thus, the final behavioral models cannot be ported directly into the fMRI analyses, and each of the main parameters (valence, arousal, valence × arousal, age, sex, duration) must still be investigated anew. Additionally, the behavioral analyses cannot predict at what point

during a trial such performance-related effects might be expressed within the BOLD signal. Alterations in performances may be related to neural activity differences during either the image viewing or interval reproduction portions of the task, so both phases must be investigated. Although it is possible that performance differences could also be due to feedback effects (i.e., differences brought about by differential effects from image type, age, or sex upon participants' abilities to use trial-by-trial feedback to modulate their subsequent performances), the fMRI analyses described in Chapter 2 only investigated feedback activations for grand mean and duration difference effects, not for specific effects of image type, age, or sex.

Chapter 2. Comprehensive fMRI Analyses of the Interval Timing Task

Introduction

The fMRI analyses presented in this chapter were geared towards understanding the overall neural correlates of performing the interval timing task across the three phases of each trial (image viewing, interval reproduction, and feedback), as well as investigating the specific effects upon BOLD responses, during viewing and reproduction periods, brought about by the interval timing task parameters and from inter-individual differences of age and sex.

Hypotheses

As noted previously, interval timing processes are believed to be carried out in a widely distributed network of subcortical and cortical regions. Significant task-related activations were anticipated in caudate, putamen, pallidum, hippocampus, anterior insula, and thalamus, posterior parietal cortex, supramarginal gyrus, central and frontal opercula, SMA, DLPFC, and IFG (Buhusi & Meck, 2005; Craig, 2009b; Matell & Meck, 2000; Meck, 2005). Differences in BOLD responses based on valence were expected to be greater within the ventral striatum and VMPFC for positive images, and greater within amygdala and insula for negative images (Ernst et al., 2009; Richards et al., 2013). Arousal effects were also expected to be seen within the amygdala and insula, given their roles in translating physiological sensations into emotional experiences (Craig, 2009a; Stein & Paulus, 2008).

Given that the task was novel, no specific sex differences in BOLD responses were anticipated.

Predictions of discrete neural localizations for linear effects of age upon BOLD signal were not made for this novel task. However, developmental models of a "maturational disconnect" between NAcc, amygdala, and PFC would predict that, within valenced image trials (which provide emotional distractors), nonlinear age effects would be seen, such that NAcc and amygdala would show exaggerated responses (i.e., "inverted-U" shape effects when plotted against age) compared to younger and older participants, whereas PFC responses would show a linear developmental trend (Casey et al., 2010; Ernst et al., 2009). Additionally, given the postulated central roles for the insula in both timing (Craig, 2009b) and emotional experience (Craig, 2009a; Stein & Paulus, 2008), the insula was also chosen for targeted nonlinear age effect investigations.

Methods

Participants

All participant information was the same for the fMRI analyses as it was for the behavioral analyses described in the Methods section of Chapter 1.

Task Parameters and Trial Layout

Each trial consisted of the following components: a trial start cue (500 ms), image presentation (1000–6000 ms), jittered interstimulus delay (1000–1500 ms), a reproduction start cue (500–1000 ms), self-paced timing reproduction (10000 ms maximum), performance feedback (1250 ms), and a variable length intertrial interval that was calculated on a trial-by-trial basis to allow for BOLD signal restabilization and to

resync the next trial onset to a predetermined upcoming TR onset (see Figure 1.2). Total trial length varied between 10 and 22 s. The fMRI scanning session consisted of 4 scans with 18 trials each, for a total of 72 trials. During task design, the ordering of trials was optimized such that no combination of short/long and positive/negative/neutral image type was related to the presentation order of the other combinations (Dale, 1999). This pseudo-randomization of trial order was determined ahead of time, and it was fixed for all participants. That is to say, all participants received the same order of trials, but those trials were placed in a fixed sequence established by optimized pseudo-random assignment to ensure that participants would be unable to determine from the previous trials which type of trial would be next.

MRI Acquisition

All images were collected at the University of Minnesota's Center for Magnetic Resonance Research, on a Siemens 3T Magnetom scanner (Erlangen, Germany) using a 12-channel head coil. The task was presented with E-Prime software (Psychology Software Tools, Inc, Pittsburgh, PA). Stimuli were projected onto a screen at the rear of the scanner bore, and participants viewed the screen with a rear-facing mirror mounted on the head coil. Participants' reproduction responses were made with right-hand button presses collected via a fiber-optic response box. During each scan, participants' respiration rates were monitored with a pneumatic compression belt, and their heart rates were monitored (via changes in blood oxygen saturation levels) with an infrared pulse oximeter clipped to the index finger of the left hand.

The fMRI scan parameters were as follows: echo planar imaging sequence with distortion correction, TR=2000 ms, TE=30 ms, 34 slices, slice thickness=4 mm, matrix size=64 × 64, FOV=220 mm × 220 mm, volumes=148, acquisition time=4 m 56 s. Prior to the first block of the task, a gradient echo fieldmap was acquired: TR=300 ms, TE1=1.94 ms, TE2=4.4 ms, voxel parameters identical to fMRI, acquisition time=41 s. T1-weighted structural scans were also acquired during the scanning session to aid in registration of functional images to standard atlas space: 3D turbo flash sequence, TR=2530 ms, TE=3.65 ms, TI=1100 ms, flip angle=7°, 240 slices, slice thickness=1 mm, FOV=256 mm × 256 mm, acquisition time=10 m 49 s.

Image Preprocessing

All functional image analyses were carried out with FSL (www.fmrib.ox.ac.uk/fsl). Preprocessing of the data included MCFLIRT motion correction (Jenkinson et al., 2002), registration of each subjects' functional to structural images with FLIRT (Jenkinson & Smith, 2001; Jenkinson, Bannister, Brady, & Smith, 2002), nonlinear registration of functional maps to MNI-152 standard space (2 mm^3) via FNIRT (Andersson, Jenkinson, & Smith, 2010), fieldmap-based EPI unwarping using PRELUDE and FUGUE (Jenkinson, 2003, 2004), interleaved slice-timing correction using Fourier-space time-series phase-shifting, non-brain removal using BET (Smith, 2002); spatial smoothing using a Gaussian kernel of FWHM 7 mm, grand-mean intensity normalization, and highpass temporal filtering with sigma=25.0 s.

Participants' data were excluded on a block-by-block-basis if head motion exceeded 2 mm in any direction or 2° of rotational movement. Additional, finer-grained

motion contamination investigations were carried out for remaining participants and blocks with FSL's *fsl_motion_outliers* program, using the framewise displacement calculations described by Power et al. (2012) to identify individual volumes within each scan that were most likely to be contaminated by motion effects.

Additional pre-processing of the respiration belt and pulse oximeter data, to derive regressors that served to remove the confounding effects of heart rate and respiration within the fMRI data, were carried out with the Physiological Log Extraction for Modeling (PhLEM) Toolbox in MATLAB (Verstynen & Deshpande, 2011) for all included participants and scans.

Data Analysis

Grand Mean, Valence, and Arousal Analyses. For the main imaging analyses, parallel analysis streams were run for the short trials and the long trials, with results to be combined and contrasted at later levels. Single-subject, single-block scans were analyzed by fitting a GLM with 15 regressors of interest defining the viewing, reproduction, and feedback periods for low arousal/positive valence, high arousal/positive valence, low arousal/negative valence, high arousal/negative valence, and neutral valence images. Several regressors of non-interest were also included: three defining the global mean signal and the mean signals within white matter and CSF, three PhLEM-derived regressors for pulse and respiration data, and a varying number of regressors identifying volumes to be withheld from the analyses 1) because of excessive motion contamination, 2) because it was a trial that was not responded to, or 3) because of erroneous loss feedback on 1000 ms trials. An additional, single regressor defining all trial events for the

other duration set (i.e., in the long trial stream, it defined all short trial events) was included to ensure that baseline/noise comparator calculations in each stream did not include any task-related variance from the other duration's trials (i.e., baseline signal changes were only ever derived from ISIs and ITIs). Single-subject, fixed effects means for the long and short trial regressors were calculated at the second level of analysis, and these means were then combined and contrasted across durations in single-subject, fixed effects calculations.

The final level of analysis combined fixed effects subject means to produce mixed effects group means. Planned group-level analyses included 1) grand mean effects plus long versus short duration comparisons for each task period (i.e., viewing, reproduction, and feedback) irrespective of image type, 2) image valence main effects just within viewing and reproduction periods, comparing combined positive and negative trials to neutral trials (paralleling the behavioral analyses), comparing positive to negative trials to neutral trials separately, and comparing positive and negative trials to each other, 3) main effects of high versus low arousal images just within the viewing and reproduction periods, and 4) valence × arousal interaction effects, comparing high and low arousal effects within positive and negative trials as well as comparing positive and negative effects within high and low trials.

Task Performance, Sex, and Age Analyses. Group-level investigations of the correlates of tsk performance (win ratios), age, and sex upon viewing and reproduction activations were carried out separately from the analyses above. Participants' mean win ratios were explored for linear correlations with BOLD signal, age was investigated for

linear and quadratic correlations, and sex differences were explored through *t*-test comparisons. Based on the behavioral findings that indicated distinct performance, age, and sex effects across durations, long and short trials were examined separately. For sex comparisons, *t*-tests comparing males' and females' BOLD responses were run with equal variances assumed across groups. For age and win ratios, continuous covariates were added to the appropriate group mean valence and arousal analysis models, with the covariate effects forced to be orthogonal to the grand means. For the win ratio analyses, the behavioral data were separated in the same manner that the imaging data were separated. That is to say, the covariate values were changed for each image type analysis to reflect performances within the trials under examination, e.g., participants' mean win ratios on positive, high arousal trial performances were correlated to signal changes in positive, high arousal viewing and reproduction periods. Specific region of interest (ROI) investigations of quadratic terms for age were carried out to test nonlinear age effects predicted by developmental models of subcortical processing. Nonlinear age effects for control-related PFC regions are not predicted by leading models (cf. Richards et al., 2013), and were not investigated. Negative quadratic curves (i.e., "inverted-U shaped") were examined in NAcc, amygdala, and insula, testing if adolescents showed stronger activations compared to younger and older participants. Two tiers of analyses were carried out: 1) deriving the sex/age effects within viewing and reproduction, regardless of trial type and then 2) estimating the effects for each image type (positive, negative, neutral, high arousal, and low arousal) separately.

Statistical Considerations. For all imaging analyses, statistical significance testing was carried out with cluster-wise thresholding, via FSL's built-in thresholding algorithm. Clusters of at least 26 contiguous voxels with minimum z values of 2.3 were considered, and only clusters with a family-wise-error-corrected $p<0.05$ probability of appearing were retained (Worsley, 2001). All images were masked by the MNI-152 brain mask included with FSL's standard atlas sets prior to thresholding, to ensure that non-brain voxels were not included in the final activation maps.

In contrasts of task conditions and in t-tests between sexes, results are only reported within regions where at least one of the conditions or groups showed, on average, positive (i.e., mean $z>0$) BOLD responses. Thus, statistical maps were masked prior to cluster-wise thresholding to include only voxels for which the "greater than" comparator had non-negative signal changes (e.g., the positive > negative viewing contrast only tested voxels where the mean positive viewing map had values of $z>0$, and the negative > positive viewing contrast only tested voxels where the negative viewing map had values of $z>0$). That is to say, contrast results were not considered meaningful if they were driven by both conditions or groups showing negative signal changes, and such comparisons were masked out.

Anatomical localization labels were derived from the Harvard-Oxford cortical, Harvard-Oxford subcortical, and FNIRT-registered cerebellar probabilistic atlases included with FSL (http://www.fmrib.ox.ac.uk/fsl/data/atlas-descriptions.html)[5]. For the

[5] VMPFC is equivalent to the Harvard-Oxford atlas label "Frontal Medial Cortex," VLPFC is the equivalent of "Frontal Orbital Cortex," and DLPFC was defined by the label "Middle Frontal Gyrus."

ROI analyses, all ROIs were derived from the Harvard-Oxford atlas sets and restricted to voxels that had at least a 50% chance of being a part of the anatomical target.

Results

Motion Contamination

One subject had grossly excessive motion for all four scans and was excluded from all analyses. Two other participants had excessive motion during the fourth block of the task. For these two participants, their data for the remaining three blocks were included in the analyses. Gross motion disturbances thus reduced the available data by 4.68%. For all remaining data, the framewise displacement analyses identified an average of 7.44 volumes (range=2–21 volumes) to be excluded for each scan, for an additional 4.98% data loss due to more subtle motion contamination. The average percent of framewise-displacement-based data loss was not significantly correlated with age (r=-0.13, p=0.47), nor did it differ significantly by sex ($t(29)$=1.63, p=0.11).

The imaging analyses produced widespread maps of task-related activations. In the interest of reducing repetition and enhancing readability, note that all activations listed below are bilateral and broadly symmetrical unless described otherwise. Also note that all figures are presented in radiological orientation, with the left hemisphere on the right side of the image and right hemisphere on the left side of the image.

Main Effects of Viewing, Reproduction, and Feedback Periods

Image Viewing Main Effects. Across all image types, the viewing period produced significant activations across the entirety of occipital cortex and within temporal-occipital fusiform gyrus, hippocampus, amygdala, temporal pole, thalamus, right pallidum, right

dorsal putamen, right anterior insula, precentral and postcentral gyri, SMA, right IFG, and left VLPFC. Comparing the long and short viewing periods showed no stronger effects for long trials, but did show significantly stronger effects for short viewing within the occipital lobe, temporal-occipital fusiform, and thalamus. Figure 2.1 presents both the viewing grand mean and duration comparison maps.

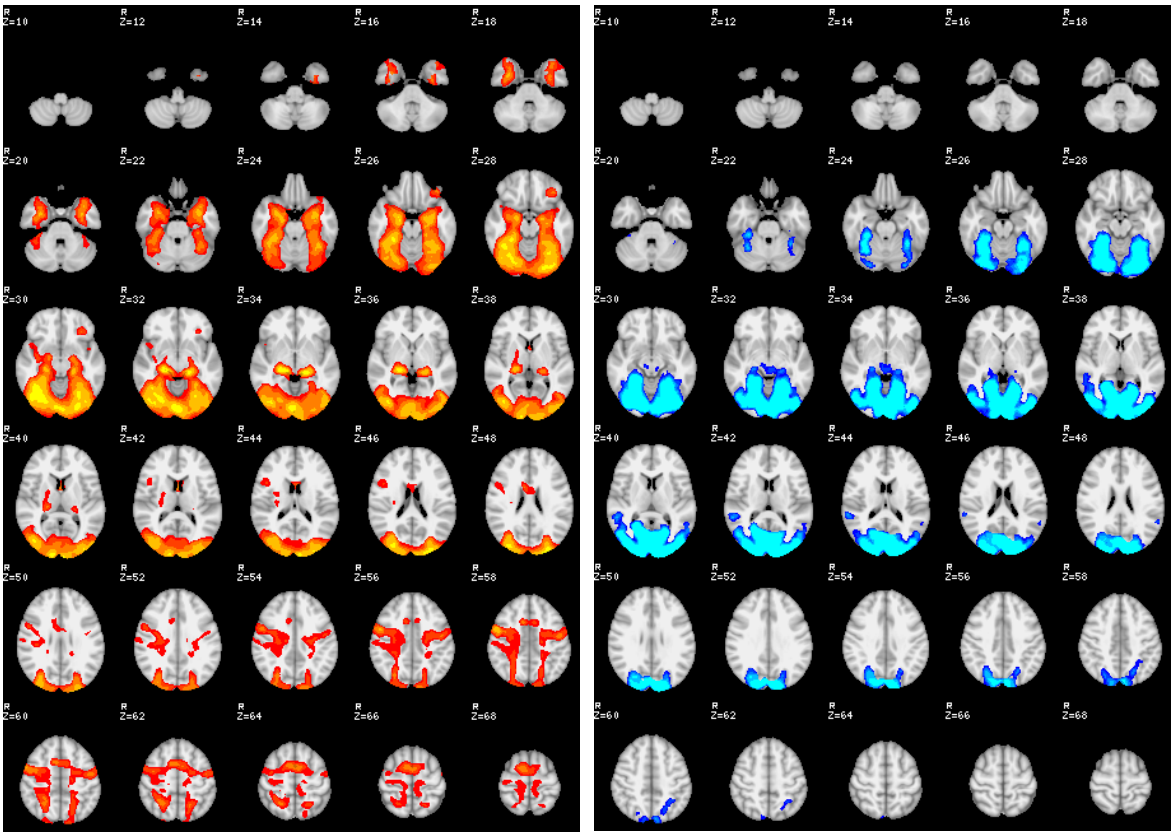

Figure 2.1: Significant Activations During Image Viewing. (A) Grand mean activations across all trials. (B) Significant differences between the long and short trials. Blue-cyan denotes stronger activations for short trials. No areas had stronger activations for the long trials. All images cluster-wise thresholded at values of $z<2.3$, $p<0.05$.

Interval Reproduction Main Effects. Across all image types, the interval reproduction period (the time from the onset of the stopwatch image to the participant's button press to end the reproduction interval) had significant activations in occipital pole,

occipital fusiform, cerebellum (crus I, crus II, area VIIa, and area VIIb), right supramarginal gyrus, left postcentral and precentral gyri, superior temporal gyrus, parietal operculum, frontal operculum, thalamus, SMA, paracingulate, ACC, pallidum, putamen, caudate, NAcc, anterior insula, and IFG. Comparing across short and long reproductions, long trials had no areas of greater relative signal change, but short trials showed stronger activations in occipital pole, SMA, central opercula, IFG, anterior insula, and the basal ganglia. The short trial reproductions also showed stronger relative activations within intracalcarine cortex, superior lateral occipital cortex, and right postcentral and precentral gyri. Figure 2.2 presents both the reproduction grand mean and duration comparison maps.

Performance Feedback Main Effects. Across all trials, feedback periods showed significant activations across the entirety of the occipital lobe, cerebellum (crus I, vermis, and area VI), right supramarginal gyrus, angular gyrus, posterior middle temporal gyrus, and posterior hippocampus. Comparisons of the short and long trial durations yielded significant differences in activation patterns to feedback. Long trials showed stronger activations within all medial occipital lobe structures, left inferior lateral occipital cortex, superior parietal lobule, right postcentral and precentral gyri, right supramarginal gyrus, right central operculum, and right IFG. Short trials produced greater positive signal changes in the superior aspects of the cerebellar regions listed above along with neighboring inferior occipital pole and fusiform, ACC, paracingulate, thalamus, caudate, NAcc, frontal operculum, anterior insula, VLPFC, and left temporal pole. Figure 2.3 presents both the feedback grand mean and duration comparison maps.

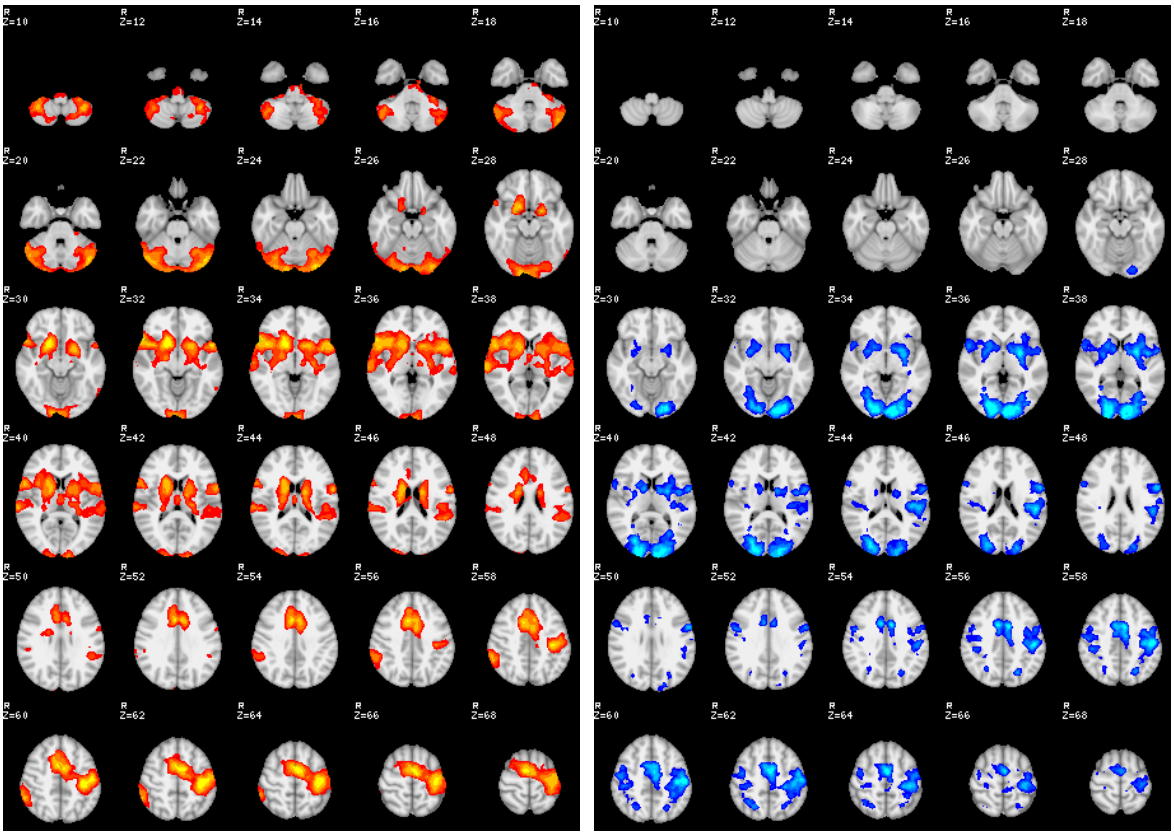

Figure 2.2: Significant Activations During Interval Reproductions. (A) Grand mean activations across all trials. (B) Significant differences between the long and short trials. Blue-cyan denotes stronger activations for short trials. No areas had stronger activations for the long trials. All images cluster-wise thresholded at values of $z<2.3$, $p<0.05$.

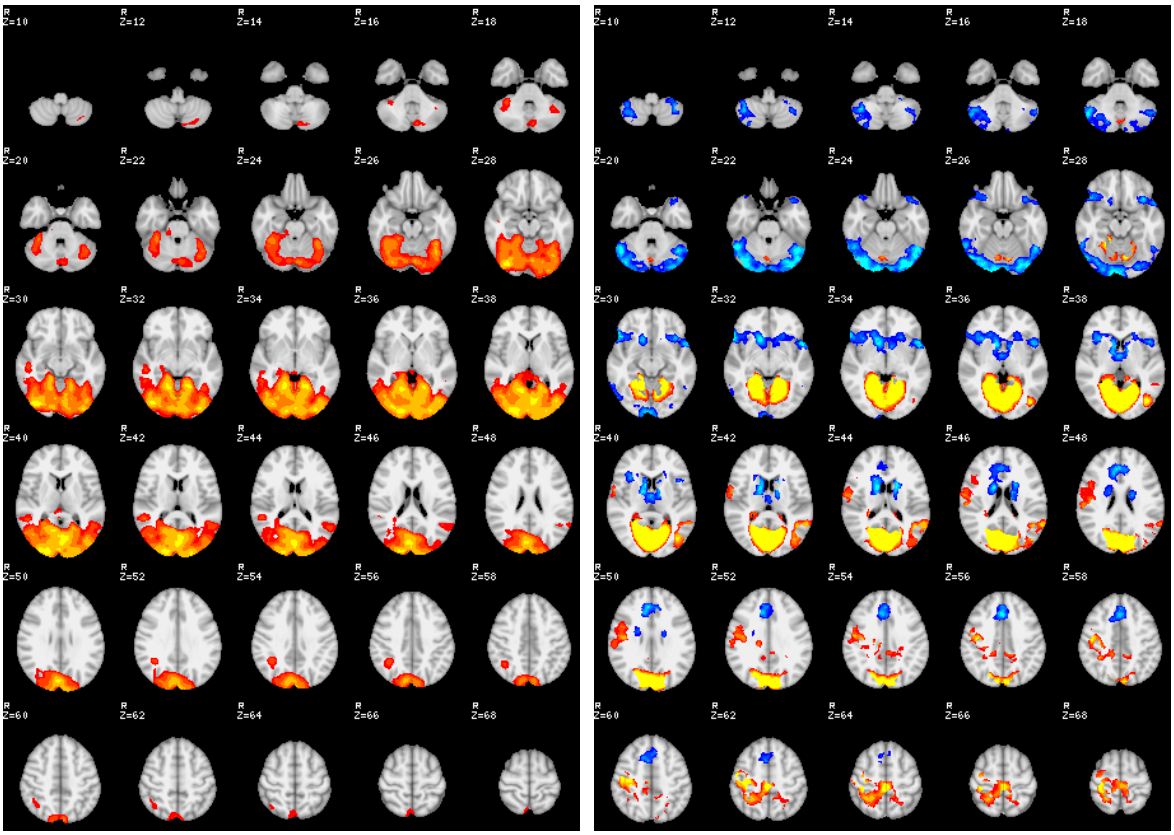

Figure 2.3: Significant Activations During Performance Feedback. (A) Grand mean activations across all trials. (B) Significant differences between the long and short trials. Red-yellow denotes stronger activations for long trials. Blue-cyan denotes stronger activations for short trials. All images cluster-wise thresholded at values of $z<2.3$, $p<0.05$.

Valence Effects

Valenced Versus Neutral Image Viewing. Comparisons of neutral images versus valenced (i.e., both positive and negative) images showed that valenced image viewing led to stronger activations in occipital pole, inferior lateral occipital cortex, temporal-occipital fusiform, superior parietal lobule, supramarginal gyrus, postcentral gyrus, periaqueductal grey matter in the brainstem, thalamus, hippocampus, amygdala, posterior insula, medial frontal pole, VLPFC, and VMPFC. Neutral image viewing showed stronger activations in the medial occipital structures of intracalcarine cortex, cuneous,

and lingual gyrus, within SMA medial precentral gyrus, lateral precentral gyrus, and in left cerebellum (crus I and area VI).

Valenced Versus Neutral Trial Reproductions. Reproduction period differences between the valenced and neutral image types were less pronounced. Valenced trial reproductions showed greater activations only in the right cerebellum (crus I and II), and neutral trials only showed greater activations in occipital pole. Figure 2.4 presents the valenced versus neutral activation contrast maps for both viewing and reproduction periods.

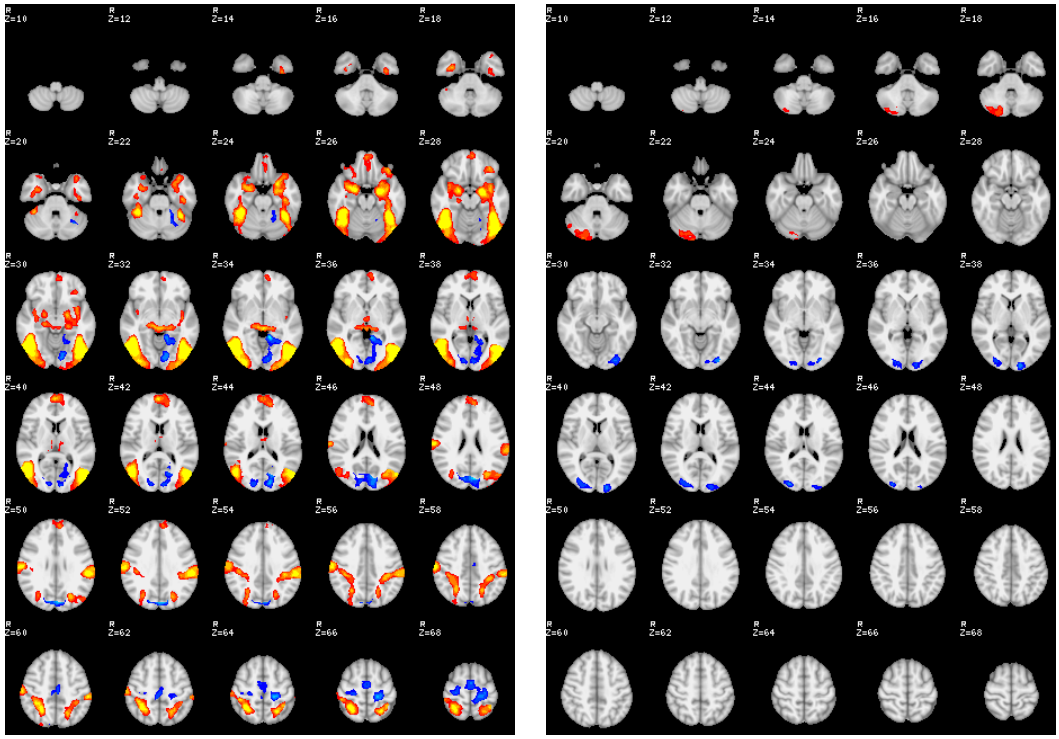

A – Valenced vs. Neutral Image Viewing **B – Valenced vs. Neutral Interval Reproduction**

Figure 2.4: Overall Valence Effects Upon Image Viewing and Interval Reproduction Activations. (A) Significant differences during image viewing. (B) Significant differences during interval reproductions. Comparisons were made between activations for all valenced (positive and negative) versus all neutral trials. Red-yellow denotes stronger activations for valenced trials. Blue-cyan denotes stronger activations for neutral trials. All images cluster-wise thresholded at values of $z<2.3$, $p<0.05$.

Positive Versus Neutral Image Viewing. Comparisons of positive images versus neutral images showed that positive image viewing led to stronger activations in inferior lateral occipital cortex, inferior temporal gyrus, temporal-occipital fusiform, paracingulate, and medial frontal pole. Neutral image viewing showed stronger activations in the medial occipital structures of intracalcarine cortex, cuneous, and lingual gyrus, and within cerebellum (areas V & VI).

Positive Versus Neutral Trial Reproductions. Reproduction period differences between the positive and neutral image types were also seen. Positive trial reproductions showed greater activations only in the left posterior superior temporal gyrus, left parietal operculum, and left Heschl's gyrus. Neutral trial reproductions only showed greater activations in occipital pole, inferior lateral occipital cortex, and occipital fusiform. Figure 2.5 presents the positive versus neutral activation contrast maps for both viewing and reproduction periods.

Negative Versus Neutral Image Viewing. The comparisons of negative versus neutral image viewing revealed widespread activation differences. Negative image viewing produced stronger activations in the cerebellum (crus II and area VI), inferior and superior lateral occipital cortex, temporal-occipital fusiform, superior parietal lobule, right supramarginal gyrus, postcentral gyrus, periaqueductal grey matter in the brainstem, thalamus, parahippocampal gyrus, hippocampus, amygdala, temporal pole, posterior insula, and VLPFC. As with the comparison above to positive image viewing, neutral images showed stronger activations in this contrast within the medial occipital structures of intracalcarine cortex, cuneous, and lingual gyrus.

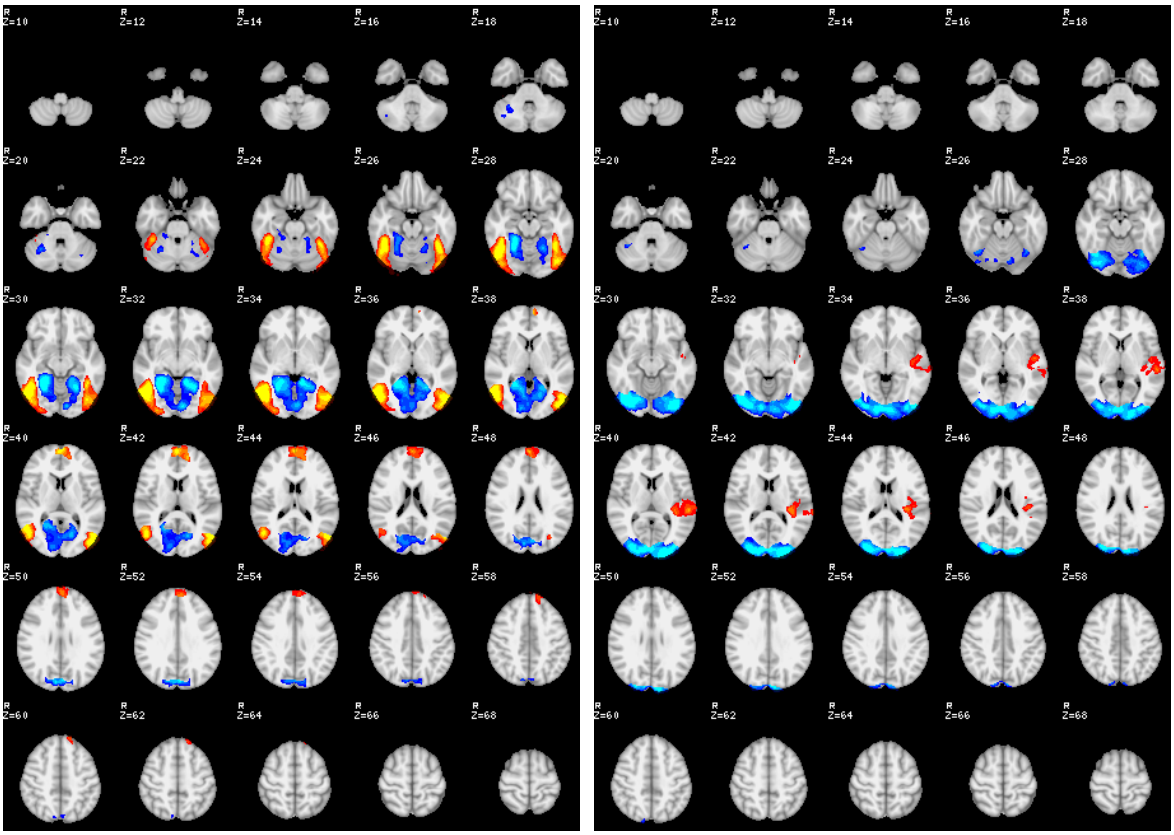

Figure 2.5: Positive Valence Effects Upon Image Viewing and Interval Reproduction Activations. (A) Significant differences during image viewing. (B) Significant differences during interval reproductions. Comparisons were made between activations for all positive versus all neutral trials. Red-yellow denotes stronger activations for positive trials. Blue-cyan denotes stronger activations for neutral trials. All images cluster-wise thresholded at values of $z<2.3$, $p<0.05$.

Negative Versus Neutral Image Reproductions. The contrast of negative versus neutral reproductions produced far less widespread differences than did the image viewing contrast. Negative trial reproductions only showed greater activations within the dorsal-most aspects of precentral gyrus, postcentral gyrus, and SMA. Neutral trial reproductions produced greater activations in inferior lateral occipital cortex and

cerebellum (area VI). Figure 2.6 presents the negative versus neutral activation contrast maps for both viewing and reproduction periods.

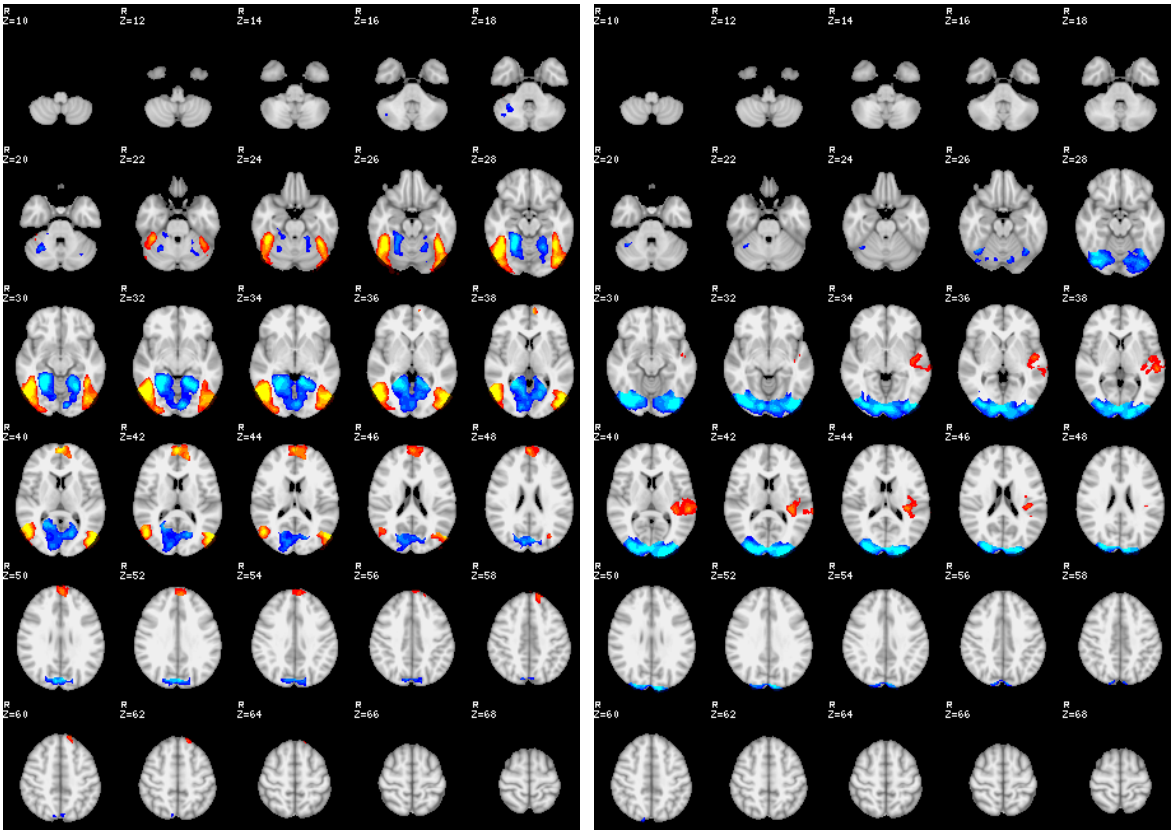

A – Negative vs. Neutral Image Viewing

B – Negative vs. Neutral Interval Reproduction

Figure 2.6: Negative Valence Effects Upon Image Viewing and Interval Reproduction Activations. (A) Significant differences during image viewing. (B) Significant differences during interval reproductions. Comparisons were made between activations for all negative versus all neutral trials. Red-yellow denotes stronger activations for negative trials. Blue-cyan denotes stronger activations for neutral trials. All images cluster-wise thresholded at values of $z<2.3$, $p<0.05$.

Positive Versus Negative Image Viewing. Compared to negative images, positive image viewing produced greater signal changes in rostral caudate, VMPFC, subgenual ACC, paracingulate, and medial frontal pole. Negative image viewing produced greater

activations within occipital pole, temporal-occipital fusiform, left supramarginal gyrus, periaqueductal grey matter, thalamus, caudal putamen, posterior insula, left PCC, parahippocampal gyrus, left hippocampus, amygdala, and left temporal pole.

Positive Versus Negative Trial Reproductions. For the positive versus negative reproduction comparison, only negative trial reproductions showed greater activations, in a cluster across the tip of occipital pole. Figure 2.7 presents the positive versus negative activation contrast maps for both viewing and reproduction periods.

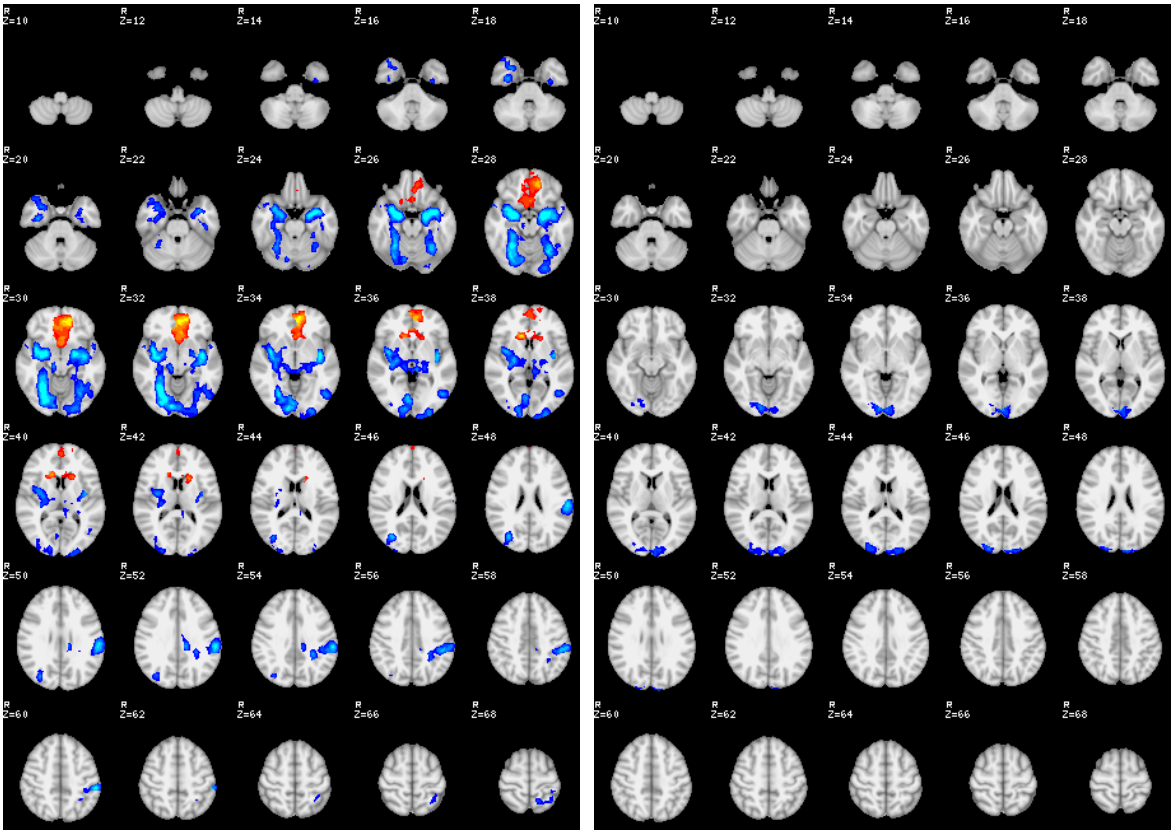

A – Positive vs. Negative Image Viewing **B – Positive vs. Negative Interval Reproduction**

Figure 2.7: Positive Versus Negative Valence Effects Upon Image Viewing and Interval Reproduction Activations. (A) Significant differences during image viewing. (B) Significant differences during interval reproductions. Comparisons were made between activations for all positive versus all negative trials. Red-yellow denotes stronger activations for positive trials. Blue-cyan denotes stronger activations for negative trials. All images cluster-wise thresholded at values of $z<2.3$, $p<0.05$.

Arousal Effects

High Versus Low Arousal Image Viewing. The comparison of high arousal to low arousal image viewing (Figure 2.8) showed that high arousal images produced greater activations in superior lateral occipital cortex, temporal-occipital fusiform, right supramarginal gyrus, right IFG, amygdala, insula, and temporal pole. Low arousal images produced greater activations in occipital pole, cuneous, lingual gyrus, and calcarine/intracalcarine cortex.

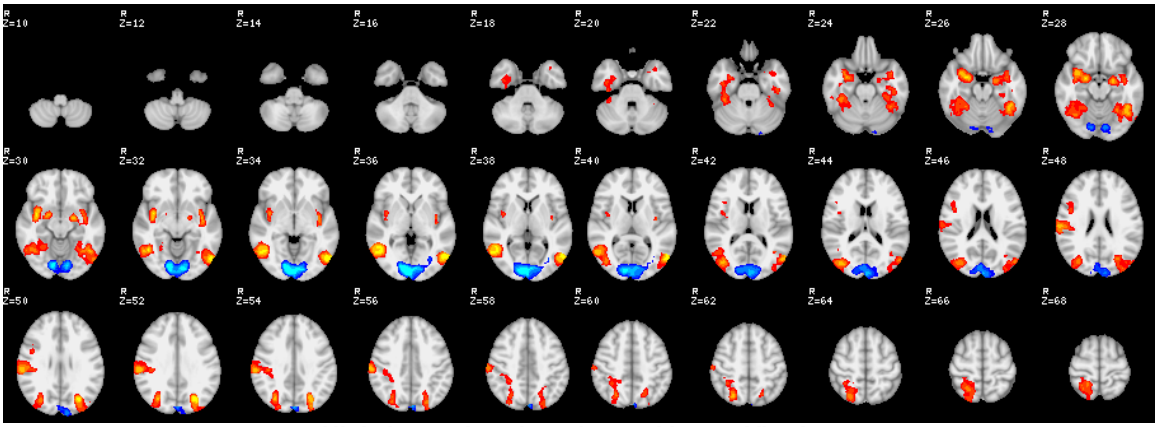

Figure 2.8: High Versus Low Arousal Effects Upon Image Viewing Activations. Comparisons were made between activations for all high arousal versus all low arousal trials. Red-yellow denotes stronger activations for high arousal trials. Blue-cyan denotes stronger activations for low arousal trials. All images cluster-wise thresholded at values of $z<2.3$, $p<0.05$. Note: No significant activation differences were seen in the reproduction period.

High Versus Low Arousal Trial Reproductions. There were no significant differences in BOLD response between high and low arousal reproduction periods.

Valence × Arousal Effects

High Versus Low Arousal, Within Positive Trials. For both the viewing and reproduction periods, the contrast maps of high versus low arousal positive images

showed similar activation differences. For viewing, positive/high images produced greater activations in cuneous, intracalcarine cortex, lingual gyrus, and cerebellum (right area VI). For reproductions, positive/high images led to greater activations within occipital pole, inferior lateral occipital cortex, lingual gyrus, and cerebellum (left area VI). Positive/low image viewings produced greater activations within VMPFC, paracingulate, medial superior frontal gyrus, and frontal pole, while positive/low trial reproduction periods showed greater activations within paracingulate and frontal pole. Figure 2.9 presents the activation contrast maps for both viewing and reproduction periods.

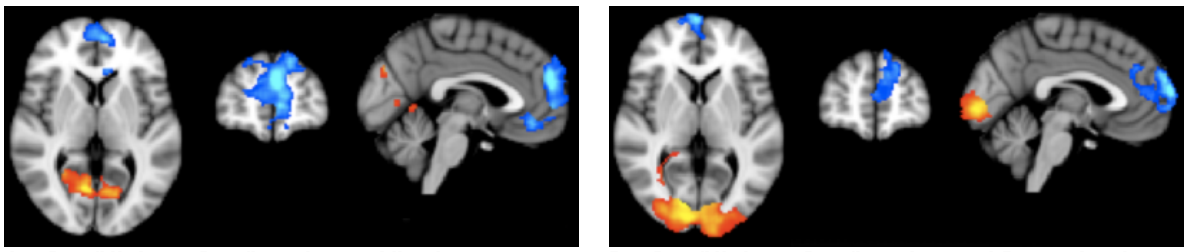

A – Pos/High vs. Pos/Low Image Viewing **B – Pos/High vs. Pos/Low Interval Reproduction**

Figure 2.9: High Versus Low Arousal Effects, Within Positive Trials, Upon Image Viewing and Interval Reproduction Activations. (A) Significant differences during image viewing. (B) Significant differences during interval reproductions. Comparisons were made between activations for all positive, high arousal trials versus all positive, low arousal trials. Red-yellow denotes stronger activations for positive, high arousal trials. Blue-cyan denotes stronger activations for positive, low arousal trials. All images cluster-wise thresholded at values of $z<2.3$, $p<0.05$. Slices in MNI-152 standard space: x=-2, y=54, z=4.

High Versus Low Arousal, Within Negative Trials. Unlike the comparisons within positive trials just above, the viewing and reproduction period contrast maps of high versus low arousal negative images were dissimilar. The map for viewing negative/high

images compared to negative/low images was an attenuated version of the overall negative versus neutral image viewing map shown above. Areas showing greater activations included inferior and superior lateral occipital cortex, lingual gyrus, temporal-occipital fusiform, superior parietal lobule, periaqueductal grey matter in the brainstem, parahippocampal gyrus, hippocampus, amygdala, and posterior insula. Negative/high reproductions only produced greater signal changes within right cerebellum (crus I and II). There were no suprathreshold activations for the negative/low greater than negative/high contrasts in either viewing or reproduction periods. Figure 2.10 presents the activation contrast maps for both viewing and reproduction periods.

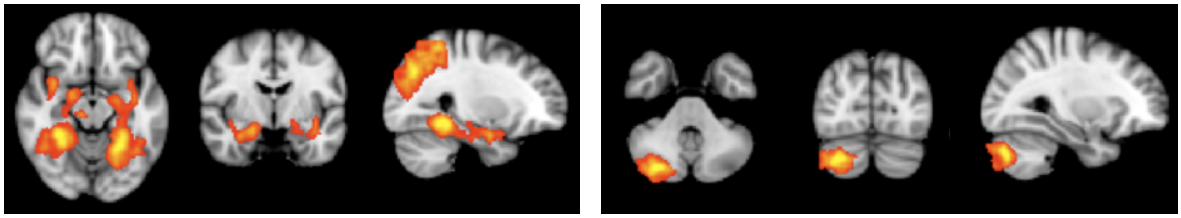

A — Neg/High vs. Neg/Low Image Viewing **B — Neg/High vs. Neg/Low Interval Reproduction**

Figure 2.10: High Versus Low Arousal Effects, Within Negative Trials, Upon Image Viewing and Interval Reproduction Activations. (A) Significant differences during image viewing. (B) Significant differences during interval reproductions. Comparisons were made between activations for all negative, high arousal trials versus all negative, low arousal trials. Red-yellow denotes stronger activations for negative, high arousal trials. No greater activations were seen for positive, low arousal trials. All images cluster-wise thresholded at values of $z<2.3$, $p<0.05$. Panel A slices in MNI-152 standard space: x=28, y=-6, z=-14. Panel B slices in MNI-152 standard space: x=30, y=-78, z=-38.

Positive Versus Negative Valence, Within High Arousal Trials. There were no areas with significantly greater activations for positive/high image viewing compared to negative/high image viewing. However, the negative/high > positive/high image viewing contrast produced a map (Figure 2.11) that was nearly identical to the negative/high >

negative/low map above (see Figure 2.10). All regions represented in that map were also in the negative/high > positive/high map, so the region listing will not be repeated here.

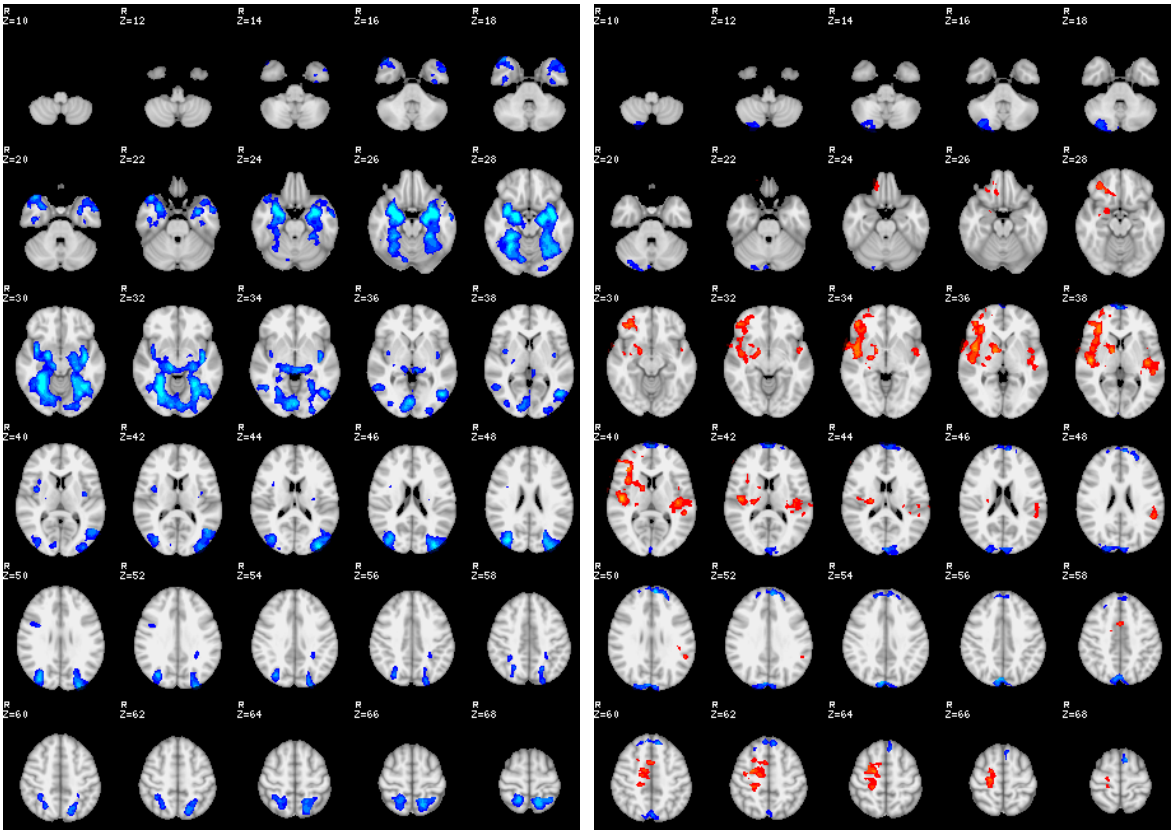

A – Pos/High vs. Neg/High Image Viewing **B – Pos/High vs. Neg/High Interval Reproduction**

Figure 2.11: Positive Versus Negative Valence Effects, Within High Arousal Trials, Upon Image Viewing and Interval Reproduction Activations. (A) Significant differences during image viewing. (B) Significant differences during interval reproductions. Comparisons were made between activations for all positive, high arousal trials versus all negative, high arousal trials. Red-yellow denotes stronger activations for positive, high arousal trials. Blue-cyan denotes stronger activations for negative, high arousal trials. All images cluster-wise thresholded at values of $z<2.3$, $p<0.05$.

In the overall positive versus negative reproduction contrasts reported above (see Figure 2.7), there were no areas that showed greater activations for positive reproductions. On the other hand, when looking at valence effects within high arousal

trials, positive/high trial reproductions produced significantly greater activations than negative/high trial reproductions across many of the regions that were also seen in the map for the main effect of interval reproductions (see Figure 2.2). In this positive/high versus negative/high reproduction contrast, significant clusters were seen within right precentral gyrus, right SMA, right superior frontal gyrus, left supramarginal gyrus, parietal operculum, Heschl's gyrus, posterior insula, right putamen, right pallidum, right anterior insula, right frontal operculum, right VLPFC, and right frontal pole. In contrast, negative/high images only produced greater activations in small clusters scattered across occipital pole, precuneous, medial superior frontal gyrus, frontal pole, and cerebellum (right crus II). Figure 2.11 presents the positive/high versus negative/high contrast maps for both viewing and reproduction periods.

Positive Versus Negative, Within Low Arousal Trials. The comparison of viewing periods for low arousal positive and negative trials (Figure 2.17) largely recapitulated the overall positive versus negative viewing contrast maps shown above (see Figure 2.10). However, in addition to the regions listed above for positive > negative viewing, there were significant clusters for positive/low > negative/low image viewing within superior frontal gyrus and more dorsal aspects of the frontal pole. Compared to the overall negative > positive viewing map above, the negative/low > positive/low viewing contrast was right lateralized (except for occipital regions) and added a cluster within right IFG.

Again, in the overall positive versus negative reproduction contrasts reported above (see Figure 2.7), there were no areas that showed greater activations for positive reproductions. Looking within just low arousal image trials, the positive/low >

negative/low reproduction contrast did yield significant activation differences, in a cluster spanning VMPFC, paracingulate, and frontal pole. The negative/low > positive/low contrast produced a more expansive version of the occipital pole cluster seen in overall negative > positive reproduction map reported above, with extensions down into cerebellum (area VI). Figure 2.12 presents the positive/high versus negative/high contrast maps for both viewing and reproduction periods.

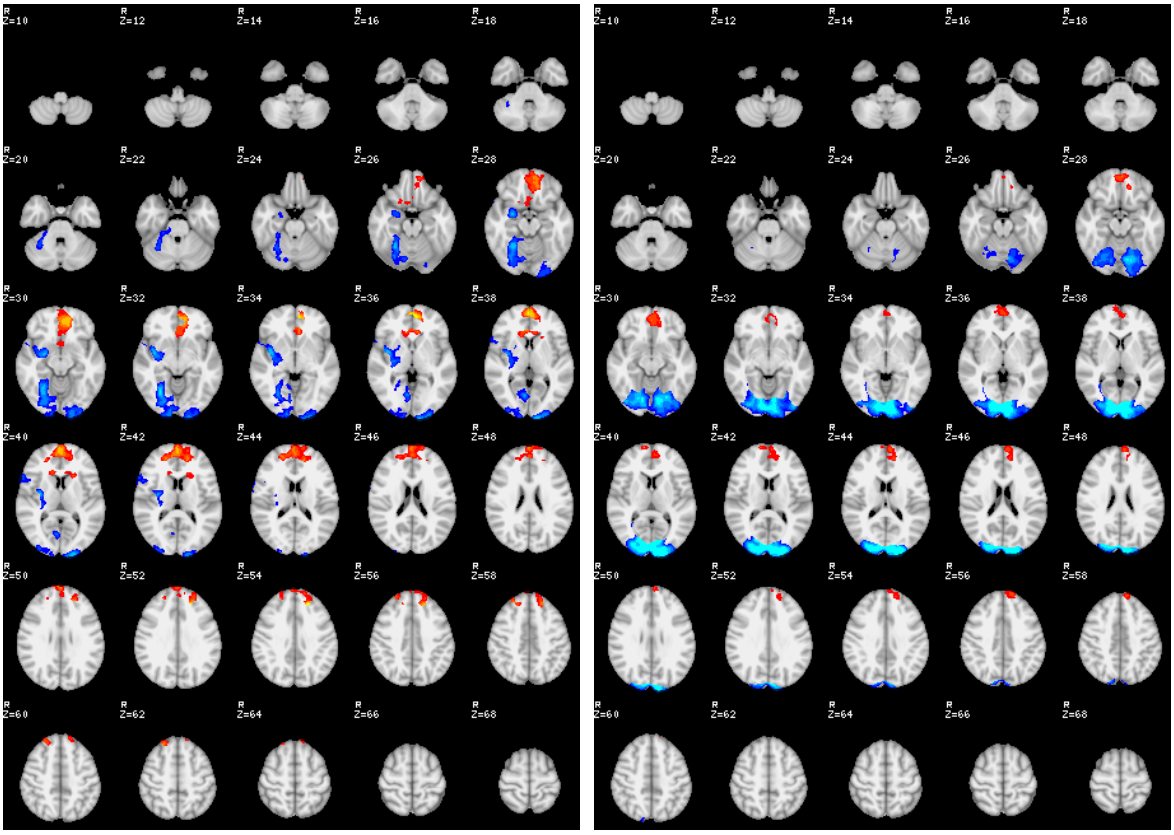

Figure 2.12: Positive Versus Negative Valence Effects, Within Low Arousal Trials, Upon Image Viewing and Interval Reproduction Activations. (A) Significant differences during image viewing. (B) Significant differences during interval reproductions. Comparisons were made between activations for all positive, low arousal trials versus all negative, low arousal trials. Red-yellow denotes stronger activations for positive, low arousal trials. Blue-cyan denotes stronger activations for negative, low arousal trials. All images cluster-wise thresholded at values of $z<2.3$, $p<0.05$.

Covariate Analyses for Win Ratios

Short Trial Viewing. Within short trials, win ratios were positively correlated with signal change during positive image viewing within clusters across VMPFC, paracingulate, and left frontal pole. Conversely, win ratios for negative trials were negatively correlated with signal change during image viewing in a cluster across ACC, paracingulate, and right frontal pole. The two maps overlapped within paracingulate. Follow-up investigations of the individual image types showed that the positive trial correlation was driven solely by positive, high arousal images, whereas both arousal types contributed equivalently to the negative trial correlation. Additionally, the map of positive behavioral correlations for positive, high arousal trials was more extensive and bilaterally represented, and for these trials there was also a negative correlation between task performance and signal change within left precentral gyrus, left postcentral gyrus, bilateral superior parietal lobule, and bilateral precuneous. Figure 2.13 presents task performance correlation maps for short trial image viewing within all positive trials and all negative trials (Figure 2.13 A), and then separately for positive, high arousal trials (Figure 2.13 B).

Short Trial Reproductions. The only task performance correlation for short trial reproductions was seen for positive, low arousal trials. A positive correlation was seen within posterior cingulate and precuneous.

Long Trial Viewing and Reproductions. There were no significant correlations between task performance and long trial image viewing for any of the image types. For reproductions, only a positive correlation was seen during positive, high arousal trials, in

clusters across SMA, right precentral gyrus, and right postcentral gyrus. Figure 2.14 presents the significant correlations between task performance and reproduction for both short, positive, low arousal trials and long, positive, high arousal trials.

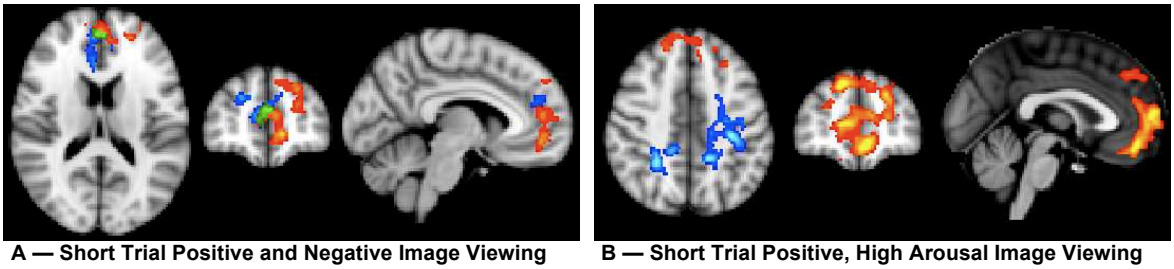

A — Short Trial Positive and Negative Image Viewing **B — Short Trial Positive, High Arousal Image Viewing**

Figure 2.13: Task Performance Effects, Within Short Trials, Upon Image Viewing. (A) Significant positive correlations during positive image viewing (red-yellow) and significant negative correlations during negative image viewing (blue-cyan). The overlap of the two maps is shown in green. (B) Significant correlations during viewing of positive, high arousal images. Red-yellow denotes positive correlations; blue-cyan denotes negative correlations. All images cluster-wise thresholded at values of $z<2.3$, $p<0.05$. All slices in MNI-152 standard space. Panel A: x=-6, y=50, z=16. Panel B: x=0, y=50, z=44.

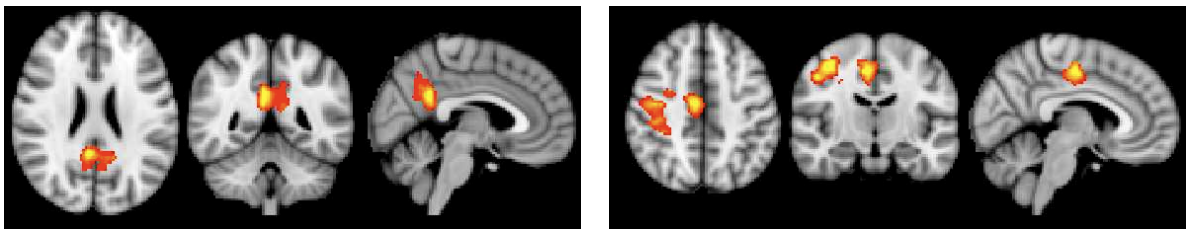

A — Short Trial Positive, Low Arousal Reproductions. **B — Long Trial Positive, High Arousal Reproductions**

Figure 2.14: Task Performance Effects Upon Interval Reproductions. (A) Significant positive correlations during positive, low arousal interval reproductions. (B) Significant positive correlations positive, high arousal interval reproductions. No significant negative correlations were seen for either condition All images cluster-wise thresholded at values of $z<2.3$, $p<0.05$. All slices in MNI-152 standard space. Panel A: x=4, y=-48, z=24. Panel B: x=6, y=-14, z=46.

T-tests of Sex Differences

Sex differences in short trial performances were identified in the LMER behavioral analyses discussed in Chapter 1, with males being more likely to win money on short trials than females. During short image viewing across all trial types, a cluster spanning subgenual ACC, paracingulate, and VMPFC was identified (Figure 2.15) wherein males had a weak positive mean activation (mean z=0.98) but females showed a strongly negative signal change (mean z=-2.88). No suprathreshold clusters were found when each image type was analyzed separately, but follow-up inquires of the mean signal change values within the VMPFC cluster indicated that the same directional trend of sex differences was seen for all valenced images, though more prominently separated for positive, high arousal images (males' mean z=1.31, females' mean z=-1.42). However, for neutral images, VMPFC signal changes were negative and statistically equivalent for males and females (males' mean z=-1.88, females' mean z=-2.62).

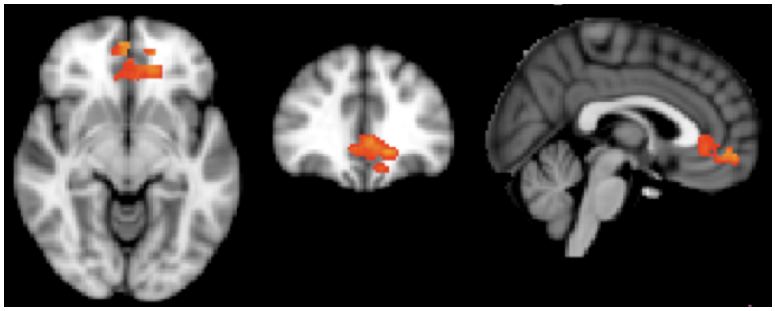

Figure 2.15: Sex Differences in Activations During Short Trial Image Viewing. Males showed weak positive signal changes, while females showed strongly negative signal changes, in medial PFC regions during short trial image viewing. Red-yellow denotes stronger activations for males compared to females. No greater activations were seen for females compared to males. All images cluster-wise thresholded at values of z<2.3, p<0.05. Slices in MNI-152 standard space: x=2, y=36, z=-8.

Long trials, for which sex was not a significant predictor of behavioral performance, nonetheless showed sex differences in the fMRI data. Moreover, long trial viewing showed a differential sex effect across valence categories (Figure 2.16 A). Averaging over all image types, females had greater activations (mean z=3.63) than males (mean z=0.38) in a cluster across right middle temporal gyrus and right temporal-occipital fusiform. Follow-up investigations of each image type showed that arousal levels had no significant impact, but that positive and negative images showed disparate sex effects. The overall image viewing sex effect was driven by female > male activations for positive images. The females versus males t-test within just positive images showed the same right temporal/occipital cluster (males' mean z=-0.03, females' mean z=3.45), but also an additional cluster spanning left medial precentral and postcentral gyri (males' mean z=-0.84, females' mean z=2.84). In contrast, for negative image viewing only, males showed greater activations in right VLPFC (males' mean z=2.88, females' mean z=-1.49), right IFG (males' mean z=2.27, females' mean z=-1.68), and left supramarginal gyrus (males' mean z=2.76, females' mean z=-1.05).

No sex differences were seen for any short reproduction periods. No sex differences were seen for long trial reproductions when analyzing across all image types, though for long neutral trial reproductions alone there was a large array of significant female > male activation differences (Figure 2.16 B). The significant clusters spanned medial superior frontal gyrus, paracingulate, left DLPFC, left IFG, left angular gyrus, and left lateral occipital cortex.

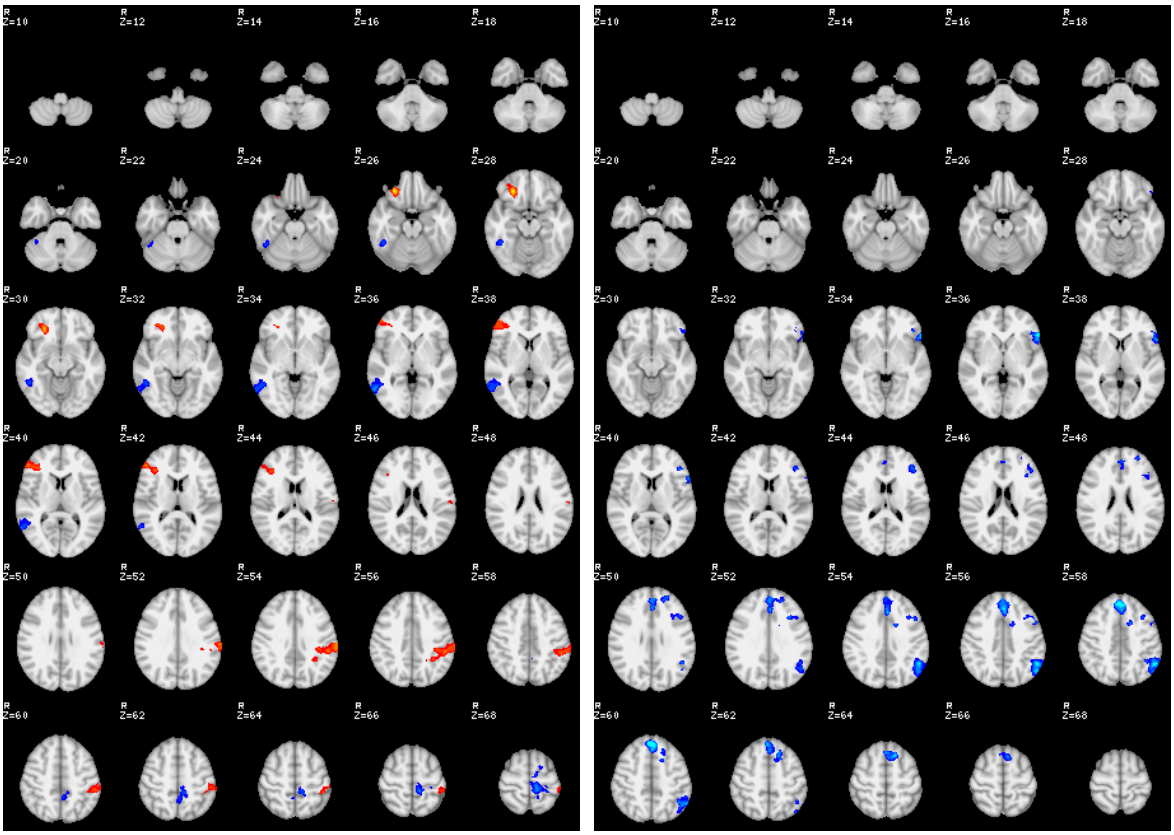

A – Males vs. Females, Positive (F>M) and Negative (M>F) Image Viewing

B – Males vs. Females, Neutral Trial Interval Reproduction

Figure 2.16: Sex Differences in Activations During Long Trial Image Viewing and Interval Reproduction. (A) Significant sex differences during image viewing were seen when analyzing positive and negative images separately. In this panel, red-yellow denotes areas where males showed stronger activations while viewing *negative* images. Blue-cyan denotes areas where females showed stronger activations during *positive* image viewing. (B) Significant sex differences were seen only during *neutral* trial interval reproductions. Blue-cyan denotes stronger activations for females compared to males. All images cluster-wise thresholded at values of $z<2.3$, $p<0.05$.

Linear and Nonlinear Analyses for Age

Linear Effects in Long Trials. Long trials, for which age was a strong predictor of performance, showed extensive BOLD signal relationships with age (Figure 2.17). Signal changes during long image viewing periods were positively correlated with age in medial precentral gyrus and posterior aspects of SMA, lateral precentral gyrus, right middle

temporal gyrus, left superior temporal gyrus, central opercula, thalamus, putamen, pallidum, caudate, right posterior insula, and the ventral tegmental area of the brainstem. All regions were represented bilaterally, though the right precentral and caudate clusters were more extensive than those in the left hemisphere. Follow-up investigations of each image type indicated that the overall correlation pattern was present for each image type at subthreshold levels. However, thresholded images revealed valence and arousal differences within the age correlation, with effects in SMA and precentral gyrus being driven by positive, high arousal images and effects in right hemisphere opercular and subcortical regions driven by negative, high arousal images. Long trial reproduction periods did not show any significant linear correlations between age and BOLD signal changes.

Linear Effects in Short Trials. Short trials, for which age was not a strong predictor of task performance, showed more circumscribed BOLD signal relationships with age during image viewing than were seen for long trials. There were no age effects for image viewing when all image types were analyzed as a whole, but negative age correlations within ACC and paracingulate (i.e., greater activations in younger participants) were seen for low arousal image viewing alone. Follow-up investigations (not shown) indicated that positive/low, negative/low, and neutral images all contributed equivalently to the correlation effect. As with long trials, short trial reproduction periods did not show any significant linear correlations between age and BOLD signal changes.

Nonlinear Age Effects. Targeted ROI investigations within NAcc, amygdala, and insula were carried out to test for the presence of negative quadratic (e.g., nonlinear,

"inverted-U") effects of age, as predicted by maturational disconnect models. There were no significant nonlinear age effects for any of the image types, for either the viewing or reproduction periods, for either short or long trials.

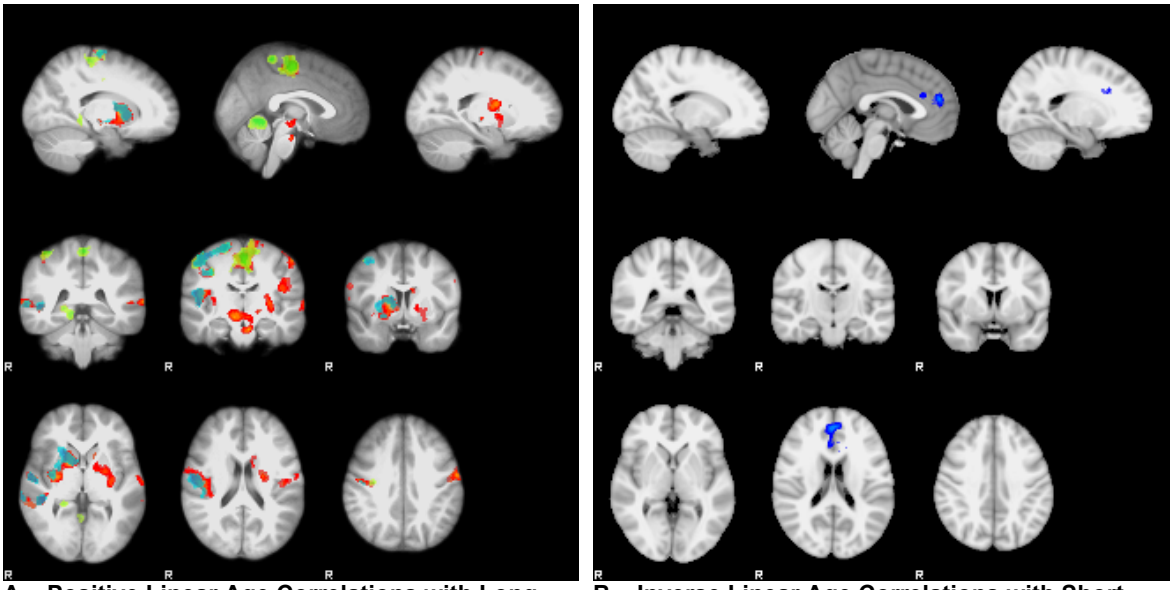

A – Positive Linear Age Correlations with Long Trial Image Viewing Activations

B – Inverse Linear Age Correlations with Short Trial, Low Arousal Image Viewing Activations

Figure 2.17: Linear Age Correlations for Image Viewing. (A) Significant positive age correlations were widespread for long trial image viewing. The image is color-coded to show the differential contributions of positive and negative high arousal trials to the overall effect. Red denotes areas of the correlation across all image types, green denotes areas significantly correlated with positive trials only, and turquoise denotes areas significantly correlated to negative trials only. (B) Significant inverse linear correlations between age and signal change for short trial image viewing were seen in medial PFC, only for low arousal images. All images cluster-wise thresholded at values of $z<2.3$, $p<0.05$. Slices are in MNI-152 standard space. Top row: sagittal slices, x=16, 0, & -20. Middle row: coronal slices, y=-40, -16, & 4. Bottom row: axial slices, z=0, 18, & 36.

Discussion

Main Effects of Viewing, Reproduction, and Feedback Periods

Overall, the interval timing task performed as designed. The task robustly engaged many areas that have been implicated as a part of a timing network in prior

studies, along with multiple regions related to emotional experience and cognitive control. Overlaying the viewing and reproduction grand mean activation maps (image not presented) showed that there was significant overlap among suprathreshold voxels within occipital pole, cerebellum (crus I), thalamus, right pallidum, right putamen, SMA, ACC, right insula, and left precentral gyrus. The occipital pole and left precentral gyrus activations reflect the visual nature of the task and the requirement for a right-hand button press. The significant activations for right precentral gyrus were not expected, but post-task debriefings indicated that a common strategy among participants was to use the left hand to tap out counts as an aid to tracking and reproducing the intervals. The thalamus putamen, pallidum, SMA, and cerebellum have roles in motor output, but are also commonly viewed as portions of an interval timing network (Buhusi & Meck, 2005; Matell & Meck, 2000; Meck, 2005). The activation of these regions across both viewing and reproduction periods implies that they are core features of the interval timing network, though it may also be that these regions' activations were in service of preparing motor responses, regardless of timing-related processing. While the insula may also play a role in timing performance (Craig, 2009b; Wittmann et al., 2011), it is more commonly regarded as a center of emotional experience and salience detection (Seeley et al., 2007; Stein & Paulus, 2008), and its activation across both task periods may be an index of active engagement with the task and exhibition of appropriate neural flexibility to reach successful trial outcomes (Menon & Uddin, 2010).

Image viewing yielded significant BOLD signal changes across multiple visual information processing centers and within timing-related regions, but the activation map

also contained areas implicated in the regulation of attention and emotion and the exercise of cognitive control. Activations were robust in the dorsal ACC and right anterior insula, portions of the salience ICN. Significant activations were also seen across posterior parietal regions of the central executive ICN, which have been shown to be more strongly correlated to executive functioning neuropsychological test performances than the frontal portions of the central executive ICN (Seeley et al., 2007). At the same time, strong deactivations were seen across many regions, including areas covered by the default mode network (images not shown). Notably, no significant activations were seen within the caudate for the viewing periods, indicating that its role in interval timing is more on the side of expression than reception or encoding.

Indeed, reproduction periods showed robust activations through the entirety of the basal ganglia, along with IFG and areas of left hemisphere motor cortex underlying participants' button presses. This section of the map appeared very similar to reproduction findings from a recent study that used an audition-based interval timing task with very similar setup to the present study (Wittmann et al., 2011). In terms of changes within ICNs of interest, activations in the salience network increased in strength and extent, as did right parietal regions of the central executive network, and areas in the default mode network continued to show strong deactivations (images not shown) throughout reproduction.

The short and long viewing periods only differed by the strength of signal change in the occipital lobes. The two separate long and short reproduction activation maps (not shown) were highly overlapping with each other and with the grand mean map, and their

direct comparison (see Figures 2.1 B and 2.2 B) showed that short trials had significantly stronger activations in areas largely found within the respective grand mean maps. These results are potentially due to technical aspects of comparing signal change calculations across time periods with a three-fold difference in length, though it is also possible that the short reproductions required a relatively more powerful "burst" of activity throughout the timing/motor output network.

On the other hand, the feedback display period was a constant length on all trials and thus it is reasonable to make stronger inferences about the nature of the activation differences, which were striking, to feedback received for long and short trials. The relative lack of salience network (i.e., ACC) activations to feedback in the long trials may be reflective of the increased likelihood of winning on long trials. Feedback may have thus been less informative and required less processing related to updating the neural representations of performance strategies. The presence of stronger NAcc responses for short trial feedback displays, which would have contained many more messages of failure, may seem counterintuitive when thinking about the NAcc as a core component of the brain's "reward centers." However, there is evidence that the NAcc is more active during the anticipation and prediction of rewards compared to the receipt of rewards (Pagnoni, Zink, Montague, & Berns, 2002) and that it also serves the function of delivering a "teaching signal" when outcomes are different from the most recently developed pattern (Abler et al., 2006; Spicer et al., 2007). Thus, as rewards become more and more predictable and the outcome pattern becomes well established (as would have

been the case for long trial wins compared to short trial wins), signaling from NAcc would dwindle.

The BOLD response differences to feedback may also reflect differences in cortical networks underlying performance strategies, if the activations are to be interpreted as the updating of neuronal models of how to properly time and reproduce intervals and to then improve performance on subsequent trials. No explicit instructions on how to manage the task were given to participants, other than to "get a sense" for how long each image was displayed to them and to end the reproduction period when they "felt" that the time was right. In post-scanning debriefings, left finger tapping to time the viewing periods was a commonly reported strategy. Such a strategy would ostensibly be more successful for long trials than short trials, and indeed, portions of right hemisphere motor cortex underlying right hand control were more strongly activated for long trial feedback displays. The presence of significant cerebellar involvement with short trial feedback perhaps speaks to differences in aspects of the timing network required to accurately time the shorter trials, as it is believed that as intervals become shorter and shorter, activity in the cerebellum becomes more and more central to timing accuracy (Buhusi & Meck, 2005; Lewis & Miall, 2003).

Overall, the grand mean activations for the task were very much in line with expectations from the interval timing literature. Within that literature is an ongoing debate over what constitutes the "core" timing network and which regions are spuriously included because overt behaviors, most often motor responses, are requirements of timing tasks or because factors such as overall difficulty are not well controlled (Livesey et al.,

2007). No timing without motor or motor without timing comparison conditions were included in the current study, so these data cannot be used to parse out which areas seen in the grand mean maps are more related to timing and which are more related to motor output, but that was not the aim of the study. Of greater interest were the effects of valence, arousal, and age across adolescent development upon BOLD signal changes during task performance.

Valence & Arousal Effects

There were no arousal main effects and very few valence main effects during interval reproduction periods, but widespread BOLD signal main effect differences between image types were seen during the viewing periods. The contrast map for valenced > neutral image viewing showed significant clusters within amygdala, insula, periaqueductal grey matter, and supramarginal gyrus, all of which have been related to processing of stimuli related to fear, pain, and disgust (Adolphs, Tranel, Damasio, & Damasio, 1994; An, Bandler, Ongur, & Price, 1998; Davis, 1992; Köchel, Schöngassner, & Schienle, 2013), and a large cluster was seen across the more positive-stimuli-associated VMPFC and into medial frontal pole. The statistical maps comparing positive > neutral, negative > neutral, and positive > negative image viewing activations showed that the positive/negative biases for these regions all fell along the lines just described.

Sections of the valenced > neutral image viewing map also covered core regions of the default mode network. Since the default mode network is generally seen as needing to be "turned off" during most cognitive tasks, one might interpret sustained activation of these areas as one reason why strongly valenced stimuli often make it difficult to

concentrate or to perform tasks accurately. However, there is evidence that default-mode regions can remain active during cognitive tasks, particularly for tasks with social cognition requirements (Laird et al., 2011). Indeed, only a handful of the neutral images used in this study contained depictions of people (most were objects or landscapes), whereas the majority of valenced images depicted people either interacting with each other or looking into the camera, towards the viewer.

The valence × arousal contrasts indicated that, within negative trials, increasing arousal simply led to increased (potentiated) activations in regions that were also active during low arousal viewing. However, within positive trials, different arousal levels prompted the engagement of disparate brain regions. The PFC clusters seen in the overall positive > neutral and positive > negative viewing contrasts were primarily due to activations during positive/low trials, whereas greater positive/high image viewing activations were primarily within visual processing areas. Interestingly, this same dichotomy was carried over into the reproduction phases, indicating that positive/low trials, on average, may have allowed for greater overall expression of cognitive and emotional control than positive/high trials. Moreover, when looking at valence effects upon reproduction periods within high arousal images, positive/high trials produced significantly greater activations within many areas implicated in the reproduction main effects map, indicating that positive/high trial reproductions may have required more mental resources. At the group mean level, the behavioral analyses from Chapter 1 showed that increasingly arousing positive images had led to poorer performances, whereas increasingly arousing negative images led to more successful timing

performances. Indeed, the task performance correlations seen in Figures 2.13 B indicated that increased activations in control-related PFC areas during image viewing were associated with improved performances on short, positive, high arousal trials. Such evidence of "extra" neural activity underlying successful performance was not seen for the other trial types. Indeed, additional superior frontal pole and medial paracingulate activation was negatively correlated with performance during short, negative trials, providing correspondence to the valence × arousal interaction in the behavioral analyses.

Additionally, the negative > positive and high arousal > low arousal main effect viewing maps both showed significant clusters in insula, amygdala, and over the posterior parietal regions associated with the central executive network (e.g., superior parietal lobule, supramarginal gyrus), whereas the positive > negative viewing map only showed a large cluster across VMPFC and into rostral caudate. All together, the behavioral and imaging results for valence and arousal align with proposals of salience ICN and central executive ICN cooperation that predict that, when arousal levels are equated, the preferential access to the salience network that is held by negative stimuli over positive stimuli more strongly activates the salience network, which in turn enhances switching from default mode to central executive processes, leading to overall improved behavioral performances (Menon & Uddin, 2010; Seeley et al., 2007). However, a performance benefit from increased arousal may be dependent upon task demands and criteria used to measure performance, as a recent developmental study demonstrated that longer reaction times (i.e., poorer performances) on a go/no-go task were present when stimuli were negatively valenced, compared to neutral conditions (Cohen-Gilbert & Thomas, in press).

Additionally, though the paracingulate and frontal pole are not generally included in conceptions of the core central executive ICN discussed above (Menon & Uddin, 2010; Seeley et al., 2007), the presence of negative correlations between activations in these regions with negative trial performances (Figure 2.13 A) may be seen as undermining an argument that negative stimuli enhance beneficial PFC-based, control-related activations.

Sex Differences

Moreover, such an interpretation does not immediately fit with the finding that in short trials, females showed strongly negative VMPFC activity during image viewing (a marker of default-mode network deactivation), yet performed less well than males. It may be, though, that VMPFC activity is not the culprit, as subthreshold investigations (not shown) of the female > male contrast indicated that, even at very weak thresholds (z>1.0), females did not show greater activations than males within areas of the salience network (e.g., amygdala, insula, ACC) during image viewing. Furthermore, the significant difference does not necessarily mean that males were excessively activating VMPFC during the short trial viewings. Indeed, the significant difference in the *t*-test was driven by the magnitude of negative signal changes for females, not by males' positive signal changes, which on average produced VMPFC voxels with z values < 1.

One study investigating sex differences in emotional reappraisal found that, when instructed to view IAPS images and reduce their reactions to the content, the regulation of negative emotions produced significantly stronger VMPFC activations for females than for males (Mak et al., 2009). Here, a somewhat contradictory finding was seen, although, again, the absence of a strong VMPFC activation for males makes the

difference more difficult to interpret. Moreover, the interval timing task was not designed to be an overt emotion regulation task, and participants were given no instructions suggesting what, if anything, they should do about their reactions to the image content, so differences in findings between the two studies are not inherently in conflict.

Even though males did not have statistically significant increases in VMPFC BOLD signal during short trial image viewing, there were other indications of differences between males and females in their approaches to regulating emotional responses to valenced images in the service of task performance. Subthreshold investigations of each image type of the male > female contrasts for short viewing (not shown) indicated that only activations during the neutral trials did not contribute to the overall viewing *t*-test results. Thus, it may be that displaying at least minor positive responses within VMPFC is beneficial to setting aside the emotional content of valenced images and carrying out the interval timing task, but that deep reductions in VMPFC activity leads to less successful regulatory control. Alternatively, it may not be an issue of needing, but failing, to neutralize one's reaction to the emotional content of the stimuli that underlies the short trial performance difference between males and females. Much like the interpretation above that amygdala and insula activations may be markers for the beneficial ways in which emotions can aid and bolster concurrent cognitive performances, a lack of engagement in other core emotion-related areas could hinder cognitive abilities. In such a scenario, underutilization of VMPFC would be considered "too cold" while sizeable increases may be "too hot" (though there is no direct evidence here to support that),

whereas the mild positive signal change seen for males would be "just right" for maximizing performance outcomes.

The presence of sex differences in BOLD signal during long trials, which did not show a behavioral difference between males and females, is an additional indication of the presence of a difference in approaches to dealing with the presence of positive or negative images. However, for long trials, this potential strategic or cognitive difference did not translate into overall differences in trial outcomes.

Age Correlations

Linear effects. Within long trials, age showed significant positive correlations with BOLD signal changes during image viewing, but not during reproduction. Given that the patterns of age correlations were not remarkably different across the different image types, there is no evidence indicating that older subjects were able to perform better because they were able to utilize separable neural networks that differentially regulated responses to particular image types. Additionally, the lack of age-related prefrontal activations suggests that the age-related performance improvement in long trials was not due to overt emotional downplaying or distraction strategies during image viewing (McCrae et al., 2009; Wager et al., 2008). Interestingly, the age correlation map was more overlapping with the grand mean reproduction map than with the grand mean viewing map (and was almost entirely distinct from the union of the viewing and reproduction maps). This may indicate that older subjects' enhanced performances were due to increased abilities to run multiple task-related networks simultaneously. To state it another way, it may be that younger subjects, perhaps by necessity of neural immaturity,

approached the task in a more step-wise manner ("Now I'm viewing…Now I'm reproducing…"), while older subjects were perhaps able to somewhat simultaneously encode the intervals and prepare to make their reproduction responses. Though PFC regions are often implicated in the expression of such multitasking abilities (Burgess et al., 2000; Roca et al., 2011), there is evidence that intact basal ganglia functioning is also requisite for multitasking (Thoma et al., 2008), making the lack of prefrontal age associations less detrimental to this interpretation.

Linear, negative correlations with age were seen only in the short, low arousal image viewing period. The negative correlation was within ACC, a portion of the brain's salience detection ICN. As low arousal is equivalent to low salience, one interpretation of this result could be that younger participants were less able "let their guard down" even when stimuli held low intrinsic motivational salience.

Nonlinear effects. This study was conducted with pre- to early-adolescent, mid- to late-adolescent, and young adult participants in order to be able to test for maturational differences in neural responses to appetitive and aversive stimuli, with particular interests in dual- and multi-system maturational disconnect models that predict exaggerated subcortical responses to emotionally salient stimuli (e.g., Casey et al., 2010; Ernst et al., 2009). Such models predict that adolescents would show greater subcortical activations, compared to children and adults, when faced with stimuli that influence incentive motivation. There were no such nonlinear associations between age and BOLD signal in targeted analyses of NAcc, amygdala, and insula. This lack of findings could be due to the fact that the interval timing task is more of an emotional challenge or distraction

regulation task, as opposed to a reward-related decision making task, which is the area of research that most maturational disconnect models are built upon (Richards et al., 2013).

Developmentally-nonlinear motivational control models generally make predictions that, compared to children and adults, adolescents will show a deficit in task performance when confronted with appetitive or aversive cues that are incidental to the task at hand, but some nonlinear model proponents also predict that adolescents will show relatively greater enhancements of task performance when incentivized with the promise of rewards following performance (Casey et al., 2010). Thus, such models predict that adolescents will be excessively distracted by irrelevant indicators of appetitive or aversive information, but will be deeply focused by the promise of pending task-relevant rewards. The interval timing task contained both incidental distractors as well as monetary reward incentives, leaving the potential interpretation that the two factors may have "canceled" each other out, masking underlying nonlinear effects. Such an interpretation may be more amenable to behavioral measurements. Within an fMRI study, such an interpretation would require an assumption that the incidental distractors and pending rewards would act equivalently, but in the opposite directions, upon the exact same neural structures.

Additionally, some research groups have argued that nonlinear behavioral and neural effects are more potent when social cues are at the forefront of the task at hand (Chein et al., 2010; Gardner & Steinberg, 2005). However, while social interaction was not an aspect of the timing task, as discussed above, the valenced images used in this experiment were replete with socially-relevant content, in ways not unlike other studies

that reported nonlinear age effects (e.g., Somerville, Hare, & Casey, 2010). Moreover, the possibility of increased potency through socially relevant cueing does not mean that a task's lack of social cues leads to a lack of nonlinear effects.

Regardless, the interval timing task itself engaged all subcortical ROI-investigated areas robustly, either during viewing or reproduction, and strong linear age relationships were seen within portions of the insula and the basal ganglia, providing seemingly fertile ground for potential adolescence-related nonlinear BOLD responses. Furthermore, the short trials showed relatively stronger recruitment of basal ganglia and insula during interval reproductions, again seemingly providing ample opportunity for expression of adolescent-specific hyperactivities within fast-paced contexts (e.g., Steinberg et al., 2008).

The lack of nonlinear age associations in this study could be interpreted as supporting the notions that either such nonlinear effects are only to be expected within circumscribed paradigms related to reward learning, protracted reward anticipation, and reward-related decision making, or in a more severe view, that nonlinear maturational disconnect models are reasonable heuristics that have produced much fruitful research, but that there truly is no pathological "teen brain" to be found and such models need to be reworked or possibly even discarded in favor of more nuanced accounts (cf. Pfeifer & Allen, 2012). This latter conclusion is decidedly unwarranted from the findings of a single study, though the present report is not alone (e.g., Bjork, Smith, Chen, & Hommer, 2010; Forbes et al., 2009; Geier et al., 2010; Pfeifer et al., 2011; Pitskel et al., 2011) in finding no evidence, or contradictory evidence, for a fundamental neural basis underlying

the adolescence-specific over-expression of sensation-seeking and reward drive along with under-expression of emotional or motivational control.

Lastly, it is also possible that the lack of adolescent-specific findings in this study was due to the manner in which adolescence was defined. As a concept, adolescence is ambiguous and is broadly defined as the period of transition between childhood and adulthood. Many definitions have been proposed based on various methodological and theoretical perspectives (e.g., studies of endocrinology, sexual reproduction, cognition, or socialization). The timeframe for adolescence is most often described as coincident with the teen years, but lines of evidence from a variety of fields point toward a timeframe that could be as expansive as age 10 through the mid-20s (Baumrind, 1987; Herdt & McClintock, 2000; Petersen, Silbereisen, & Soerensen, 1993). In such a view, all participants in this study (ages 11 to 24) would be adolescents, rendering spurious any attempts to find adolescent-specific effects by further splitting the age range. However, the ages recruited for this study were roughly aligned with age ranges presented in research reports with nonlinear behavioral and imaging findings (e.g., Galvan et al., 2005; Somerville, Hare, & Casey, 2010).

Limitations and Future Directions

This study potentially suffered in its search for nonlinear age differences by having relatively small sample sizes within the three target age ranges. However, with 31 total participants, this sample is not unlike other developmental fMRI studies. An expanded age range to include younger participants could be helpful, but then even stronger considerations of the image content would have to be made. Alternatively,

elimination of low arousal conditions, and heightening of the arousal content (e.g., by including increasingly graphic or explicit images) could serve to make the interval timing task a more vigorous emotional challenge task. However, reaping significant benefits from such changes would need to be a near certainty, when weighed against the increased risk of harm to minor participants by exposing them to potentially unsuitable or disturbing content.

It is also possible that enhancement of anticipation for rewards could maximize the likelihood of finding adolescent-specific BOLD signal changes in NAcc (Knutson & Greer, 2008). Participants in this study were not told how much each winning trial was worth or how many trials they would perform, only that they could win up to a total of $5.00 through their efforts across the entire task. The trial outcomes were also limited to winning additional money or having their winnings remain at the same level. Increasing the sizes of rewards, explicitly stating how much each win is worth, or the introduction of a loss/punishment condition are important considerations for further iterations of this task. Such alterations would not be made in service of making the task more engaging, as the participants' accuracy rates (64.59% wins on short trials, 84.76% wins on long trials) indicated that they were sufficiently engaged with the task as it is. Rather, these alterations would be made in attempts to access adolescent-specific responsiveness to evermore arousing or distracting appetitive and aversive information.

Comparison conditions of stimuli viewing without timing or timing without imagery could also be included, to allow for increased specificity of neural correlates of timing versus emotional experiences. Such enhancements could lead to isolation of brain

regions specifically involved in responses to image content, making targeted nonlinear developmental tests potentially more profitable.

From a methodological standpoint, conducting fMRI analyses that classify images by individual ratings rather than mean ratings could be useful. Such an approach would allow for further parallel examinations of the behavioral findings from Chapter 1 which indicated that individual ratings had a larger influence upon trial outcomes than did mean image categorizations and that females and males tended to have shifted mean ratings of positivity, negativity, and arousal. However, analyses that code regressors as 0/1/2/3/4 rather than as positive/negative would require the assumption that neural responses to images would be parametrically parallel to the ratings scale.

Additionally, this study looked at fMRI data only, but future investigations could incorporate structural data (e.g., cortical morphometry, white matter tractography) as well. As with any MRI study, more elaborate analytic techniques hold the potential for more comprehensive explanations of the biological and psychological relationships underlying overt behaviors and internal experiences. However, as with the use of penalized fit indices in the behavioral analyses, increasing complexity must always be weighed against the need for parsimony and clarity.

Summary

Overall, the analyses confirmed that the task broadly performed as intended, with not only meaningful behavioral differences but also significantly different neural responses to the duration, valence, and arousal manipulations. Notably, however, the interval timing task was not able to elicit adolescent-specific exaggerated BOLD signal

changes within key subcortical structures of emotional and motivational control, which was a major aim of the study.

The fMRI analyses showed significant activations indicative of engagement of networks associated with interval timing, emotional evaluation, heightened arousal, and executive control across the viewing and reproduction portions of the task. During image viewing (and interval experiencing), cortical components of a putative timing network were active, whereas during interval reproduction, neural activity turned more towards the subcortical aspects of this network. Differences in activations between short and long trial viewing and reproduction were more about extent and magnitude within similar regions rather than about separable configurations of activated brain regions. In contrast, activations to feedback on short and long trial performances showed markedly different patterns of activation, which may reflect differences in the utility of feedback between more and less predictable rewards across task conditions.

Valence and arousal manipulations showed main effects and interaction effects. For positive > negative viewing, collapsed across arousal levels, there were significant activation differences within key medial prefrontal areas associated with subjectively positive experiences. On the other hand, regions shown in the negative > positive image viewing contrast contained key aspects of the brain's salience detection network. Even though valence and arousal were not confounded in the image set, the contrast maps for negative > positive image viewing and high > low arousal image viewing were largely overlapping. Comparing arousal levels within negative trials showed that arousal potentiated activations within regions common to the two conditions. On the other hand,

high versus low arousal level comparisons within positive trials indicated that arousal alterations led to differential engagement of disparate neural regions.

Reproduction period differences among trials containing the different image types were scant. However, in the comparison of positive/high versus negative/high interval reproductions, positive/high trials were shown to require significantly greater activations across regions seen in the main effect map for reproductions.

Linear, positive correlations with age were seen within long duration trials across a wide array of cortical and subcortical regions. The age-correlated regions were seen during image viewing but were largely within reproduction-related regions, indicating that increasing age was associated with viewing and reproduction activations that were more and more similar. That is to say, as age increased, increased viewing-related activations were seen within areas from the grand mean map for reproductions. As age and task performance were also positively correlated, the BOLD signal/age correlation may reflect enhancement of performance through lesser "partitioning" of neural systems activated across the different phases of the task. Linear, negative correlations of ACC activations with age were seen during short, low arousal image viewing periods, indicating that, with increasing age, participants had less recruitment of a portion of the brain's salience detection network within low salience contexts.

Though sex did not meaningfully predict long trial performances, there were demonstrable sex differences in BOLD signal changes for both long trial viewing (positive and negative images) and reproduction (neutral images) periods. Sex effects were present but mild for task performance in short trials, and there was a concomitant

sex difference in VMPFC for short trial viewing periods that, as it was driven by a sizeable mean deactivation among females contrasted to a negligible mean activation for males, provided no straightforward interpretation. However, in conjunction with potential interpretations of beneficial effects of arousing, negative stimuli upon performance, the VMPFC-based sex difference could reflect a lack of emotional engagement leading to less efficient switching default mode and performance-demanded (e.g., salience, central executive) network activations.

No nonlinear associations with age were seen within targeted analyses of subcortical regions most commonly implicated in adolescence-specific hyper-reactivity to emotionally salient stimuli.

Along with Chapter 1, this chapter presented a comprehensive accounting of the timing study as it was designed to be analyzed. There are, however, other ways to make beneficial use of the same data, and the following chapter presents an attempt to use the interval timing data to perform a conceptual replication and extension of a recent study purporting to provide evidence for the NAcc's role in processing negatively valenced stimuli.

Chapter 3. The Role of Arousal Upon Bivalent Stimulus Processing Within the Nucleus Accumbens

Introduction

The purpose of scientific research is to develop an array of models of how the world works, and then to rigorously, perhaps aggressively, attempt to falsify those models in service of creating more and more accurate descriptions of the natural world (Popper, 1959/2002). This fundamental process of proposal, revision, and expansion has of course played itself out many times over within all fields of scientific inquiry, and the field of affective neuroscience is no exception. There is currently a debate over the primary role of the nucleus accumbens (NAcc) in processing emotionally or motivationally relevant stimuli, with some groups favoring a model of NAcc function as responding nearly exclusively to appetitive information, while others argue that hedonic valence is less important and propose models wherein NAcc responds to any stimulus that contributes to instrumental learning and goal attainment. This study is focused on the NAcc and uses interval timing task data as described in the previous two chapters, but a brief history of a similar recent (and ongoing) debate over amygdala functioning provides a worthwhile backdrop of parallel issues.

Following the legacy of Broca (1878), the first half of the 20th century saw seminal work by Jakob (1907/1908), Bard (1928), Cannon (1929), Papez (1937), and MacLean (1949) describing the roles of subcortical (e.g., amygdala, hippocampus, hypothalamus, basal ganglia) and medial cortical structures (e.g., cingulate, orbitofrontal

cortex) on the production of motivated behaviors. Those pioneers developed the concepts of the "visceral brain" and "limbic system" that, despite their anatomical and functional ambiguities, remain informative and influential today (LeDoux, 2000; Panksepp, 1998; Triarhou, 2008). Contemporary research built upon those early forays in affective neuroscience has developed, and will continue to develop, more nuanced views of the ways in which subcortical structures influence behavior. Animal studies of drug addiction and reward learning (Kelley & Berridge, 2002; Schultz, 2000; Spear, 2000) and human studies of reward anticipation (Knutson et al., 2001; Kuhnen & Knutson, 2005; Rademacher et al., 2010) have identified the dorsal striatum (caudate and putamen) and ventral striatum (particularly NAcc), thalamus, and amygdala as important structures for learning the associations of particular behaviors with subsequent outcomes and then solidifying later re-executions of the same behaviors.

Revisions to Views on Amygdala Functioning.

Within this framework, the amygdala has generally been associated with fear conditioning, perception of negative stimuli (i.e., threats), and avoidance of aversive punishments (Davis, 1992; LeDoux, 2000). For example, rats receiving lesions to the amygdala show impairments in learning to avoid punishing conditioned stimuli (e.g., non-response to cues paired with foot shocks) as well as displaying natural fear responses to innately fear-inducing stimuli, such as predators (Davis, 2006). Adolphs and colleagues (e.g., Adolphs, Tranel, Damasio, & Damasio, 1994; Adolphs & Tranel, 1999; Tranel, Gullickson, Koch, & Adolphs, 2006) reported on a patient with amygdalar calcification lesions who could not recognize facial expressions of fear, could not make

decisions of "trustworthiness" from photographs of faces, and displayed a lack of fear responses in day-to-day situations, such as viewing scary movies.

It is clear that the amygdala is fundamentally involved in fear- and threat-related responses, but recent fMRI investigations have led to revisions of the fear/threat model of amygdala functioning and broadened the view of the amygdala's "preferred" types of stimuli. The characterization of the amygdala as a fear-specific operator is being reworked in somewhat of a return to the conceptions derived from early direct electrical stimulation studies in cats, which showed that amygdalar stimulation immediately brings on behaviors of environmental appraisal and assessment (Ursin & Kaada, 1960). For example, social phobia patients show exaggerated amygdala signaling in response to blank facial expressions (Birbaumer et al., 1998), whereas individuals with Williams syndrome, who are characteristically *not* fearful or anxious in social situations, show exaggerated amygdala activity to threat imagery only when the scenes are non-social in nature (Dodd & Porter, 2011). Beyond social information, it has been demonstrated that amygdalar responses to images of food are greater when participants are hungry than when they are sated (LaBar et al., 2001), and for cigarette smokers seeking clinical assistance with quitting, the strength of amygdalar activation while viewing smoking-related imagery positively correlates with scores on measures of attentional biases toward smoking imagery (Janes et al., 2010). Further demonstrations of amygdalar activations in response to positive and neutral stimuli that are important to enhancing task performance have indicated that the amygdala responds to a more abstract category of information: *salient* or *relevant* stimuli, with relevance capable of being defined from either a base

biological or behaviorally functional viewpoint (see Adolphs, 2008; Pessoa, 2010; and Sander, Grafman, & Zalla, 2003 for comprehensive reviews). Thus, ongoing studies of the role of the amygdala in promoting aspects of affective behavior have broadened from an early focus on threat appraisal. Similarly, current research focused on the NAcc has evolved from an initial focus on that structure's role in promoting positive incentive-related behavior.

Nucleus Accumbens and Reward-Related Processing.

For some time, the consensus view of the role of the ventral striatum (i.e., NAcc) has been that it is predisposed towards processing information associated with approach to appetitive rewards (Apicella, Ljungberg, Scarnati, & Schultz, 1991; Bowman, Aigner, & Richmond, 1996; Lavoie & Mizumori, 1994). This view rests upon a deep and well-established base of research in animals. For example, single-unit recordings in the ventral and dorsal striata of monkeys show activity in these structures when executing a task in order to receive rewards, with twice the number of neurons active in the ventral striatum compared to the dorsal striatum when the rewards were received (Apicella et al., 1991). However, the reward-specific conception of the gross nature of NAcc activity has received significant challenges and reconsiderations, similar to the recent revisions and expansions to models of amygdala functioning.

It is clear that the NAcc is fundamentally involved in processing reward-related information. The vast animal research base will not be covered here, but a brief sample of human imaging studies will be discussed. For example, one early fMRI study on the neural correlates of reward receipt investigated neural responses from cocaine-addicted

subjects during acute injection with either saline or cocaine (in a double-blind administration), while the subjects provided real-time ratings of their cravings for cocaine and the perceived rush of achieving a high from the injection (Breiter et al., 1997). Subjects who received cocaine showed robust activity in the NAcc, amygdala, hippocampus, basal forebrain, putamen, thalamus, ventral tegmental area, and cingulate. Their subjective ratings of craving were strongly positively correlated with NAcc, amygdala, and parahippocampal activity, whereas euphoric rush ratings were related to activations in the remaining structures just listed. None of these effects were found in the saline-injected subjects.

Without resorting to studying the overpowering reward effects of addictive drugs, human-subject parallels of oral juice delivery studies run in animals have shown that the anticipation of a sweet reward elicits activity in the ventral tegmental area, which projects heavily to the NAcc (O'Doherty, Deichmann, Critchley, & Dolan, 2002). Delgado, Nystrom, Fissell, Noll, and Fiez (2000) focused on the neural responses to receipt of monetary rewards with a guessing-game task. Activation in NAcc and caudate was observed for rewarded, punished, and neutral trials, but the activity was sustained for rewards and quickly diminished upon punishment or neutral feedback. Further work with this task, augmented by the inclusion of cues indicating the probability of a certain guess being correct, showed that caudate activity was not related to the hedonic value of feedback, but rather to the contingency learning aspects of the task (Delgado, Miller, Inati, & Phelps, 2005), leaving the interpretation that NAcc activity was responsible for coding hedonic information about each trial's outcome.

These studies are but a handful from the lineage of human fMRI research showing NAcc's involvement in reward-related processing. There are now more than enough individual human imaging studies on reward processing available to begin pooling results on a large scale. A recent meta-analysis (Knutson & Greer, 2008) looked at 21 human studies of outcome anticipation before decision-making and concluded that, across research groups and paradigms, the NAcc is reliably activated during 1) reward expectation, 2) approach behaviors in the face of uncertain outcomes, and 3) self-reported increases in positive arousal.

Bivalence and Salience in Nucleus Accumbens Functioning.

Such results are aligned with the model of NAcc functioning as biased only towards hedonically positive information (the "valence" model, e.g., Ikemoto & Panksepp, 1999; Schultz, 2000). However, an even broader meta-analysis of 142 fMRI studies of reward anticipation, receipt, and evaluation demonstrated that NAcc is robustly involved in processing both positive and negative outcomes, though with stronger activations for positive information (Liu, Hairston, Schrier, & Fan, 2011). Additionally, another meta-analysis of 206 fMRI studies investigating bivalent subjective value judgments showed that appetitive information processing and aversive information processing are *both* dependent upon the same array of brain regions, including dorsal and ventral aspects of the striatum, anterior cingulate cortex (ACC), posterior cingulate cortex (PCC), ventromedial prefrontal cortex (VMPFC), and the insula (Bartra et al., 2013). Such results are aligned with the model of NAcc functioning as biased towards information that is relevant to current goals or signals an outcome that is unexpected and

may help to alter behaviors to better fit the environment, regardless of hedonic value of the information (the "salience" model, e.g., Berridge & Robinson, 1998; Salamone, 1994).

Several recent lines of research have demonstrated that the NAcc is not merely sensitive to reward value but to the broader dimension of salience that reflects an individual's perspective on the worth or importance of incoming information. When rewards are made more or less salient to participants by manipulating receipt contingency (i.e., receiving rewards based either on performance—highly salient—or being explicitly dissociated from performance and based on chance alone—not salient), NAcc only responds to the rewards that can meaningfully inform future behavior rather than those that appear by chance (Zink et al., 2004). Making participants exert greater or lesser amounts of effort in order to receive the same level of reward results in lower NAcc activation during high-effort trials (Botvinick, Huffstetler, & McGuire, 2009). Altering the delay time between response and reward receipt is related to striatal activation, with larger activations to quicker receipts, whether the delays differ by just a few seconds (Gregorios-Pippas, Tobler, & Schultz, 2009; Wittmann, Lovero, Lane, & Paulus, 2010) or on the order of days and weeks (Kable & Glimcher, 2010; Marco-Pallarés, Mohammadi, Samii, & Münte, 2010).

The juice-delivery paradigm discussed above (O'Doherty et al., 2002) was elaborated through the addition of infrequent, unpredictable delays in sweet reward receipt, allowing for the evaluation of reward prediction error signals. When delivery was delayed by 4 seconds, the NAcc responded at the time of an expected, but not actual,

delivery (Pagnoni, Zink, Montague, & Berns, 2002). Additionally, the coding of prediction error within NAcc activation has been shown to be linearly related to the expected probability of reward receipt. As probability of receiving rewards increases, NAcc activation in response to reward *omission* also increases, demonstrating that NAcc is highly sensitive to unexpected (novel) situations compared to expected (routine) outcomes (Abler et al., 2006).

While such studies demonstrate differential levels of NAcc activation dependent upon salience levels, they are still concerned with reward-related information processing and thus do directly challenge the valence model of NAcc functioning. Beyond rewards, punishing or aversive stimuli have also been shown to elicit activity within the NAcc and interconnected regions. For example, application of heat directly to the back of the hand leads to a coupling of activations in NAcc and somatosensory pain-related circuitry such as the insula, thalamus, and periaqueductal grey area (Becerra et al., 2001). Similarly, cueing participants that a negative image is about to be shown to them induces greater activation in NAcc, insula, and thalamus, compared to expectations of pending positive or neutral images (Herwig et al., 2007). The NAcc is also active when using aversive stimuli as reinforcers to guide behavior (Jensen et al., 2007; Niznikiewicz, & Delgado, 2011), primarily when one can take an active role—but not a passive role—in determining future outcomes (Bar-Haim et al., 2009; Levita et al., 2012).

A Potential for Conceptual Replication and Extension.

Indeed, the findings of such studies argue for a more expansive role of NAcc signaling in motivational learning and behavioral control. Most of this literature is

concerned with instrumental learning of approach and avoidance behaviors, and a minority of it is concerned with NAcc's role in the primary experiences of appetitive and aversive stimuli. The interval timing task described in prior chapters is not designed in a way that can contribute directly to the debate on the role of NAcc in learning and conditioning, but it does offer an opportunity to add to the debate on primary emotional experiences, through a conceptual replication and extension of one of the few studies demonstrating bivalent NAcc signaling during primary experiences of valenced stimuli (Levita et al, 2009).

In that study, Levita and colleagues examined changes in BOLD response to the onset and offset of hedonically positive and negative sounds, in a young adult (ages 20-31) sample. Though the sounds were played for 2 to 6 seconds, only the initial and terminal moments (100 ms each) of the playback period were examined, in order to test the notion that NAcc responses to aversive stimuli may only be due to the experience of relief upon their disappearance. The task design also involved only passively listening to the sounds, as NAcc involvement with negative stimuli could be confounded by the role of the striatum in motor output. Levita et al. (2009) found that not only did the NAcc show BOLD activation responses to the onsets of sounds and deactivations upon their offsets regardless of valence, but also that the magnitude of NAcc signal change was larger for negative compared to positive sounds. Thus, they demonstrated that the NAcc was involved in the processing of aversive stimuli but also, importantly, that this involvement was not strictly related to relief at removing the stimulus from the

environment. The study also indicated that there are contexts in which a presumed NAcc activation bias for positive stimuli is not merely absent, but reversed.

The current set of analyses used the interval timing task data described in Chapters 1 and 2 to attempt a conceptual replication and extension to the Levita et al. (2009) study. In particular, the interval timing data set has the advantage of using stimuli that were rated not only on valence, but also on arousal, with the overall stimulus set balanced along valence and arousal dimensions. The negative recordings played to the participants in Levita and colleague's study were described as 1000 Hz tones layered onto white noise and punctuated bursts of 1000 Hz tones. In contrast, the positive sounds were recordings of wind chimes. The sounds used were clearly rated by the study's participants as distinctly negative or positive, but ratings of levels of arousal for the sounds were notably absent, as both valence and arousal have long been known to be fundamental dimensions of appetitive and aversive stimuli (Lang et al., 1999) and arousal can be taken as an analog for, or marker of, salience (Cooper & Knutson, 2008; Gerdes et al., 2010).

Without reported arousal ratings, it cannot be stated with certainty that the two stimulus sets (noise bursts and wind chimes) differed on arousal levels. However, skin conductance response (SCR) data were collected during the experiment and reported for a third of the participants. The negative sounds produced significantly greater SCRs (more than double the response magnitude) than did positive sounds, indicating that the recordings did indeed, from a physiological standpoint, come from very different regions of the arousal spectrum. Thus, the absence of an imaging analysis that incorporated both

valence and arousal ratings begs the question of whether or not the study's finding of negative > positive BOLD responses within NAcc was truly due to valence differences or to arousal differences.

In addition to incorporating arousal ratings, the interval timing task differed from Levita et al.'s in that it contained an explicit cognitive demand and motor component. While there were excellent reasons for the lack of a motor component in the Levita study, the presence of one in the interval timing task allows for a test of whether or not NAcc responses to valenced stimuli are specific to stimulus onsets or if the presence of task demands in the current study could show a shift NAcc activation profiles relative to Levita et al.'s findings.

Hypotheses

Thus, these analyses sought to answer three questions: 1) Is NAcc activity specific to stimulus onset, or is it markedly influenced by context? (here, a task to obtain rewards), 2) When NAcc activity is seen—at either onset or offset, depending on the answer to question 1—will it be greater for negative stimuli than positive stimuli?, and 3) When NAcc activity is seen, is it better explained by arousal ratings than by valence ratings? It was predicted that 1) the presence of a task would alter the activation profile of the NAcc, 2) that NAcc activations would not be greater during trials with negative stimuli compared to those with positive stimuli, and 3) that arousal ratings would indeed account for NAcc signal change above and beyond valence ratings.

Methods

All participant, task, MRI acquisition, and fMRI preprocessing procedures are the same as described in the full task analyses in Chapters 1 and 2.

MRI Analyses

Two parallel analyses were conducted: one using only image valence ratings in the model and a second that incorporated both valence and arousal ratings. The valence only model acts as a re-creation of the analysis conducted by Levita et al. (2009) and provides a within-dataset comparison of activation shifts brought about by the model incorporating arousal. Each analysis stream evaluated BOLD signal changes to just the initial 100 ms of the image displays and the 100 ms immediately following the end of the displays, which was the same duration for the onset/offset regressors used in the comparison study (Levita, personal communication).

The two studies were similar in their use of stimuli presented for shorter and longer durations. Levita et al. (2009) reported no differences in onset and offset activation profiles across their trial durations (2 to 6 seconds), so potential effects of different trial durations in the interval timing task (1 to 6 seconds) were not examined in the current analyses.

Single-subject, single-block scans were analyzed by fitting a GLM with regressors defining onset and offset points for each trial, split by image type. For the valence-only model, the image types were positive, negative, and neutral. For the valence plus arousal model, the image types were positive/high, positive/low, negative/high, negative/low, and neutral, which were then combined to create estimates of valence and arousal effects. The

same global, white matter, CSF, and motion contamination covariates of non-interest described in the Methods section in Chapter 2 were included in these analyses. An additional single regressor describing the remainder of all the task periods (e.g., reproduction, feedback) was included to ensure that onset- and offset-related variance in BOLD fluctuations was not contaminated with other task-related variance. This "task remainder" regressor also included the portion of the viewing period between the 100 ms onset and offset points, to ensure that no timepoints containing task-related variance would be included in baseline/noise comparator calculations.

Activation maps for positive, negative, high arousal, low arousal, and grand mean onsets and offsets, as well as positive versus negative and high versus low arousal for the two events, were calculated as single-subject fixed effect means across all four scanning blocks. The resulting statistical maps were resampled to 2 mm^3 resolution and registered to the MNI-152 reference brain. These standard-space parameter estimate volumes were then entered into group-level random effects analyses to obtain the onset, offset, and condition contrast means. Follow-up inquiries of NAcc-specific signal change statistics were carried out with an NAcc mask derived from the Harvard-Oxford subcortical probabilistic atlas included with FSL (**http://www.fmrib.ox.ac.uk/fsl/data/atlas-descriptions.html**), with the mask restricted to voxels that had at least a 50% chance of being classified as NAcc. All group analyses were statistically controlled for effects of sex and age. Corrections for family-wise error inflation were carried out with cluster-wise thresholding. Clusters of at least 26 voxels with minimum z values > 2.3 were considered,

and only clusters with a corrected $p < 0.05$ probability of appearing were retained (Worsley, 2001).

Results

Image Ratings

It must be reiterated that analyses in Chapter 1 demonstrated that valence and arousal were not confounded in the current study's stimulus set. High and low arousal images differed significantly on arousal ratings, and positive, negative, and neutral images all differed significantly on valence ratings. However, positive and negative images did not differ in mean arousal ratings, and high and low arousal images did not differ in mean valence ratings.

Onset and Offset Grand Means

Onset Grand Mean. The results for grand mean activations for image onset and offset were nearly identical across the valence-only and valence plus arousal pipelines. For concision of presentation, only the full model results are shown (Figure 3.1).

Signal change to image onset was robust and widespread, but did not include any portions of the basal ganglia or ventral striatum. It is not the case that activations within the striatum were present but merely subthreshold in strength; rather, striatal signal change to image onset was negative (mean *z*-stat in NAcc = -1.59). Areas that did show significant activations included dorsal aspects of the brainstem, the full extent of the occipital lobes, the temporal-occipital fusiform, posterior hippocampus, parahippocampal gyrus, angular gyrus, postcentral gyrus, supramarginal gyrus, thalamus, amygdala,

anterior insula, central and frontal operculum, VLPFC, posterior and anterior cingulate, paracingulate, and IFG.

Offset Grand Mean. Regions with significant activations upon image offset included cuneous and precuneous, superior and inferior lateral occipital cortex, lingual gyrus, intracalcarine/calcarine cortex, cerebellum (crus I), temporal-occipital fusiform, middle temporal gyrus, angular gyrus, supramarginal gyrus, thalamus, caudate, putamen, pallidum, NAcc, posterior and anterior cingulate, SMA, DLPFC, and IFG.

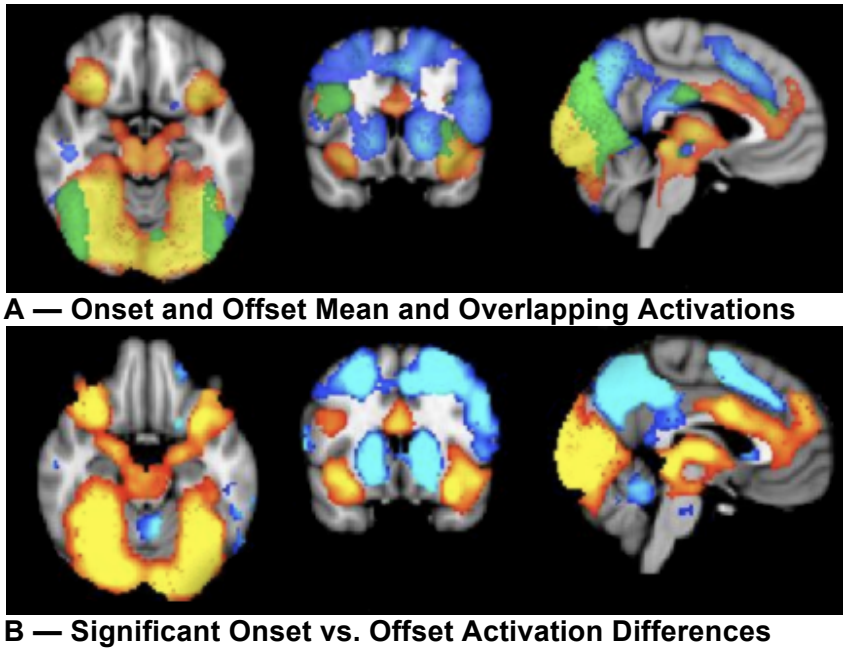

Figure 3.1: Onset and Offset Main Effects, Similarities, and Differences. (A) Grand mean activations for onset and offset were largely distinct, but overlapped in several areas. Red-yellow denotes areas with a significant activation upon image onset, blue-cyan denotes areas with significant activations upon image offset, and green denotes areas of shared activation. (B) The contrast of onset and offset activations showed that the shared activation regions seen in panel A generally had greater activations in response to image onsets. Red-yellow denotes stronger activations for onsets. Blue-cyan denotes areas with stronger activations in response to image offsets. All images cluster-wise thresholded at values of $z<2.3$, $p<0.05$. Panel A slices in MNI-152 standard space: x=-4, y=14, z=-16. Panel B slices in MNI-152 standard space: x=-2, y=14, z=-20.

Onset Versus Offset. When simply overlaid on each other, the onset and offset mean maps showed overlap within cuneous, lateral occipital cortex, lingual gyrus, temporal-occipital fusiform, middle temporal gyrus, thalamus, posterior and anterior cingulate, anterior insula, and IFG. When directly contrasted, all non-overlapping areas of activation between the two maps were statistically significantly different from each other, including activations within the NAcc being significantly greater at offset (mean z=2.84) than at onset (mean z=-1.59). Figure 3.1 presents the onset and offset grand means, their areas of overlap, and their significant differences.

Positive Image Onset Versus Negative Image Onset

Valence Only Model. Within the valence-only model, there were significant differences between BOLD responses to positive and negative image onsets. Positive image onsets produced stronger activations within cuneous and precuneous, right lingual gyrus, anterior cingulate, paracingulate, and right DLPFC/frontal pole. Negative image onsets produced greater activations within left inferior lateral occipital cortex, left temporal-occipital fusiform, left angular gyrus, left anterior supramarginal gyrus, left precentral gyrus, left posterior insula, and left amygdala (Figure 3.2 A).

Valence and Arousal Model. When arousal was added to the model, the positive > negative onset map (Figure 3.2 B) added new clusters within occipital pole and inferior precuneous, completely lost suprathreshold clusters in right DLPFC and right lingual gyrus, and showed slight reductions to the size of the clusters within anterior cingulate and cuneous. The negative > positive onset map added to the size of the supramarginal gyrus cluster, and completely lost the clusters in left inferior lateral occipital cortex, left

temporal-occipital fusiform, and left amygdala. The overall downward signal change in NAcc at the time of image onsets was not due to one image type showing activations while the other showed stronger deactivations. The mean NAcc signal change values for the onsets were below zero for both positive (mean z=-1.41) and negative (mean z=-1.61) images.

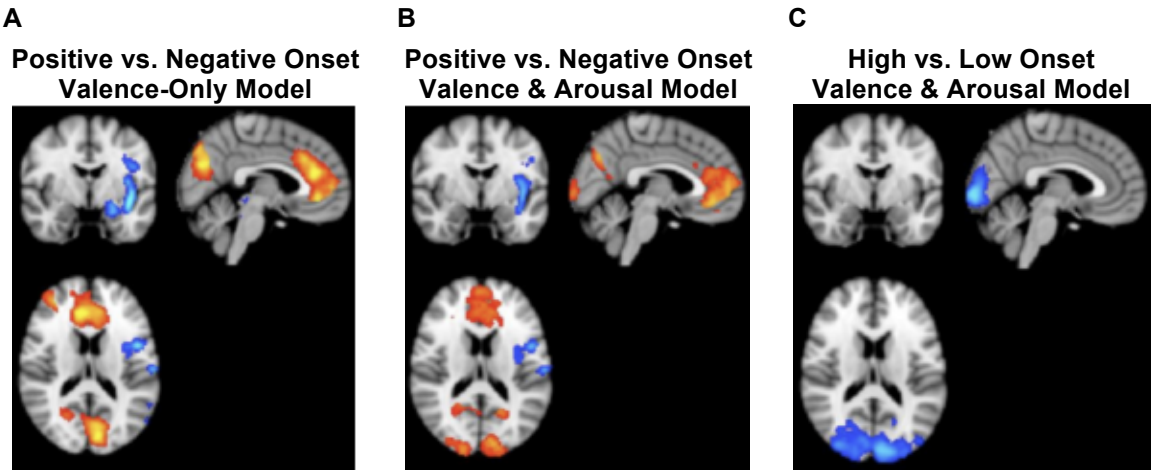

Figure 3.2: Valence and Arousal Effects Upon Image Onset Activations. (A) The contrast of activations to image onset between positive and negative images, within the valence-only analysis stream. Red-yellow denotes areas with stronger activations for positive images; blue-cyan denotes areas with stronger activations for negative images. (B) Attenuated positive vs. negative image onset effects from within the full model (valence plus arousal) analysis stream. Red-yellow denotes areas with stronger activations for positive images; blue-cyan denotes areas with stronger activations for negative images. (C) Effects of arousal upon image onsets, from the full model analysis. No high arousal > low arousal activations were seen. Blue-cyan denotes areas where low arousal image onsets led to stronger activations. All images cluster-wise thresholded at values of $z<2.3$, $p<0.05$. Slices in all panels are in MNI-152 standard space: x=4, y=-2, z=16.

High Arousal Image Onset Versus Low Arousal Image Onset

Though the inclusion of arousal accounted for variance in ways that altered the thresholded statistical maps for the positive versus negative comparisons, the "lost"

clusters did not simply transfer into the high > low arousal and low > high arousal maps (Figure 3.2 C). In fact, there were no suprathreshold voxels for high > low arousal onsets, and the low arousal onsets only showed greater activations within occipital pole. Investigations of signal change statistics within NAcc showed that both high and low arousal images produced below-zero mean values, but with nominally more negative values for high arousal images (mean z=-2.08) than for low arousal images (mean z=-0.71).

Positive Image Offset Versus Negative Image Offset

Valence Only Model. In the valence-only pipeline, contrasts of activations upon positive and negative image offsets still did not show differences within basal ganglia structures (Figure 3.3 A). Though positive image offsets did show nominally stronger activations within NAcc (mean z=3.89) compared to negative image offsets (mean z=2.38), the difference did not pass thresholding procedures. There was one significant positive > negative cluster, covering right inferior lateral occipital cortex and right cerebellum (crus I). Clusters showing significant negative > positive offset activations were found in intracalcarine cortex and lingual gyrus.

Valence and Arousal Model. When arousal was added to the model, the positive > negative offset activation map added a left hemisphere cluster across cerebellum (crus I) and inferior lateral occipital cortex (a contralateral analog to the cluster noted above), as well as a cluster across dorsal aspects of cuneous and precuneous (Figure 3.3 B). Accounting for arousal also caused all negative > positive offset activations to fall below threshold. Compared to the mean z statistics in the valence only model, accounting for

arousal variance reduced the strength of activations upon image offset for both positive (mean z=2.76) and negative (mean z=1.96) images.

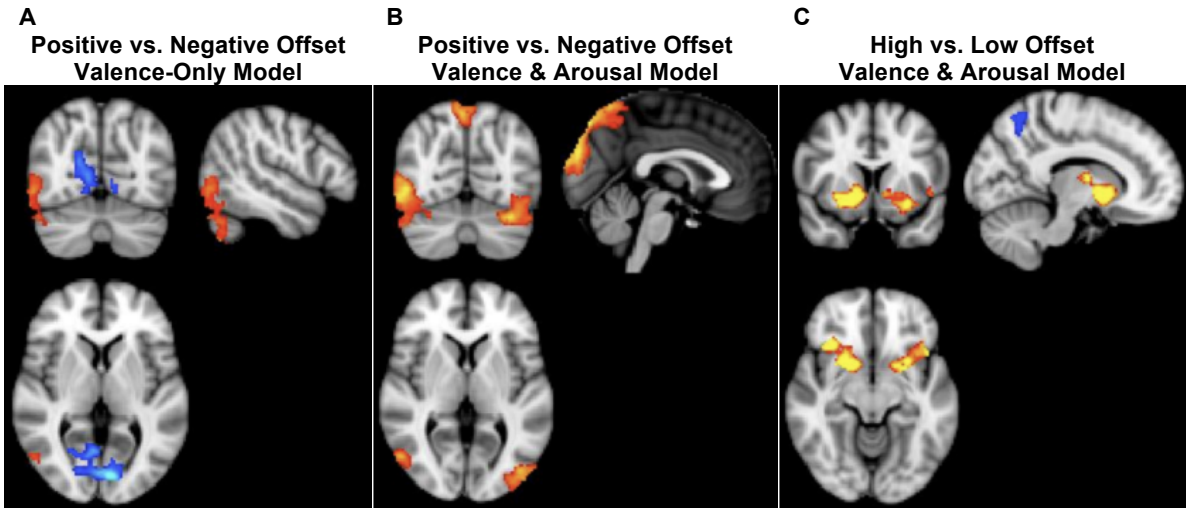

Figure 3.3: Valence and Arousal Effects Upon Image Offset Activations. (A) The contrast of activations to image offset between positive and negative images, within the valence-only analysis stream. Red-yellow denotes areas with stronger activations for positive images; blue-cyan denotes areas with stronger activations for negative images. Slices: x=50, y=-68, z=4. (B) Enhanced positive offset activations and reduced negative offset activations were seen with the addition of arousal to the analysis model. Red-yellow denotes areas with stronger activations for positive images. No negative > positive effects were seen. Slices: x=0, y=-68, z=4. (C) Effects of arousal upon image offsets, from the full model analysis. Markedly stronger activations were seen within basal ganglia, including NAcc, for high arousal image offsets (red-yellow). Blue-cyan denotes areas where low arousal image onsets led to stronger activations. Slices: x=12, y=10, z=-10. All images cluster-wise thresholded at values of z<2.3, p<0.05. Slices in all panels are in MNI-152 standard space.

High Arousal Image Offset Versus Low Arousal Image Offset

The offset of low arousal images only produced greater activations in precuneous, compared to the offset of high arousal images (Figure 3.3 C). However, the high > low arousal contrast yielded significant clusters within thalamus, pallidum, putamen, caudate, NAcc, insula, VLPFC, frontal operculum, IFG, and DLPFC/frontal pole. Both high

arousal and low arousal image offsets led to positive signal changes within NAcc, though more strongly for high arousal images (mean z=3.84) than for low arousal images (mean z=0.93).

Overall, NAcc activations were not seen upon onset of images, but were seen upon the offset of images. The offset-related activations were stronger for high arousal images compared to low arousal images, but did not differ between positive and negative images (Table 3.1).

Table 3.1
Mean z statistics for NAcc signal changes for each image type and in aggregate.

	Onset Signal Change *z* statistics M(SD)	Offset Signal Change *z* statistics M(SD)
Positive	-1.41 (2.38)	2.76 (1.21)
Negative	-1.61 (2.92)	1.96 (2.05)
High Arousal	-2.08 (2.68)	3.84 (1.42)
Low Arousal	-0.71 (2.59)	0.93 (1.68)
All Images	-1.60 (3.13)	2.84 (1.93)

Discussion

This study sought to perform a conceptual replication and extension of a prior report of bivalent activation profiles within the nucleus accumbens, by designing analyses to answer three main questions: 1) Is NAcc activity specific to stimulus onset, regardless of stimulus valence?, 2) When NAcc activity is seen (either upon onset or offset), is it greater for negative stimuli or positive stimuli?, and 3) Is NAcc activity elicited by stimulus presentation better explained by arousal ratings than by valence ratings?

Main Effects of Onset and Offset

The main effect analyses sought to answer the first research question, regarding the possibility of context-irrespective specificity of NAcc activation to the onset of valenced stimuli. Prior research has shown that NAcc activity is highly sensitive to outcome and performance differences, such as the predictability of rewards (Zink et al., 2004) or the amount of effort required to receive rewards (Botvinick et al., 2009). However, such alterations of activity are usually seen during processes of learning reward contingencies or decision-making, not necessarily to the primary experience of inherently appetitive or aversive stimuli without demands of complex associative learning or decision-making. The current results confirm that NAcc responses to transient displays of valenced stimuli are also sensitive to the larger context within which those stimuli are presented, and that Levita and colleagues were well-advised to remove any motor component from their experimental design when attempting to address the concern that NAcc offset-related activation could be affected by the presence of instrumental behavior. If Levita et al.'s results are representative of the NAcc's primary response to valenced stimuli, then the current study's results support the notion that other cognitive demands alter the responsivity of NAcc and can shift its activation profiles.

Positive Versus Negative Image Activations at Offset

According to these results, the answer to the second research question, whether or not onset/offset NAcc responses would be greater for negative compared to positive images, was no. NAcc activations were only seen upon image offsets. Though there was a nominal difference of positive > negative NAcc offset values (Table 3.1), the difference

was not statistically significant. Thus, the experience of viewing positive versus negative images did not alter NAcc activation levels upon image offset.

Certainly, the major difference of task/no task precludes straightforwardly interpreting offset activations within this dataset to the offset results of the Levita et al. comparison study. Participants performing the interval timing task were gearing up to perform their interval reproductions upon image offset, so the interpretation that NAcc activity at image offset within the interval timing task is solely due to the perception and experience of appetitive or aversive content is not supportable. However, to the extent that the appetitive and aversive content across image types was responsible for making the timing task more or less difficult to perform (as the behavioral results reported in Chapter 1 confirm), it would be reasonable to assume that brain regions that are implicated in emotional perception and experience and are also recruited by the task would have their activation levels either potentiated or dampened during task performance as a results of the stimulus content (a general assumption of many affective neuroscience experiments). Under that assumption, the lack of activation differences within NAcc for the offset of positive and negative images can be interpreted to support Levita and colleagues' results that the NAcc has significant roles in the processing of both appetitive and aversive information—that there is a bivalent side to the NAcc. The lack of a difference also indicates that there may have been something particular to the Levita et al. experimental stimuli that was responsible for the negative > positive NAcc activation finding. Thus, the answer to the second question then begs the third question in this study, on the role that arousal levels can play in altering NAcc activations.

High Arousal Versus Low Arousal Image Activations at Offset

The third research question in this study asked whether or not arousal levels would provide a better explanation of NAcc activity than valence levels. The answer was yes. When arousal levels were included in the fMRI analysis model, the main effect onset and offset findings did not change, indicating that the extra regressors did not fundamentally alter the nature of variance being accounted for at the grand mean level (e.g., through introducing multicollinearity). However, accounting for arousal variance clearly showed that high arousal images were associated with significantly greater NAcc activations upon image offset than low arousal images were, regardless of valence. In fact, as the images disappeared and participants prepared to perform their interval reproductions, the high arousal trials showed greater activations across multiple subcortical and PFC regions, indicating that high arousal image viewing either required "extra" neural processing or potentiated the activity already underway in those regions. Furthermore, introducing arousal into the model reduced the values of valence-related NAcc signal change statistics but did not change the underlying relationship of positive versus negative trial NAcc activations at offset; NAcc activations at offset were still present for both positive and negative trials, and they were still not significantly different from each other.

Thus, arousal levels accounted for the differences in NAcc activations, not valence levels. This suggests that the Levita et al. (2009) findings may have been due to comparing the effects of experiencing a high arousal stimulus (bursts of white noise and pure tones) to those of a low arousal stimulus (wind chimes).

Limitations

The largest limitation upon this study's aims to replicate and extend Levita and colleagues' (2009) findings is that the analysis was conducted post-hoc and within the presence of a cognitive task. The interpretation here is that such a presence can alter the timing and profile of NAcc's responses to strongly valenced stimuli. This interpretation comes from making a task/no task comparison across results of separate studies, but the strongest test of this hypothesis would come from a comparison of task/no task conditions within the same subjects. Without such a within-subjects comparison, it could be argued that the NAcc activations shown here are not related to emotional experiences but are instead related to "cool" cognitive processes. However, as noted above, the behavioral analyses of the interval timing task (Chapter 1) demonstrated that manipulations of image valence and arousal brought about alterations in task performance, and prior fMRI studies of interval timing have not implicated NAcc as a key component of a timing network (cf. Buhusi & Meck, 2005). Thus, the cross-study comparison cannot be negated on the argument that the stimuli used in the interval timing task did not layer emotional experiences on top of the task-related cognitive processing.

A notable difference between the two studies is within sample demographics. The interval timing study was designed as a developmental study, whereas Levita et al. (2009) recruited young adults. In these analyses, age was included as a covariate, in order to derive group mean effects that were statistically independent of any age-related effects. This sets the interpretation of the grand means as the activations expected of a person at the mean age of the sample (here, 17.22 years), which leaves open the possibility that the

cross-study differences could be reflected in part by effects of continued development into young adulthood. Additionally, the fMRI results in Chapter 2 showed several sex differences in the full task fMRI analyses, leaving the possibility that sex differences contributed to the current findings. However, as with age, participant sex was statistically controlled in the current group mean analyses. Additionally, the age and sex differences in Chapter 2 were not seen within NAcc, the focus of the current study.

Conclusions

The notion that NAcc is deeply involved in both positive and negative information processing is supported by these analyses. Thus, the findings from this set of analyses do not negate or fundamentally contradict the basic conclusion Levita et al. (2009) drew from their results, that NAcc has a bivalent side and can be active in the presence of (and in response to) both appetitive and aversive stimuli. However, these results indicate that explaining Levita et al.'s (2009) findings solely through a discussion of stimulus valence may be mistaken. The benefit provided by the current study is an analytical extension that helps to explain how the NAcc, so commonly regarded as a positivity-biased structure, can be induced to show stronger responses to negative than to positive stimuli. Namely, that differing levels of stimulus salience (i.e., arousal), regardless of stimulus valence, will differentially affect NAcc signaling in ways that are more important than valence manipulations.

These results are aligned with the salience model of NAcc functioning and give support to the expanded view, which, like the recently expanded view of amygdala functioning, proposes that the strength of activations within neural structures involved in

using environmental information to modulate and guide one's future actions (NAcc included) will be determined primarily by the degree to which one finds that information to be important, necessary, or instrumentally advantageous.

It should be noted, however, that some research groups argue that the valence and salience models of NAcc function are not mutually exclusive and that both models could simply be aspects of yet another unifying model purporting that NAcc has multiple functional roles, which could include evaluating both hedonic valence and motivational salience (Brooks & Berns, 2013; McClure, Daw, & Montague, 2003). Based on the variety of substructures within the NAcc and the complex network of connections to and from NAcc (Haber & Knutson, 2010; Sesack & Grace, 2010), such a multifactorial functioning view is possible. The articulation of such a model is in the very early stages (Humphries & Prescott, 2010), though with continued challenges, revisions, and expansions to current views, such a model may soon become fully fleshed out and ready for testing of its own.

General Summary and Discussion

Adolescence is a time of transition between childhood and adulthood, both in terms of physical characteristics and in terms of cognitive and emotional functioning, and it is marked by increases in responsivity to hedonically arousing information as well as novelty-seeking, social affiliation, and risk-taking (Spear, 2000). These changes can lead to beneficial behaviors but also carry substantial risks, such as difficulty regulating emotional responses or controlling dysfunctional reward-seeking behavior. Mitigating the risks posed by the functional reorganizations of adolescent behaviors, and maximizing their benefits, requires the capacity for, and execution of, motivational control.

Recently, much research has focused on the construction of models outlining the neurobiological changes underlying the development of motivational control. The common theme among these models is a specific emphasis on the interactions between subcortical and prefrontal brain regions, as differences in the maturational rates of these structures implies that adolescence may be a time of reduced functional integration among them (Ernst et al., 2009; Luna, 2009; Somerville et al., 2010; Steinberg, 2010). Specifically, these lines of research have delineated important roles for brain regions such as the nucleus accumbens (NAcc) and the amygdala in reflexive responses to the immediate presence of hedonic stimuli (which may lead to rash or poorly-planned behaviors), whereas regions within the prefrontal cortex are implicated in reflective, planful behaviors in the service of long-term goal achievement.

However, studies of adolescent reward responsiveness and emotional control do not often use paradigms that elicit appetitive and aversive information processing within the context of demands for executive control. The development of such a task was an explicit goal of this dissertation, with the additional intentions of using the task within a developmental sample to better understand 1) the extent to which control processes can be exerted under different emotional conditions, 2) the neural correlates of such processes, and 3) the alteration of these processes by development across adolescence. Thus, the interval timing task was created, which at its core required executive attention and control, but also had the additional manipulation of requiring participants to view affect-laden images while performing the task.

The behavioral analyses described in Chapter 1 of this dissertation showed that the image content manipulations successfully altered participants' abilities to experience and reproduce discrete time intervals through combinations of strongly and weakly valenced stimuli. The task was built with expectations that valence and arousal levels would have independent effects upon interval timing abilities. Valence effects were robust, however, arousal levels alone did not markedly influence task performances. Rather, strong arousal effects were present only in interaction with valence.

Among the parallels between the behavioral analyses in Chapter 1 and the fMRI analyses in Chapter 2, image valence had a strong influence upon task performance and was accompanied by the engagement of disparate neural structures, as shown between contrasts of positive, negative, and neutral image trials. Additionally, the neural correlates of overall task performance were different between positive and negative trials,

with effects driven particularly by apparent requirements for increased PFC-mediated control on positive, high arousal trials. Thus, for valence the presence of behavioral differences was accompanied by neural differences that were a matter of kind, not just degree. However, there was also evidence that differences in degree of activation were related to differences in behaviors, particularly across arousal levels.

Notably, the activation contrast maps comparing brain activations for the viewing of negative > positive and high arousal > low arousal images were markedly similar. Both showed extensive activations within regions involved in the detection of salient stimuli, underscoring the preferential access that negative stimuli have to the brain's salience-detection network. The examination of valence × arousal interactions in the behavioral analyses showed that it was easier to be successful on negative, high arousal trials compared to negative, low arousal trials, in line with expectations that heightened activation of the salience network facilitates subsequent engagement of task-required, central executive control networks (Menon & Uddin, 2010). However, the contrast of subsequent reproduction periods for negative/high greater than negative/low trials did not show significant differences within cortical central executive regions, but rather within a cerebellar region (crus II) that is structurally associated with prefrontal cortex and functionally involved in working memory (Stoodley & Schmahmann, 2009).

The importance of stimulus salience (i.e., arousal ratings) to neural activation profiles was also shown within the alternative task analyses described in Chapter 3. These secondary analyses sought to inform the current debate over the specificity of NAcc activation to appetitive information versus a broader view of NAcc being activated by the

presence of motivationally salient information, regardless of hedonic valence. Through the comparison of two analysis streams, one accounting only for valence and the other accounting for valence and arousal, it was demonstrated that the strength of NAcc activations was better accounted for by arousal levels, and that the amount of BOLD signal variance within salience network regions (i.e., amygdala) previously attributed to negative valence was attenuated by the inclusion of arousal in the analysis model.

Beyond the creation of a task that reliably engaged attentional, motivational, and cognitive control structures, this dissertation sought to employ the task within a developmental sample to test hypotheses of nonlinear developmental effects upon neural responses to highly arousing stimuli. Based on a review of the literature, the presence of such nonlinear associations between age and BOLD signal within specific regions of interest (ROIs) of NAcc, amygdala, and insula were expected, particularly within trials containing highly arousing images. However, no such relationships were found. Rather, only linear relationships between age and BOLD signal changes were seen in response to viewing images during long trials. While the regions showing a positive correlation between age and signal change contained multiple subcortical structures, including thalamus, caudate, putamen, pallidum, and the ventral tegmental area, that are functionally and structurally related to the target ROIs, the clusters of significantly correlated voxels did not extend into NAcc, insula, or amygdala.

Potential explanations for the lack of nonlinear age relationships were thoroughly discussed in Chapter 2. Primary among potential explanations are 1) the use of an underlying executive control task with incidental emotionally salient stimuli rather than a

task that requires reward-related decision-making, reward anticipation, or reward contingency learning (Richards et al., 2013), 2) the potential that the presence of post-task performance incentives may have prompted the marshaling of extra control resources within adolescents (Casey et al., 2010), and 3) the age range chosen to represent adolescence (Herdt & McClintock, 2000; Petersen, Silbereisen, & Soerensen, 1993). Regardless, the presence of linear age relationships, coupled with a lack of nonlinear age relationships, within the interval timing data can be informative to the broader study of adolescent cognitive and emotional development.

The increases in potentially negative behavioral changes (e.g., sensation-seeking, risk-taking) noted at the opening of this section can have dire consequences. For example, over two-thirds of adolescent deaths are caused by unintended injuries (Centers for Disease Control and Prevention, 2010). Additionally, adolescence is a period in life that carries an overall two-fold increase in rates of mortality and psychiatric morbidity (Dahl, 2004), particularly for the onset of substance use disorders (Chambers et al., 2003) and mood disorders (Kessler et al., 2005). However striking such statistics are, they belie the fact that adolescence is also a time of rapid cognitive skill acquisition that allows increasingly proficient problem-solving and planning abilities (Luciana, Conklin, Hooper, & Yarger, 2005; Luna et al., 2001; Steinberg & Cauffman, 1996), and that adolescents can regularly demonstrate adult-level abilities to properly assess risk, exert control over their motivated behaviors across many situations, and perform complex decision-making tasks within calm, rational contexts (Reyna & Farley, 2006).

As important as it is to understand the ways in which adolescents' increased drives for seeking out novel and rewarding experiences can lead to negative outcomes, it is equally important to understand when those drives are not expressed or when they do not lead to detrimental behaviors. That is to say, knowing when things go right for adolescents is as important as knowing when things go wrong. Thus, the lack of adolescent-specific neural hyperactivity to valenced stimuli within the present study was certainly against expectations laid out during study design, but it does not represent a failure in describing adolescent behavior. Instead of a task that can demonstrate times when adolescents are unable to exert sufficient motivational and cognitive control, the interval timing task turned out to be one that followed the expected linear increase in executive control task performance capacity (Best et al., 2009; Davidson et al., 2006; Luciana & Nelson, 2002; Luciana et al., 2005) and also showed concomitant linear age relationships within the fMRI data. This is not to say that the interval timing task was unsuccessfully designed and was purely a cognitive control task, as the valence and arousal manipulations did clearly impact performance and bring about differential changes within attention, motivation, and cognitive control brain networks.

Thus, the "When can things go right?" side of the equation turned out to be the starting point for research employing the interval timing task in the study of adolescent motivational control. Seeking answers to the "When can things go wrong?" side will be the charge for future work, perhaps using alterations to the task design as described in the Discussion section of Chapter 2, such enhancing anticipation before the display of

valenced stimuli or receipt of rewards, or increasing the monetary stakes of winning and losing performances.

Models of maturational disconnects and functional imbalances within the brains of adolescents are well suited to the generation of knowledge on the biological sources of problematic and costly adolescent behaviors. However, this study adds to the growing body of literature (cf. Pfeifer & Allen, 2012) indicating that such imbalance models should not be assumed to be the de facto state of functioning for adolescents confronted with emotionally engaging stimuli. As common as it is to pathologize adolescence, it must be remembered that the majority of individuals not only survive this period of life but also thrive, successfully navigating the transition into adulthood with minimal risk exposure. Thus, while psychological research often characterizes the "teen brain" as one that generates unbridled impulsivity and chronically suboptimal decision-making, from a population mode standpoint, it is imperative to keep in mind that, while the "teen brain" is one that that certainly does carry an enhanced potential for expressing injurious impulsiveness and making detrimental decisions, it also holds the capacity to act appropriately and planfully, with the promise of continued refinement in cognitive and emotional control.

References

Abler, B., Walter, H., Erk, S., Kammerer, H., & Spitzer, M. (2006). Prediction error as a linear function of reward probability is coded in human nucleus accumbens. *NeuroImage*, *31*, 790–795.

Adleman, N. E., Menon, V., Blasey, C. M., White, C. D., Warsofsky, I. S., Glover, G. H., et al. (2002). A developmental fMRI study of the Stroop color-word task. *NeuroImage*, *16*, 61–75.

Adolphs, R. (2008). Fear, faces, and the human amygdala. *Current Opinion in Neurobiology*, *18*, 166–172.

Adolphs, R., & Tranel, D. (1999). Preferences for visual stimuli following amygdala damage. *Journal of Cognitive Neuroscience, 11,* 610–616.

Adolphs, R., Tranel, D., Damasio, H., & Damasio, A. (1994). Impaired recognition of emotion in facial expressions following bilateral damage to the human amygdala. *Nature*, *372*, 669–672.

Angrilli, A., Cherubini, P., Pavese, A., & Manfredini, S. (1997). The influence of affective factors on time perception. *Perception and Psychophysics*, *59*, 972–982.

An, X., Bandler, R., Ongür, D., & Price, J. L. (1998). Prefrontal cortical projections to longitudinal columns in the midbrain periaqueductal gray in macaque monkeys. *The Journal of Comparative Neurology*, *401*, 455–479.

Andersson, J., M. Jenkinson, and S. Smith (2010), Non-linear registration, aka spatial normalisation. FMRIB technical report, available from http://fsl.fmrib.ox.ac.uk/analysis/techrep/tr07ja1/

Apicella, P., Ljungberg, T., Scarnati, E. & Schultz, W. (1991). Responses to reward in monkey dorsal and ventral striatum. *Experimental Brain Research*, *85*, 491–500.

Aupperle, R. L., & Paulus, M. P. (2010). Neural systems underlying approach and avoidance in anxiety disorders. *Dialogues in Clinical Neuroscience*, *12*, 305–319.

Bar-Haim, Y., Fox, N. a, Benson, B., Guyer, A. E., Williams, A., Nelson, E. E., Perez-Edgar, K., et al. (2009). Neural correlates of reward processing in adolescents with a history of inhibited temperament. *Psychological Science*, *20*, 1009–1018.

Bard, P. (1928). A diencephalic mechanism for the expression of rage with special reference to the sympathetic nervous system. *American Journal of Physiology*, *84*, 490–515.

Bartra, O., McGuire, J. T., & Kable, J. W. (2013). The valuation system: A coordinate-based meta-analysis of BOLD fMRI experiments examining neural correlates of subjective value. *NeuroImage*, *76*, 412–427.

Baumrind, D. (1987). A developmental perspective on adolescent risk taking in contemporary America. In Irwin Jr., C. E. (Ed.). *Adolescent social behavior and health*. San Francisco: Jossey-Bass.

Becerra, L., Breiter, H. C., Wise, R., Gonzalez, R. G., & Borsook, D. (2001). Reward circuitry activation by noxious thermal stimuli. *Neuron*, *32*, 927–946.

Berntson, G. G., Norman, G. J., Bechara, A., Bruss, J., Tranel, D., & Cacioppo, J. T. (2011). The insula and evaluative processes. *Psychological Science*, *22*, 80–86.

Berridge, K. C., & Robinson, T. E. (1998). What is the role of dopamine in reward: hedonic impact, reward learning, or incentive salience? *Brain Research Reviews*, *28*, 309–369.

Best, J. R., Miller, P. H., & Jones, L. L. (2009). Executive functions after age 5: Changes and correlates. *Developmental Review*, *29*, 180–200.

Birbaumer, N., Grodd, W., Diedrich, O., Klose, U., Erb, M., et al. (1998). fMRI reveals amygdala activation to human faces in social phobics. *NeuroReport*, *9*, 1223–1226.

Bjork, J. M., Knutson, B., Fong, G. W., Caggiano, D. M., Bennett, S. M., & Homer, D. W. (2004). Incentive-elicited brain activation in adolescents: Similarities and differences from young adults. *The Journal of Neuroscience*, *24*, 1793–1802.

Bjork, J. M., Smith, A. S., Chen, G., & Hommer, D. W. (2010). Adolescents, adults, and rewards: Comparing motivational neurocircuitry recruitment using fMRI. *PLoS One*, *5*, e11440.

Botvinick, M. M., Huffstetler, S., & McGuire, J. T. (2009). Effort discounting in human nucleus accumbens. *Cognitive, Affective, & Behavioral Neuroscience*, *9*, 16–27.

Bourgeois, J., Goldman-Rakic, P. S., & Rakic, P. (1994). Synaptogenesis in the prefrontal cortex of rhesus monkeys. *Cerebral Cortex*, *4*, 78–96.

Bowman, E. M., Aigner, T. G. & Richmond, B. J. (1996). Neural signals in the monkey ventral striatum related to motivation for juice and cocaine rewards. *Journal of Neurophysiology*, *75*, 1061–1073.

Breiter, H. C., Gollub, R. L., Weisskoff, R. M., Kennedy, D. N., Makris, N., Berke, J. D., et al. (1997). Acute effects of cocaine on human brain activity and emotion. *Neuron*, *19*, 591–611.

Broca, P., 1878. Anatomie comparée des circonvolutions cérébrales: Le grand lobe limbique et la scissure limbique dans la série des mammifères. *Revue d'Anthropologie - Deuxième Série (Paris)*, *1*, 385–498.

Brooks, A. M., & Berns, G. S. (2013). Aversive stimuli and loss in the mesocorticolimbic dopamine system. *Trends in Cognitive Sciences*, *17*, 281–286.

Buhusi, C. V., & Meck, W. H. (2005). What makes us tick? Functional and neural mechanisms of interval timing. *Nature Reviews Neuroscience*, *6*, 755–765.

Bunge, S. A., Dudukovic, N. M., Thomason, M. E., Vaidya, C. J., & Gabrieli, J. D. E. (2002). Immature frontal lobe contributions to cognitive control in children: Evidence from fMRI. *Neuron*, *33*, 301–311.

Burgess, P. W., Veitch, E., de Lacy Costello, a, & Shallice, T. (2000). The cognitive and neuroanatomical correlates of multitasking. *Neuropsychologia*, *38*, 848–863.

Cannon, W. B. (1929). *Bodily Changes in Pain, Hunger, Fear, and Rage: An Account of Recent Researches into the Function of Emotional Excitement*. New York and London: D. Appleton and Company.

Carver, A. C., Livesey, D. J., & Charles, M. (2001). Age related changes in inhibitory control as measured by stop signal task performance. *The International Journal of Neuroscience*, *107*, 43–61.

Casey, B. J., Jones, R. M., & Hare, T. A. (2008). The adolescent brain. *Annals of the New York Academy of Sciences*, *1124*, 111–126.

Casey, B. J., Duhoux, S., & Malter Cohen, M. (2010). Adolescence: What do transmission, transition, and translation have to do with it? *Neuron*, *67*, 749–760.

Casey, B. J., Trainor, R. J., Orendi, J. L., Schubert, A. B., Nystrom, L. E., Giedd, J. N., et al. (1997). A developmental functional MRI study of prefrontal activation during performance of a go-no-go task. *Journal of Cognitive Neuroscience*, *9*, 835–847.

Centers for Disease Control and Prevention, National Center for Injury Prevention and Control. (2010). "Unintentional Injuries, Violence, and the Health of Young People." Available at http://www.cdc.gov/healthyyouth/injury/facts.htm

Chambers, R. A., Taylor, J. R., & Potenza, M. N. (2003). Developmental neurocircuitry of motivation in adolescence: A critical period for addiction vulnerability. *American Journal of Psychiatry*, *160*, 1041–1052.

Chein, J., Albert, D., O'Brien, L., Uckert, K., & Steinberg, L. (2010). Peers increase adolescent risk taking by enhancing activity in the brain's reward circuitry. *Developmental Science*, F1–F10, DOI: 10.1111/j.1467-7687.2010.01035.x

Cohen-Gilbert, J. E., & Thomas, K. M. (In press). Inhibitory control during emotional distraction across adolescence and early adulthood. *Child Development*. doi:10.1111/cdev.12085

Cooper, J. C., & Knutson, B. (2008). Valence and salience contribute to nucleus accumbens activation. *NeuroImage*, *39*, 538–547.

Craig, A. D. (2009a). How do you feel--now? The anterior insula and human awareness. *Nature Reviews Neuroscience*, *10*, 59–70.

Craig, A. D. (2009b). Emotional moments across time: A possible neural basis for time perception in the anterior insula. *Philosophical transactions of the Royal Society of London. Series B, Biological sciences*, *364*, 1933–1942.

Dahl, R. E. (2004). Adolescent brain development: A period of vulnerabilities and opportunities. *Annals of the New York Academy of Sciences*, *1021*, 1–22.

Dale, A. M. (1999). Optimal experimental design for event-related fMRI. *Human Brain Mapping*, *8*, 109–114.

Damoiseaux, J. S., Rombouts, S. a R. B., Barkhof, F., Scheltens, P., Stam, C. J., Smith, S. M., & Beckmann, C. F. (2006). Consistent resting-state networks across healthy subjects. *Proceedings of the National Academy of Sciences of the United States of America*, *103*, 13848–13853.

Davidson, M. C., Amso, D., Cruess Anderson, L., & Diamond, A. (2006). Development of cognitive control and executive functions from 4 to 13 years: Evidence from manipulations of memory, inhibition, and task switching. *Neuropsychologia*, *44*, 2037–2078.

Davis, M. (1992). The role of the amygdala in fear and anxiety. *Annual reviews of Neuroscience*, *15*, 353–375.

Davis, M. (2006). Neural systems involved in fear and anxiety measured with fear-potentiated startle. *American Psychologist*, *61*, 741–756.

Delgado, M. R., Miller, M. M., Inati, S., & Phelps, E. A. (2005). An fMRI study of reward-related probability learning. *NeuroImage*, *24*, 862–873.

Delgado, M. R., Nystrom, L. E., Fissell, C., Noll, D. C., & Fiez, J. A. (2000). Tracking the hemodynamic responses to reward and punishment in the striatum. *Journal of Neurophysiology*, *84*, 3072–3077.

Dodd, H. F., & Porter, M. A. (2011). There's that scary picture: Attention bias to threatening scenes in Williams syndrome. *Neuropsychologia*, *49*, 247–253.

Droit-Volet, S., & Meck, W. H. (2007). How emotions colour our perception of time. *Trends in Cognitive Sciences*, *11*, 504–513.

Ernst, M., & Fudge, J. L. (2009). A developmental neurobiological model of motivated behavior: Anatomy, connectivity and ontogeny of the triadic nodes. *Neuroscience and Biobehavioral Reviews*, *33*, 367–382.

Ernst, M., & Paulus, M. P. (2005). Neurobiology of decision-making: A selective review from a neurocognitive and clinical perspective. *Biological Psychiatry*, *58*, 597–604.

Ernst, M., Pine, D. S., & Hardin, M. (2006). Triadic model of the neurobiology of motivated behavior in adolescence. *Psychological Medicine*, *36*, 299–312.

Ernst, M., Romeo, R. D., & Anderson, S. L. (2009). Neurobiology of the development of motivated behaviors in adolescence: A window into a neural systems model. *Pharmacology, Biochemistry and Behavior*, *93*, 199–211.

Forbes, E. E., Hariri, A. R., Martin, S. L., Silk, J. S., Moyles, D. L., Fisher, P. M., Brown, S. M., et al. (2009). Altered striatal activation predicting real-world positive affect

in adolescent major depressive disorder. *The American Journal of Psychiatry*, *166*, 64–73.

Fox, M. D., Snyder, A. Z., Vincent, J. L., Corbetta, M., Van Essen, D. C., & Raichle, M. E. (2005). The human brain is intrinsically organized into dynamic, anticorrelated functional networks. *Proceedings of the National Academy of Sciences of the United States of America*, *102*, 9673–9678.

Galvan, A., Hare, T. A., Davidson, M., Spicer, J., Glover, G., & Casey, B. J. (2005). The role of ventral frontostriatal circuitry in reward-based learning in humans. *The Journal of Neuroscience*, *25*, 8650–8656.

Galvan, A., Hare, T. A., Parra, C. E., Penn, J., Voss, H., Glover, G., & Casey, B. J. (2006). Earlier development of the accumbens relative to orbitofrontal cortex might underlie risk-taking behavior in Adolescents. *The Journal of Neuroscience*, *26*, 6885–6892.

Gardner, M., & Steinberg, L. (2005). Peer influence on risk taking, risk preference, and risky decision making in adolescence and adulthood: An experimental study. *Developmental Psychology*, *41*, 625–635.

Geier, C. F., Terwilliger, R., Teslovich, T., Velanova, K., & Luna, B. (2010). Immaturities in reward processing and its influence on inhibitory control in adolescence. *Cerebral Cortex*, *20*, 1613–1629.

Gerdes AB, Wieser MJ, Mühlberger A, Weyers P, Alpers GW, Plichta MM, Breuer F, Pauli P. (2010). Brain activations to emotional pictures are differentially

associated with valence and arousal ratings. *Frontiers in Human Neuroscience*, *4*, 175.

Giedd, J. N., Blumenthal, J., Jeffries, N. O., Castellanos, F. X., Liu, H., & Zijdenbos, A. et al. (1999). Brain development during childhood and adolescence: a longitudinal MRI study. *Nature Neuroscience*, *2*, 861–863.

Gil, S., & Droit-Volet, S. (2012). Emotional time distortions: the fundamental role of arousal. *Cognition & Emotion*, *26*, 847–862.

Gregorios-Pippas, L., Tobler, P. N., & Schultz, W. (2009). Short-term temporal discounting of reward value in human ventral striatum. *Journal of Neurophysiology*, *101*, 1507–1523.

Groenewold, N. a, Opmeer, E. M., de Jonge, P., Aleman, A., & Costafreda, S. G. (2013). Emotional valence modulates brain functional abnormalities in depression: Evidence from a meta-analysis of fMRI studies. *Neuroscience and Biobehavioral Reviews*, *37*, 152–163.

Haber, S. N., & Knutson, B. (2010). The reward circuit: Linking primate anatomy and human imaging. *Neuropsychopharmacology*, *35*, 4–26.

Hardin, M. G., Mandell, D., Mueller, S., Dahl, R. E., Pine, D. S., Ernst, M. (2009). Inhibitory Control in anxious and healthy adolescents is modulated by incentive and incidental affective stimuli. *Journal of Child Psychology and Psychiatry*, *50*, 1550–1558.

Herdt, G., & McClintock, M. (2000). The magical age of 10. *Archives of Sexual Behavior*, *29*, 587–606.

Herwig U, Abler B, Walter H, Erk S. (2007). Expecting unpleasant stimuli--an fMRI study. *Psychiatry Research*, *154*, 1–12.

Humphries, M. D., & Prescott, T. J. (2010). The ventral basal ganglia, a selection mechanism at the crossroads of space, strategy, and reward. *Progress in Neurobiology*, *90*, 385–417.

Hurvich, C., & Tsai, C. (1989). Regression and time series model selection in small samples. *Biometrika*, *76*, 297–307.

Ikemoto, S, & Panksepp, J. (1999). The role of nucleus accumbens dopamine in motivated behavior: a unifying interpretation with special reference to reward-seeking. *Brain Research Reviews*, *31*, 6–41.

Ikemoto, Satoshi, & Wise, R. a. (2004). Mapping of chemical trigger zones for reward. *Neuropharmacology*, *47 Suppl 1*, 190–201.

Jakob, C. (1907/1908). Localización del alma y de la inteligencia. Buenos Aires: El Libro.

Janes, A. C., Pizzagalli, D. A., Richardt, S., Frederick, B. de B., Holmes, A. J., et al. (2010). Neural substrates of attentional bias for smoking-related cues: An fMRI study. *Neuropsychopharmacology*, *35*, 2339–2345.

Jenkinson, M., Bannister, P., Brady, M., & Smith, S. M. (2002). Improved optimisation for the robust and accurate linear registration and motion correction of brain images. *NeuroImage*, *17*, 825–841.

Jenkinson, M., & Smith, S. M. (2001). A global optimisation method for robust affine registration of brain images. *Medical Image Analysis*, *5*, 143–156.

Jenkinson, M. (2003). Fast, automated, N-dimensional phase-unwrapping algorithm. *Magnetic Resonance in Medicine*, *49*, 193–197.

Jenkinson, M. (2004). Improving the registration of B0-disorted EPI images using calculated cost function weights. Tenth International Conference on Functional Mapping of the Human Brain.

Jensen, J., Smith, A. J., Willeit, M., Crawley, A. P., Mikulis, D. J., Vitcu, I., & Kapur, S. (2007). Separate brain regions code for salience vs. valence during reward prediction in humans. *Human Brain Mapping*, *28*, 294–302.

Kable, J. W., & Glimcher, P. W. (2010). An "as soon as possible" effect in human intertemporal decision making: Behavioral evidence and neural mechanisms. *Journal of Neurophysiology*, *103*, 2513–2531.

Kalkut, E. L., Han, S. D., Lansing, A. E., Holdnack, J. A., Delis, D. C. (2009). Development of set-shifting ability from late childhood through early adulthood. *Archives of Clinical Neuropsychology*, *24*, 565–574.

Kelley, A. E., & Berridge, K. C. (2002). The neuroscience of natural rewards: Relevance to addictive drugs. *The Journal of Neuroscience*, *22*, 3306–3311.

Kessler, R. C., Berglund, P., Delmer, O., Jin, R., Merikangas, K. R., & Walters, E. E. (2005). Lifetime prevalence and age-of-onset distributions of DSM-IV disorders in the National Comorbidity Survey Replication. *Archives of General Psychiatry, 62*, 593–602.

Knutson, B., Adams, C. M., Fong, G. W., & Hommer, D. (2001). Anticipation of increasing monetary reward selectively recruits nucleus accumbens. *The Journal of Neuroscience*, *21*, RC159.

Knutson, B., & Greer, S. M. (2008). Anticipatory affect: neural correlates and consequences for choice. *Philosophical Transactions of the Royal Society of London B*, *363*, 3771–3786.

Köchel, A., Schöngassner, F., & Schienle, A. (2013). Cortical activation during auditory elicitation of fear and disgust: A near-infrared spectroscopy (NIRS) study. *Neuroscience Letters*, *549*, 197–200.

Kuhnen, C. M., & Knutson, B. (2005). The neural basis of financial risk taking. *Neuron*, *47*, 763–770.

LaBar, K. S., Gitelman, D. R., Parrish, T. B., Kim, Y.-H., Nobre, A., & Mesulam M.-M. (2001). Hunger selectivity modulates corticolimbic activation to food stimuli in humans. *Behavioral Neuroscience*, *115*, 493–500.

Laird, A., Fox, P., Eickhoff, S., Turner, J. A., Ray, K. L., Mckay, D. R., Glahn, D. C., et al. (2011). Behavioral interpretations of intrinsic connectivity networks. *Journal of Cognitive Neuroscience*, *23*, 4022–4037.

Lang, P. J., Bradley, M. M., & Cuthbert, B. N. (1995). The International Affective Picture System (lAPS): Photographic Slides. Gainesville, FL: University of Florida.

Lavoie, A. M. & Mizumori, S. J. Y. (1994). Spatial-, movement- and reward-sensitive discharge by medial ventral striatum neurons of rats. *Brain Research*, *638*, 157–168.

LeDoux, J. E. (2000). Emotion circuits in the brain. *Annual Reviews in Neuroscience*, *23*, 155–184.

Levita, L., Hare, T. A., Voss, H. U., Glover, G., Ballon, D. J., & Casey B. J. (2009). The bivalent side of the nucleus accumbens. *NeuroImage*, *44*, 1178–1187.

Levita, L., Hoskin, R., & Champi, S. (2012). Avoidance of harm and anxiety: A role for the nucleus accumbens. *NeuroImage*, *62*, 189–198.

Lewis, P. A., & Miall, R. C. (2003). Distinct systems for automatic and cognitively controlled time measurement: Evidence from neuroimaging. *Current Opinions in Neurobiology*, *13*, 250–255.

Liu, X., Hairston, J., Schrier, M., & Fan, J. (2011). Common and distinct networks underlying reward valence and processing stages: A meta-analysis of functional neuroimaging studies. *Neuroscience and Biobehavioral Reviews*, *35*, 1219–1236.

Livesey, A. C., Wall, M. B., & Smith, A. T. (2007). Time perception: Manipulation of task difficulty dissociates clock functions from other cognitive demands. *Neuropsychologia*, *45*, 321–331.

Long, J. (2012). *Longitudinal Data Analysis for the Behavioral Sciences Using R*. Thousand Oaks, CA: Sage Publications.

Luciana, M., Collins, P. F., Olson, E. A., & Schissel, A. M. (2009). Tower of London performance in healthy adolescents: The development of planning skills and

associations with self-reported inattention and impulsivity. *Developmental Neuropsychology*, *34*, 461–475.

Luciana, M., Conklin, H. M., Hooper, C. J., & Yarger, R. S. (2005). The development of nonverbal working memory and executive control processes in adolescents. *Child Development*, *76*, 697–712.

Luciana, M., & Nelson, C. A. (2002). Assessment of neuropsychological function in children through the Cambridge Neuropsychological Testing Automated Battery (CANTAB): Normative performance in 4 to 12 year-olds. *Developmental Neuropsychology*, *22*, 595–624.

Luciana, M., Wahlstrom, D., Porter, J. N., & Collins, P. F. (2012). Dopaminergic modulation of incentive motivation in adolescence: Age-related changes in signaling, individual differences, and implications for the development of self-regulation. *Developmental Psychology*, *48*, 844–61.

Luna, B. (2009). The maturation of cognitive control and the adolescent brain. In F. Aboitiz and D. Cosmelli (Eds.) *From Attention to Goal-Directed Behavior*. Berlin: Springer-Verlag.

Luna, B., Thulborn, K. R., Munoz, D. P., Merriam, E. P., Garver, K. E., et al. (2001). Maturation of widely distributed brain function subserves cognitive development. *NeuroImage*, *13*, 786–793.

MacLean, P. D. (1949). Psychosomatic disease and the "visceral brain": Recent developments bearing on the Papez theory of emotion. *Psychosomatic Medicine*, *11*, 338–353.

Mak, A. K. Y., Hu, Z., Zhang, J. X. X., Xiao, Z., & Lee, T. M. C. (2009). Sex-related differences in neural activity during emotion regulation. *Neuropsychologia*, *47*, 2900–2908.

Marco-Pallarés, J., Mohammadi, B., Samii, A., & Münte, T. F. (2010). Brain activations reflect individual discount rates in intertemporal choice. *Brain Research*, *1320*, 123–129.

Matell, M. S., & Meck, W. H. (2000.) Neuropsychological mechanisms of interval timing behavior. *BioEssays*, *22*, 94–103.

May, J. C., Delgado, M. R., Dahl, R. E., Stenger, V. A., Ryan, N. D., Fiez, J. A., & Carter, C. S. (2004). Event-related functional magnetic resonance imaging of reward-related brain circuitry in children and adolescents. *Biological Psychiatry*, *55*, 359–366.

McClure, S. M., Daw, N. D., & Read Montague, P. (2003). A computational substrate for incentive salience. *Trends in Neurosciences*, *26*, 423–428.

McRae, K., Hughes, B., Chopra, S., Gabrieli, J. D. E., Gross, J. J., & Ochsner, K. N. (2010). The neural bases of distraction and reappraisal. *Journal of Cognitive Neuroscience*, *22*, 248–262.

Menon, V., & Uddin, L. Q. (2010). Saliency, switching, attention and control: A network model of insula function. *Brain Structure & Function*, *214*, 655–667.

Nelson, E. E., Leibenluft, E., McClure, E. B., & Pine, D. S. (2005). The social re-orientation of adolescence: a neuroscience perspective on the process and its relation to psychopathology. *Psychological Medicine*, *35*, 163–174.

Niznikiewicz, M., & Delgado, M. (2011). Two sides of the same coin: Learning via positive and negative reinforcers in the human striatum. *Developmental Cognitive Neuroscience*, *1*, 494–505.

O'Doherty, J. P., Deichmann, R., Critchley, H. D., & Dolan, R. J. (2002). Neural responses during anticipation of a primary taste reward. *Neuron*, *33*, 815–826.

Pagnoni, G., Zink, C. F., Montague, P. R., & Berns, G. S. (2002). Activity in human ventral striatum locked to errors of reward prediction. *Nature Neuroscience*, *5*, 97–98.

Panksepp, J. (1998). *Affective Neuroscience: The Foundations of Human and Animal Emotion*. New York: Oxford University Press.

Papez, J. W., 1937. A proposed mechanism of emotion. *Archives of Neurology and Psychiatry*, *38*, 725–743.

Paulus, M. P., Tapert, S. F., & Schulteis, G. (2009). The role of interoception and alliesthesia in addiction. *Pharmacology, Biochemistry, and Behavior*, *94*, 1–7.

Pessoa, L. (2010). Emotion and cognition and the amygdala: From "what is it?" to "what's to be done?" *Neuropsychologia*, *48*, 3416–3429.

Petersen, A. C., Silbereisen, R. K. & Soerensen, S. (1993). Adolescent development: A global perspective. In W. Meeus, M. de Goede, W. Kox & K. Hurrelmann (Eds.), *Adolescence, careers, and cultures*. Berlin/New York: W. de Gruyter.

Pfeifer, J. H., & Allen, N. B. (2012). Arrested development? Reconsidering dual-systems models of brain function in adolescence and disorders. *Trends in Cognitive Sciences*, *16*, 322–329.

Pfeifer, J. H., Masten, C. L., Moore, W. E., Oswald, T. M., Mazziotta, J. C., Iacoboni, M., & Dapretto, M. (2011). Entering adolescence: Resistance to peer influence, risky behavior, and neural changes in emotion reactivity. *Neuron*, *69*, 1029–1036.

Pitskel, N. B., Bolling, D. Z., Kaiser, M. D., Crowley, M. J., & Pelphrey, K. A. (2011). How grossed out are you? The neural bases of emotion regulation from childhood to adolescence. *Developmental Cognitive Neuroscience*, *1*, 324–337.

Popper, K. (1959/2002). *The Logic of Scientific Discovery*. New York: Routledge Classics.

Power, J. D., Barnes, K. a, Snyder, A. Z., Schlaggar, B. L., & Petersen, S. E. (2012). Spurious but systematic correlations in functional connectivity MRI networks arise from subject motion. *NeuroImage*, *59*, 2142–2154.

Pöppel, E. (2009). Pre-semantically defined temporal windows for cognitive processing. *Philosophical transactions of the Royal Society of London. Series B, Biological sciences*, *364*, 1887–1896.

R Development Core Team (2012). R: A language and environment for statistical computing. R Foundation for Statistical Computing, Vienna, Austria. ISBN 3-900051-07-0, URL http://www.R-project.org/.

Rademacher, L., Krach, S., Kohls, G., Irmak, A., Gründer, G., & Spreckelmeyer, K. N. (2010). Dissociation of neural networks for anticipation and consumption of monetary and social rewards. *NeuroImage*, *49*, 3276–3285.

Raichle, M. E., MacLeod, a M., Snyder, a Z., Powers, W. J., Gusnard, D. a, & Shulman, G. L. (2001). A default mode of brain function. *Proceedings of the National Academy of Sciences of the United States of America*, *98*, 676–682.

Reyna, V. F., & Farley, F. (2006). Risk and rationality in adolescent decision-making: Implications for theory, practice, and public policy. *Psychological Science in the Public Interest*, *7*, 1–44.

Richards, J. M., Plate, R. C., & Ernst, M. (2013). A systematic review of fMRI reward paradigms used in studies of adolescents vs. adults: the impact of task design and implications for understanding neurodevelopment. *Neuroscience and Biobehavioral Reviews*, *37*, 976–991.

Robinson, T. E., & Berridge, K. C. (2003). Addiction. *Annual review of psychology*, *54*, 25–53.

Roca, M., Torralva, T., Gleichgerrcht, E., Woolgar, A., Thompson, R., Duncan, J., & Manes, F. (2011). The role of Area 10 (BA10) in human multitasking and in social cognition: A lesion study. *Neuropsychologia*, *49*, 3525–3531.

Salamone, J. D. (1994). The involvement of nucleus accumbens dopamine in appetitive and aversive motivation. *Behavioural Brain Research*, *61*, 117–133.

Sander, D., Grafman, J., & Zalla, T. (2003). The human amygdala: An evolved system for relevance detection. *Reviews in the neurosciences*, *14*, 303–316.

Schultz, W. (2000). Multiple reward signals in the brain. *Nature Reviews Neuroscience*, *1*, 199–207.

Seeley, W. W., Menon, V., Schatzberg, A. F., Keller, J., Glover, G. H., Kenna, H., Reiss, A. L., et al. (2007). Dissociable intrinsic connectivity networks for salience processing and executive control. *The Journal of Neuroscience*, *27*, 2349–2356.

Sesack, S. R., & Grace, A. a. (2010). Cortico-Basal Ganglia reward network: Microcircuitry. *Neuropsychopharmacology, 35*, 27–47.

Smith, S. M. (2002). Fast robust automated brain extraction. *Human Brain Mapping, 17*, 143-155.

Smith, S. M., Fox, P. T., Miller, K. L., Glahn, D. C., Fox, P. M., Mackay, C. E., Filippini, N., et al. (2009). Correspondence of the brain's functional architecture during activation and rest. *Proceedings of the National Academy of Sciences of the United States of America*, *106*, 13040–13045.

Somerville, L. H., Hare, T., & Casey, B. (2011). Frontostriatal maturation predicts cognitive control failure to appetitive cues in adolescents. *Journal of Cognitive Neuroscience*, *23*, 2123–2134.

Somerville, L. H., Jones, R. M., & Casey, B. J. (2010). A time of change: Behavioral and neural correlates of adolescent sensitivity to appetitive and aversive environmental cues. *Brain and Cognition*, *72*, 124–133.

Sowell, E. R., Thompson, P. M., Holmes, C. J., Jernigan, T. J., & Toga, A. W. (1999). In vivo evidence for post-adolescent brain maturation in frontal and striatal regions. *Nature Neuroscience*, *2*, 859–860.

Sowell, E. R., Thompson, P. M., Leonard, C. M., Welcome, S. E., Kan, E., & Toga, A. W. (2004). Longitudinal mapping of cortical thickness and brain growth in normal children. *The Journal of Neuroscience*, *24*, 8223–8231.

Spear, L. P. (2000). The adolescent brain and age-related behavioral manifestations. *Neuroscience and Biobehavioral Reviews*, *24*, 417–463.

Spicer, J. Galvan, A., Hare, T. A., Voss, H., Glover, G., and Casey, B. J. (2007). Sensitivity of the nucleus accumbens to violations in expectation of reward. *NeuroImage*, *34*, 455–461.

Sporns, O. (2011). The human connectome: A complex network. *Annals of the New York Academy of Sciences*, *1224*, 109–125.

Stein, M. B., & Paulus, M. P. (2009). Imbalance of approach and avoidance: The yin and yang of anxiety disorders. *Biological psychiatry*, *66*, 1072–1074.

Steinberg, L. (2008). A social neuroscience perspective on adolescent risk-taking. *Developmental Review*, *28*, 78–106.

Steinberg, L., (2010). A dual systems model of adolescent risk-taking. *Developmental Psychobiology*, *52*, 216–224.

Steinberg, L., & Cauffman, E. (1996). Maturity of judgment in adolescence: Psychosocial factors in adolescent decision making. *Law and Human Behavior*, *20*, 249–272.

Stoodley, C. J., & Schmahmann, J. D. (2009). Functional topography in the human cerebellum: A meta-analysis of neuroimaging studies. *NeuroImage*, *44*, 489–501.

Thoma, P., Koch, B., Heyder, K., Schwarz, M., & Daum, I. (2008). Subcortical contributions to multitasking and response inhibition. *Behavioural Brain Research*, *194*, 214–222.

Tranel, D., Gullickson, G., Koch, M., & Adolphs, R. (2006). Altered experience of emotion following bilateral amygdala damage. *Cognitive Neuropsychiatry*, *11*, 219–232.

Triarhou, L. C. (2008). Centenary of Christfried Jakob's discovery of the visceral brain: An unheeded precedence in affective neuroscience. *Neuroscience and Biobehavioral Reviews*, *32*, 984–1000.

Ulbrich, P., Churan, J., Fink, M., & Wittmann, M. (2007). Temporal reproduction: Further evidence for two processes. *Acta Psychologica*, *125*, 51–65.

Ursin, H., & Kaada, B. R. (1960). Functional localization within the amygdaloid complex in the cat. *Electroencephalography and Clinical Neurophysiology*, *12*, 1–20.

Verstynen, T. D., & Deshpande, V. (2011). Using pulse oximetry to account for high and low frequency physiological artifacts in the BOLD signal. *NeuroImage*, *55*, 1633–1644.

Wager, T. D., Davidson, M. L., Hughes, B. L., Lindquist, M. A., & Ochsner, K. N. (2008). Prefrontal-subcortical pathways mediating successful emotion regulation. *Neuron*, *59*, 1037–1050.

Wittmann, M. (2009). The inner experience of time. *Philosophical transactions of the Royal Society of London. Series B, Biological sciences*, *364*, 1955–1967.

Wittmann, M., Lovero, K. L., Lane, S. D., & Paulus, M. P. (2010). Now or later? Striatum and insula activation to immediate versus delayed rewards. *Journal of Neuroscience, Psychology, and Economics*, *3*, 15–26.

Wittmann, M., Simmons, A. N., Flagan, T., Lane, S. D., Wackermann, J., & Paulus, M. P. (2011). Neural substrates of time perception and impulsivity. *Brain Research*, *1406*, 43–58.

Worsley, K. J. (2001). Statistical analysis of activation images. In P. Jezzard, P.M. Matthews, & S.M. Smith (Eds.), *Functional MRI: An Introduction to Methods*. Oxford: Oxford University Press.

Yurgelun-Todd, D. (2007). Emotional and cognitive changes during adolescence. *Current Opinion in Neurobiology*, *17*, 251–257.

Zink, C. F., Pagnoni, G., Martin-Skurski, M. E., Chappelow, J. C., & Berns, G. S. (2004). Human striatal responses to monetary reward depend on saliency. *Neuron*, *42*, 509–517.